MOMENT-CURVATURE RELATIONSHIP

OF

REINFORCED CONCRETE BEAMS

BY

OKOLI, Obumneme Godwin

being a report of research work submitted to the

Postgraduate School in partial fulfillment of the requirements

for the award of Doctor of Philosophy degree

in Ahmadu Bello University

Department of Building

Faculty of Environmental Design

Ahmadu Bello University

Zaria

DECLARATION

I hereby declare that this thesis has been prepared by me and that is a record of my research work. It has not been submitted in any previous application for higher degree. All quotations are indicated and the sources of information are specifically acknowledged by means of reference.

Signed.....

Engr. Okoli O. Godwin

CERTIFICATION

This dissertation\research work entitled:
MOMENT-CURVATURE RELATIONSHIP OF REINFORCED CONCRETE BEAMS
by OKOLI, Obumneme Godwin meets the regulations governing the award of the degree of Doctor of Philosophy of Ahmadu Bello University, and is approved for its contribution to knowledge and literary presentation.

..... 20/8/93
Dr. S. Kus
Chairman, Supervisory Committee — Date

..... 25/7/94
Dr. A.A. Husseini
Member, Supervisory Committee — Date

..... 11/07/94
Dr. S.P. Ejeh
Member, Supervisory Committee — Date

..... 11.07.1994
Head of Department — Date

..... 2/7/96
Dean Postgraduate School — Date

DEDICATION

This Thesis is dedicated to

my wife CHIOMA

and my children

CHI-CHI and K.C.

ACKNOWLEDGEMENT

I wish to express my indebtedness to my Supervisor Dr. Stanislaw Kus who is the mentor of this research work. His constructive criticisms, dynamism, and unrestricted access to himself was invaluable to me.

I am equally indebted to other members of the Supervisory Committee: Dr A.A Husseini and Dr S.P Ejeh for thier criticisms and advises throughout the period of this work. I also wish to specially thank Mr Z.J Sikora: Head, Department of Building for his personal concern, interest, advises and assistance always and throughout the period of this work.

My thanks go equally to the entire staff of Building Department for assistance rendered at various times especially Mal. Abubakar Saliu, Mal. Audi Salihu and Mal. Aliyu Saidu.

I am grateful to Mr D.E. Madu, Mal. I.K. Zubairu and Mr. Ken. Aimiwu through whom it was possible for me to get some journal publications from Europe.

I am most grateful to the Head: Department of Civil Engineering Prof. A.O. Adebisi for permitting me to use the Concrete and Structures Laboratory to conduct my experiments. My thanks go to the entire laboratory staff particularly Mr. A.R.O. Bello and Mr. Jacob Olumarade for their advice and assistance throughout the period of the experiment.

I also wish to acknowledge with thanks the concern, personal interest and goodwill always shown to me by Prof. O. Solanke. I am very gratiful to you.

Special thanks to my younger brother Mr. Uche Nkwoike for his financial assistance especially when the going was very tough.

Many thanks to Dr. Ray Nkado who patiently typed the manuscript. I appreciate his excellent work.

There are obviously people numerous to list who have in one way or the other contributed to the successful completion of this thesis, I am grateful to you all.

Finally, I will like to express my heart-felt gratitude to my darling wife: Mrs Chioma. A, Okoli and my children Chi-Chi and K.C. for their endurance at the most critical periods.

ABSTRACT

Rigorous analysis of reinforced concrete members loaded into the inelastic range requires the knowledge of the relationship between moment and curvature. This knowledge is necessary for better evaluation of the deflections and possible redistribution of bending moments after cracking in statically indeterminate reinforced concrete members.

In this research work, a considerably simplified theory for the analysis of moment-curvature relationship and hence deflection of reinforced concrete beams in the cracking stage is presented. The theory assumes concrete to have a non-zero tensile capacity. The non-linear behaviour of concrete in compression was accounted for by assuming a parabolic stress-strain relationship. For the purpose of this work, the stress-strain diagram of concrete in tension was approximated by a bilinear curve.

These assumptions led to a third degree equation to determine the position of the neutral axis according to the equilibrium of internal forces. Having the position the position of the position of the neutral axis, it was possible to find the moments and the curvatures for an assumed value of strain in the tensile reinforcement.
By increasing the value of the strain and repeating the above procedure, we obtain the moment-curvature diagrams.

Good agreement was found between the results of this the

and the experimental results of previous investigators.

To further confirm the validity the theory, six full sized reinforced concrete beams grouped into two sets were tested. The first set of beams have cross sectional dimensions 300mm by 100mm and the second set has dimensions 100mm by 300mm. Each of the beams has total span 4.0m. All the beams were reinforced with deformed bars of varying diameters. Stirrups were provided throughout the length of each beam.

It was found that results of the experiments were in good agreement with the theory.

TABLE OF CONTENTS

	Page
TITLE PAGE	i
DECLARATION	ii
CERTIFICATION	iii
DEDICATION	iv
ACKNOWLEDGEMENT	v
ABSTRACT	vii
LIST OF TABLES	x
LIST OF FIGURES	xi
LIST OF SYMBOLS	xii
LIST OF APPENDICES	xiii
CHAPTER ONE	
1.0 INTRODUCTION	1
1.1 General Background	1
1.1.1 The Shape of Moment-Curvature Curve	5
1.1.2 Application of Moment-Curvature Relationship for deflection calculation	13
1.1.3 Need for the study	17
1.2 Aims and Objectives	18
1.3 Scope and Limitations	19
1.4 Methodology	20
CHAPTER TWO	
2.0 LITERATURE REVIEW	24
2.1 The Shape of Stress-Strain Diagram of Concrete	24

2.1.1 Numerical approximations of Stress-Strain Curves 25

2.1.2 Tensile Stress-Strain Relationship of Concrete 32

2.1.3 Simplified Stress-Strain Curves of Tensile Concrete for Obtaining Moment-Curvature Relationship 35

2.1.4 Concluding Remarks on Stress-Strain Relationship 43

2.2 Moment-Curvature Relationship 44

2.2.1 Codes Provisions for Beam Deflection 57

CHAPTER THREE

3.0 THEORETICAL CONSIDERATIONS 60

3.1 Assumptions 60

3.2 Derivation of Formulae for Calculating Moment-Curvature Relationship 64

3.2.1 Formulae for Calculating *M*-κ Relationship Neglecting the Contrbution of Tensile Concrete. 64

3.2.2 Consideration of Tensile Concrete Using Rectangular Approximation 74

3.2.3 Consideration of Tensile Concrete Using Triangular Approxmation of tensile Stress-Strain Curve 80

3.2.3.1 Stage I of Triangular Approximation 81

3.2.3.2 Second Stage of Triangular Approximation 87

3.2.3.3 Third Stage of Triangular Approximation 98

3.2.3.4 Computation of Moment-Curvature Relationship 104

CHAPTER FOUR

4.1 Comparison of Results 105

CHAPTER FIVE

5.0 Experimental Programme 104

5.1 Concrete Mix 111

5.1.1 Test Beams 112

5.1.2 Fabrication of Beams 113

5.1.3 Test Arrangement 113

5.1.4 Cube Tests/Cylinder Tests 117

5.1.5 Evaluation of Measured Data and the Results 117

5.1.6 Observations 125

5.2 Conclusions and Recomendations 135

5.2.1 Conclusions 135

5.2.2 Recomendations 138

References 140

Appendix I Aggregate Grading Curve 146

Appendix II Some Seleted Photographs 145

Appendix III Listed Programs for calculating Moment-Curvature Relationship 150

LIST OF TABLES

TABLE		Page
2.1	Fomulae for the ascending branch of Stress-Strain diagram of concrete.	27
5.1	Aggregates Sieve Analysis	114
5.2	General Details of Test Beams	115

LIST OF FIGURES

FIGURES	Page
1.1 Deformation of a Flexural Member and Strain distribution in the Cross-Section of a deformed member	4
1.2 Complete Stress-Strain Curve of concrete in tension and compression.	7
1.3 Typical stress-strain curve for steel reinforcement	8
1.4 Typical Moment-Curvature curve of reinforced concrete beam	12
1.5 Example of idealized moment-curvature diagrams (Monnier 1970)	12
1.6 Application of moment-curvature curve for deflection evaluation	15
1.7 Application of moment-curvature curve for deflection evaluation.	16
2.1 Typical stress-strain curve for concrete in compression	30
2.2 Comparison of several formulae for stress-strain diagram of concrete	30
2.3 Hognestad's stress-strain curve	31
2.4 Assumed concrete compressive stress-strain curve	31
2.5 Typical concrete tensile stress-strain curve	34
2.6 Approximation of tensile Stress-strain curve by Vebo and Ghali	40
2.7 Approximation of tensile stress-strain curve by Bazant and Oh.	40
2.8 Representative tensile stress-strain curve of concrete component by Prakhya and Morley	41
2.9 Stress-strain relationship adopted by Prakhya and Morley	41
2.10 Stress-strain curve used by Kaminska and Czkwianiac	42

2.11 Typical moment-curvature curve showing the influence of tensile concrete 47

2.12 Stress-strain distribution adopted by Monnier 48

2.13 Monnier's idealized moment-curvature diagram 48

2.14 Stress and Strain distribution adopted by Bazant and Oh 49

2.15 Stress-strain distribution adopted by Prakhya and Morley 49

2.16 Trilinear approximation of moment-curvature relationship by Alwis 56

2.17 Branson's moment-curvature relationship for calculating I_{eff} 56

3.1 Idealised stress-strain diagram for reinforcing steel 61

3.2 Stress-strain curve of concrete showing rectangular approximation of tensile zone 62

3.3 Stress-strain curve of concrete showing triangular approximation of tensile zone 63

3.4 Stress-strain distribution for calculating moment-curvature relationship without tensile concrete 71

3.5 Rectangular approximation. (Ultimate strain within the section) 72

3.6 Rectangular approximation (Ultimate strain outside the section) 73

3.7 Stress-strain distribution showing the deformative stages used in triangular approximation 85

3.8 Stress and strain distribution for stage I 86

3.9 Stress and Strain distribution for stage II 102

3.10 Stress and Strain distribution for Stage III 103

4.1 Comparison of results of rectangular approximation with Monnier's experimental results 106

4.2 Comparison of results of triangular approximation with Monnier's experimental result (Beam A1) 107

4.3 Comparison of result of triangular approximation with Monnier's experimental result (Beam A2) 108

4.4 Comparison of result of triangular approximation with Monnier's experimental result (Beam A3) 109

4.5 Comparison of result of triangular approximation with Monnier's experimental result (Beam A4) 110

5.1(a) Typical layout of reinforcement for beams B-I, B-II, and B-III 118

5.1(b) Cross-section of beams B-I, B-II and B-III 118

5.2(a) Typical layout of reinforcement for beams B-IV B-V and B-VI 119

5.2(b) Cross-section of beams B-IV, B-V and B-VI 119

5.3 Test arrangement showing bending moment and shear force diagrams 120

5.4 Arrangement of measuring instruments 120

5.5 Stress-strain curve for beams B-I, and B-IV 121

5.6 Stress-strain curve for beams B-III and B-VI 122

5.7 Stress-strain curve for beams B-II and B-V 113

5.8 Assumed parabola for analyzing the experimental data 126

5.9 Comparison of experimental and theoretical results beam B-I 127

5.10 Comparison of experimental and theoretical results beam B-II 128

5.11 Comparison of experimental and theoretical results beam B-III 129

5.12 Comparison of experimental and theoretical results beam B-IV 130

5.13 Comparison of experimental and theoretical results beam B-V 131

5.14 Comparison of experimental and theoretical results beam B-VI 132

5.15 Comparison of experimental results of beams cross section 300mm by 100mm. 133

5.16 Comparison of experimental results of beams cross section 100mm by 300mm. 134

LIST OF SYMBOLS

Except where otherwise stated, the following meanings of symbols are used throughout the text:

A - co-efficient of the third degree equation.

B - co-efficient of the third degree equation.

C - co-efficient of the third degree equation.

D - co-efficient of the third degree equation.

A_s - area of tensile reinforcement.

A_s' - area of compression reinforcement.

B_w - width of rectangular section or width of flange for flanged beam

d_o - depth of beam

E_s - modulus of elasticity of steel reinforcement.

E_{bo} - modulus of elasticity of concrete at the origin of the concrete stress-strain diagram.

$(EI)_o$ - bending stiffness in the uncracked state.

$(EI)_c$ - bending stiffness in the cracked state.

$(EI)_{cr}$ - bending stiffness of fully cracked section (no tension).

f_t - tensile strength of concrete.

f_t' - compressive strength of concrete.

f_{cu}' - cube strength of concrete.

h - distance from extreme compressive fibre to the centroid of tensile reinforcement.

I_{bo} - moment of inertia of uncracked section including quantity of steel.

$K_w \cdot B_o$ - web thickness of flanged beam.

$K_d \cdot h$ - distance from extreme compressive fibre to centroid of compressive reinforcement.

$K_{ho} \cdot h$ - flange thickness of flanged beam

$K_x \cdot h$ - depth of neutral axis

l - span of beam

M - bending moment in the cross-section

M_c - bending moment in cross-section neglecting tensile concrete

M_t - bending moment in cross-section due to tensile concrete

M_y - yield moment

M_{cr} - cracking moment

N_a - resultant steel tensile force

N_a' - resultant steel compressive force

N_b - resultant concrete tensile force

N_b' - resultant compressive concrete force

$n = \frac{E_a}{E_{bo}}$ - ratio of modulus of elasticity of steel to that of concrete

R - radius of curvature

r_a - ratio $\frac{\varepsilon_a}{\varepsilon_c'}$

r_d ratio $\frac{\varepsilon_b'}{\varepsilon_c'}$

r_d ratio $\frac{\varepsilon'_b}{\varepsilon'_c}$

W_{bo} - section modulus of uncracked cross-section including quantity of reinforcement

Φ - diameter of steel reinforcement bars or stirrups

ε_a - strain of tensile reinforcement

ε'_a - strain of compressive reinforcement

ε_{ay} - strain at commencement of yielding of tensile reinforcement

ε_b - concrete strain at extreme tensile fibre

ε'_b - concrete strain at extreme compressive fibre

ε_c - concrete compressive strain

ε'_c - concrete compressive strain at maximum compressive stress

ε_m - concrete tensile strain at maximum tensile stress.

ε_t - concrete tensile strain

ε_{tu} - ultimate tensile strain in concrete

β - stress block parameter

κ - curvature of beam axis

σ_a - stress in tensile reinforcement

σ'_a - stress in compressive reinforcement

σ_b - concrete stress at extreme tensile fibre

σ_c - concrete compressive stress

σ_t - concrete tensile stress

ω - tensile steel ratio

ω' - compressive steel ratio

CHAPTER-ONE

INTRODUCTION

1.1 GENERAL BACKGROUND

Load deformation characteristics of flexural members depends mainly on the moment-curvature relationship of the sections. This is because most of the deformations of members arise from strains associated with flexure. Considerations of the load-deformation characteristics of members is necessary for the following reasons:

i) Brittle failure of members should not occur. In the extreme event of a structure being loaded to failure, it should be capable of undergoing large deformations prior to maximum load carrying capacity. This may save lives by giving warning of failure and preventing total collapse.

ii) The possible distribution of bending moments different from that obtained from a linear elastic structural analysis can be achieved if moment redistribution can take place. That is, as ultimate load is approached, some sections may reach the ultimate resisting moments before others; but if plastic rotation can occur there, while the ultimate moment is maintained, additional load can be carried as the moment elsewhere increase to their ultimate

value. Use of moment redistribution can convey advantages because it may reduce the congestion of reinforcement at the supports of continuous members, and enables reduction in the peak bending moments in bending moment envelopes.

iii) In areas subjected to earthquakes, a very important design consideration is the ductility of the structure when subjected to seismic loading. This is because seismic design is based on energy absorption and dissipation by post-elastic deformation for the survival of major earthquakes. Thus structures incapable of showing ductile deformation must be designed for much higher seismic forces if collapse is to be avoided.

The curvature of a structural member can be defined as rotation per unit length of the member. Let us consider an initial straight element of a reinforced concrete member (Fig. 1.1) with equal end moments.

The rotation between the ends of the element of length dx is given by:

$$\frac{dx}{R} = \frac{\varepsilon'_b \, dx}{K_x \, h} - \frac{\varepsilon_a \, dx}{h(1 - K_x)} \qquad (1.1)$$

$$\frac{1}{R} = \frac{\varepsilon'_b}{K_x \, h} - \frac{\varepsilon_a}{h(1 - K_x)} \qquad (1.2)$$

where $\frac{1}{R}$ is the curvature of the element. It is denoted by the symbol kappa, κ Therefore,

$$\kappa = \frac{\varepsilon_s}{h(1 - K_x)} = \frac{\varepsilon'_b}{K_x h} \quad \ldots (1.3)$$

The radius of curvature R, is measured to the neutral axis. The neutral axis depth is $K_x h$, the radius of curvature R, and the concrete strain in the extreme compression fibre ε'_b and steel strain ε_s vary along the length of the member because in-between the cracks, concrete still carries some tensile forces.

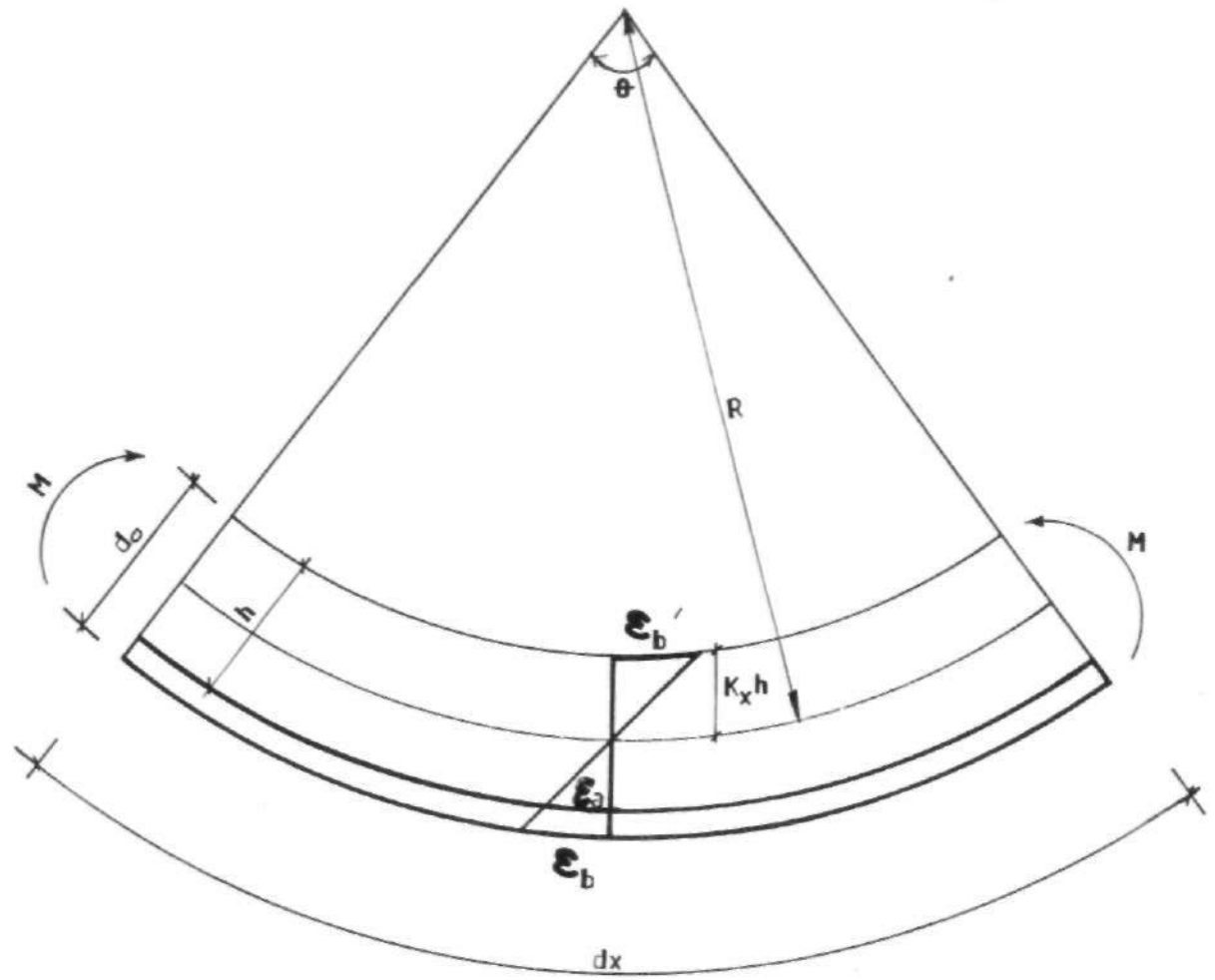


Fig. 1.1. Deformation of flexural member and strain distribution in the cross-section of a deformed member.

1.1.1 The Shape of Moment-Curvature Curve

The important factors which affects the shape of the moment-curvature curves of reinforced concrete beams are:

i) The shape of the stress-strain curve of concrete in tension and compression which completely describes the deformative properties of concrete (Fig. 1.2). Knowledge of the descending branch of the tensile stress-strain relationship is of particular importance because of its sensitive influence on the shape of moment-curvature curves. This aspect is fully discussed under literature review.

ii) The stress-strain relationship of steel reinforcement also influence the shape of moment-curvature curves. Steel having definitive yield point gives different shape of moment-curvature relation compared to steel without definite yield point for the same percentage of reinforcement (Fig. 1.3).

iii) Geometry of cross-section (rectangular or T-section), ratio of reinforcement, placement of reinforcement etc. also affect the shape of moment-curvature curve. In the case of T-beams, various cases of the positions of the neutral axis as well as tensile stress peaks need be distinguished. Percentage and placement of reinforcement strongly affects the shape of moment-curvature curve.

Heavily reinforced sections have steep moment-curvature curves while lightly reinforced section produces S-shaped moment-curvature relationship.

iv) Other factors which are not considered include include, among others, environmental factors (humidity and temperature), time dependent behaviours of concrete (shrinkage and creep), and loading history, etc.

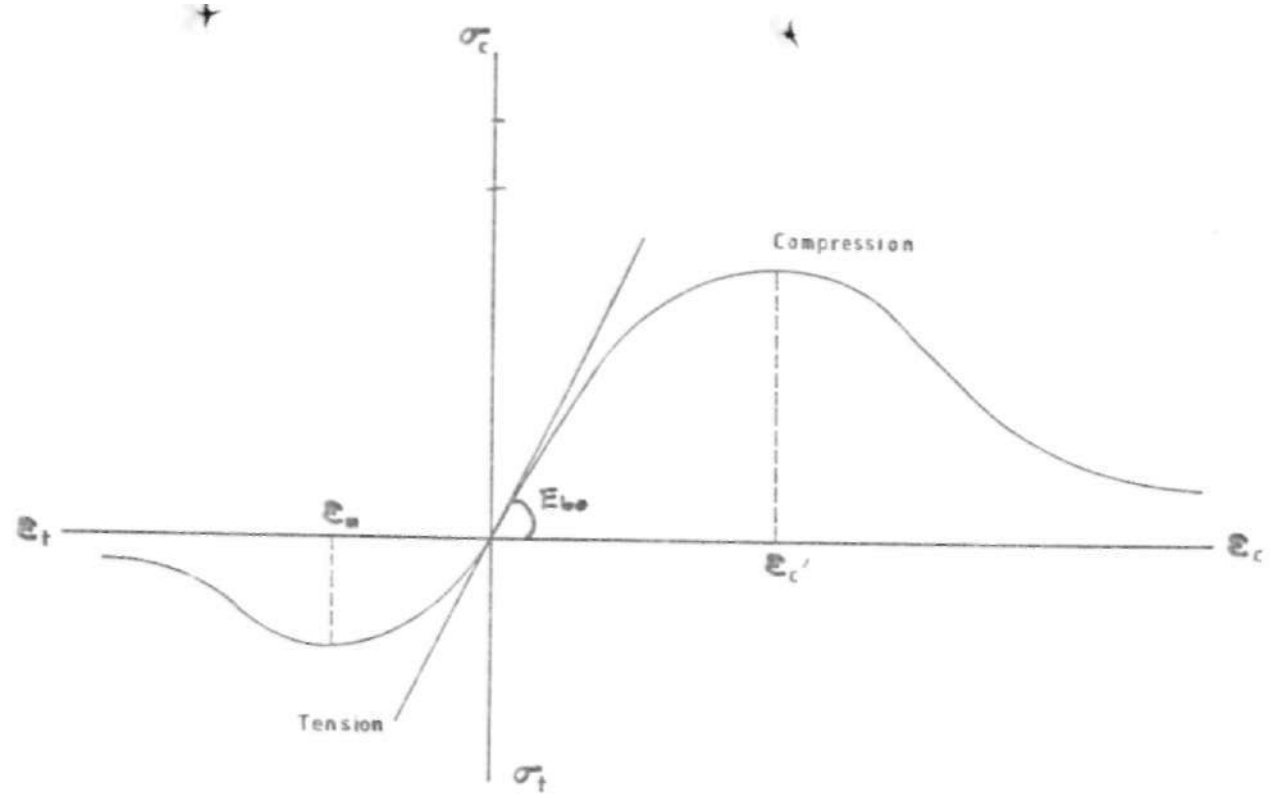


Fig. 1.2. Complete stress-strain curve of concrete in tension and compression.

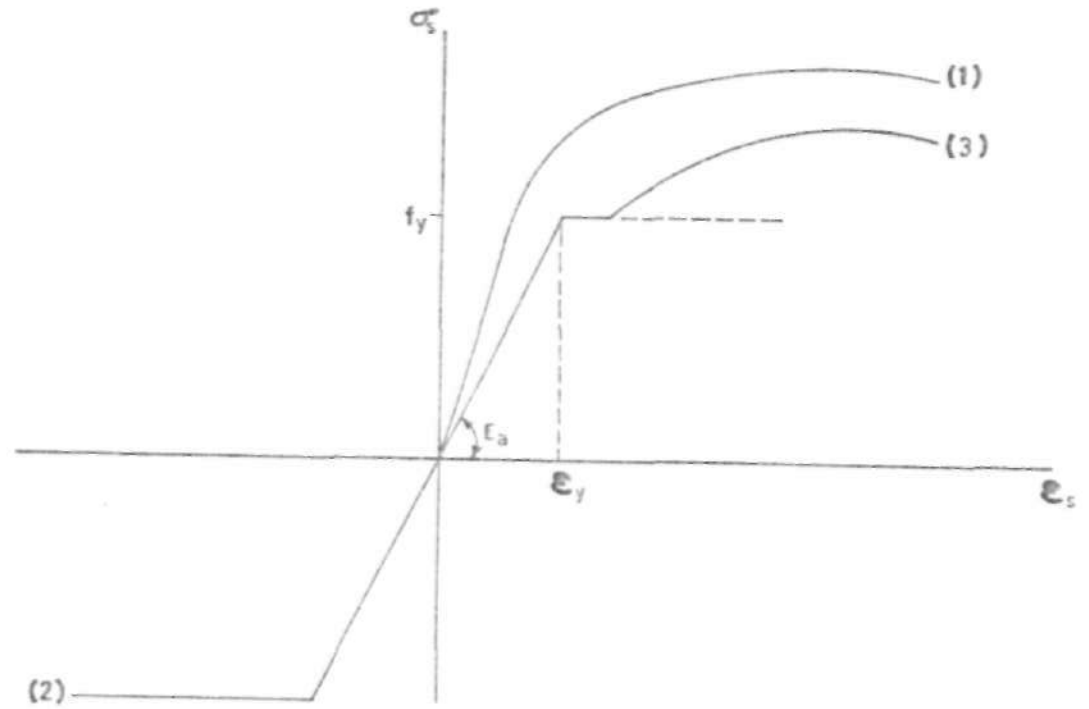


Fig.1.3. Stress - strain curves for reinforcement :
1) Steel having no definite yield plateau
2) Idealized stress-strain curve for computing M-K relationship .
3) Steel with definite yield plateau

Moment Curvature curve of a reinforced concrete beam is obtained experimentally by measuring the strains (ε'_b and ε_b) at the extreme fibres of a cross-section of a reinforced concrete beam as bending moment is increased to failure.

Curves obtained are usually linear in the initial stage up to the so called "Cracking moment" M_{cr} . At this stage, the relationship between moment and curvature is given by the classical elastic equation:

$$(EI)_o = \frac{M}{\kappa} = constant \qquad \ldots\ (1.4)$$

Where:

$(EI)_o$ -bending stiffness of uncracked cross-section

M -bending moment in the cross-section

κ -curvature corresponding to the moment in the cross-section.

Cracking moment is fictitious; it does not exist in reality because micro crack formation in reinforced concrete members is a continuous process hence no value of bending moment can be assigned to its formation.

The first stage therefore shades off smoothly into the second stage.

With the increase in bending moment, cracking of the concrete reduces the flexural rigidity of the section and the curve deviates from the initial straight line. The reduction is greater for lightly reinforced sections than for heavily reinforced sections. This stage represents the flexural rigidity of cracked cross-section. The curve grows asymptotically to the flexural stiffness of fully cracked section up to yield of tensile reinforcement. The stiffness of the fully cracked cross-section is represented by a straight line from the origin. Figure 1.4 shows a typical moment-curvature curve.

The behaviour of the section after cracking (stage 2) depends mainly on the steel content. Lightly reinforced cross-sections result in an S-shaped moment-curvature curves up to the point of yielding of tensile reinforcement. At yield, a large increase in curvature occurs at nearly constant bending moment.

This is shown in idealized form in Figure 1.5.

In heavily reinforced sections, the moment-curvature curve is steep; almost a straight line from the origin to the point of yield stress of tensile reinforcement. Failure in this case can be quite brittle unless concrete is confined by closed stirrups at close centres.

If concrete is not confined, it crushes at relatively small curvature before the steel yields causing a decrease in the moment carrying capacity of the member.

The flexural stiffness in the cracked state $(EI)_g$ can be obtained at any value of the bending moment using the relation:

$$(EI)_g = \frac{\Delta M}{\Delta \kappa} \quad \ldots\ (1.5)$$

where: ΔM - bending moment

$\Delta \kappa$ - curvature

$(EI)_g$ - bending stiffness in the cracked state

To ensure ductile behaviour in practice, steel content less than balanced design but greater than the minimum design value are always used for beams.

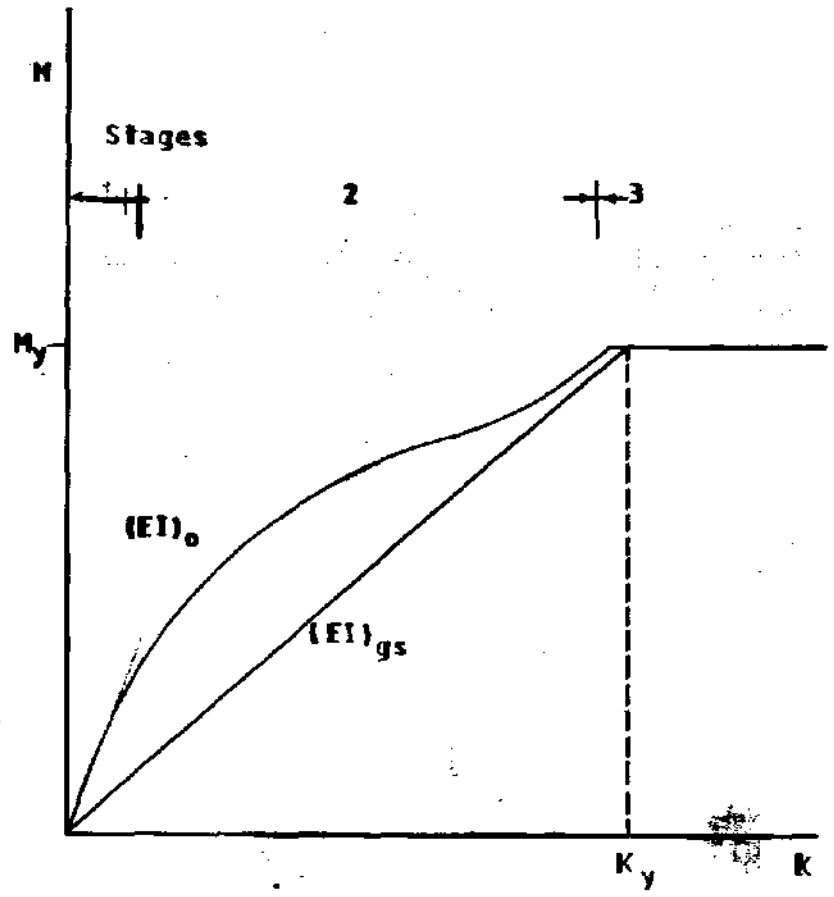


Fig. 1.4. Typical M-K curve of reinforced concrete beam.

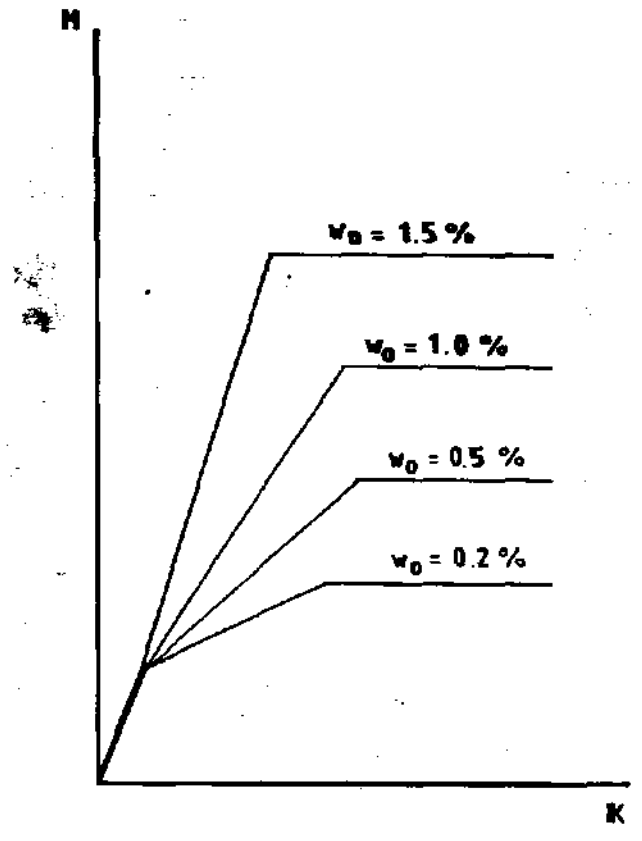


Fig. 1.5. Examples of idealized M-K diagrams (Monnier, 1970).

1.1.2 Application of $M - \kappa$ Relationship for Deflection Calculation

Short-time deflections of reinforced concrete members are affected by the strengths of concrete and reinforcement, the cross-sectional dimensions and the applied bending moment. However, the major cause of difficulty in the analysis of deflections is the variability of the stiffness due to cracking of concrete and the non-linear distribution of stress both in the compression and tensile zones of concrete. Moment-curvature relationship is used for calculating more accurately the flexural stiffness at any section of a beam knowing the value of the bending moment at that section. Having obtained the flexural stiffness, deflections can be calculated for those sections using any available method of finding deflection. For example, congugate beam method.

Deflections calculated in this way are more realistic than most approximate methods in which stiffness is assumed uniform over the entire beam length. Figure 1.6 shows the application of moment-curvature in calculating the flexural stiffness.

The principal types of deflection problems commonly found in practice may be classed into:

i) Where excessive deflections results in either aesthetic or functional problems. Examples include objectionable visual sagging, "ponding" of water on roof slabs which may result in accelerated deterioration, prevention of proper operation of machinery such as in gantry beams, jamming of doors and windows.

ii) Where structural members are joined to each other or to non-structural elements that may be damaged by large deflections. Examples include excessive rotation of joints causing unsightly cracks which may permit the entrance of water; damage to partitions, cladding, ceilings and other brittle finishes.

Cracking and deflection are related problem which are treated under serviceability limit state in reinforced concrete members. Curvature is related to crack width because curvature is calculated from concrete strain on extreme tensile or compressive fibre of the cross-section. Excessive cracking affects the appearance and ductility of structural members due to corrosion of reinforcement. Excessive crack width may be unconducive to occupants and may lead to a feeling of unsafe.

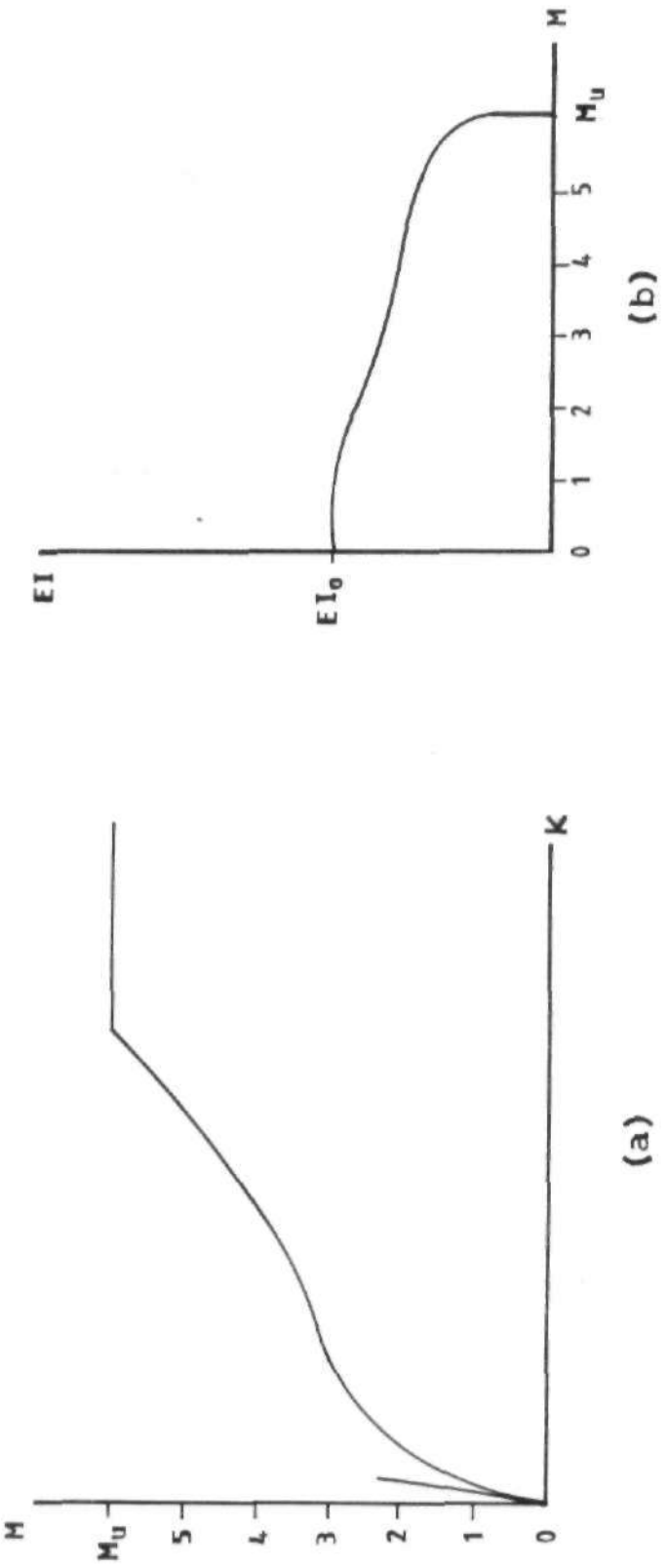


Fig. 1.6.a) Moment-curvature diagram ; b) Stiffness-moment diagram

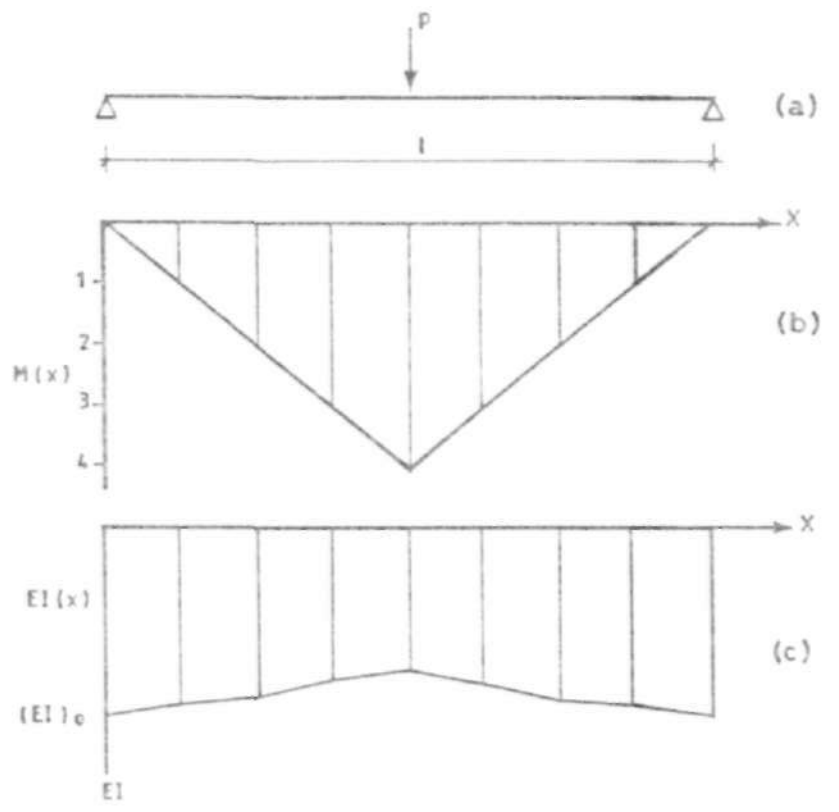


Fig. 1.7 :(a) Simply supported beam
(b) Bending moment diagram
(c) Diagram of stiffness at various beam sections.

1.3 Need for the Study

Rigorous analysis of reinforced concrete members loaded into the inelastic range requires the knowledge of the relationship between moment and curvature. This knowledge is necessary for better evaluation of deflections and the possible redistribution of bending moment after cracking in statically indeterminate reinforced concrete members.

Moment-curvature curves are indispensable for calculating the real stiffness and then deflections of cracked reinforced concrete beams.

In most of the approximate procedures available to compute deflections for un-cracked sections under service loads, linearly elastic stress-strain diagrams are assumed for concrete in compression and tension. For the cracked cross-section, the tensile strength of concrete is often ignored, while the concrete in compression is considered linearly elastic.

These conditions are used to compute the moment of inertia in terms of the ratio K_x for both un-cracked and cracked sections respectively.

The ratio K_x is defined as the distance from the zero strain surface to the extreme fibre in compression

divided by the effective depth.

The bending stiffness of reinforced concrete beams under service loads is considerably smaller than the stiffness calculated on the basis of un-cracked cross-section. Since most concrete sections in a beam are assumed partially cracked, transition values are required between these two extremes limits for deflection calculations. The I-effective method is the most widely accepted of all the approximate methods for computing deflections of partially cracked members under service loads.

In this study, an analytical procedure is developed for obtaining the moment-curvature relationship taking into account the stiffness contribution of tensile concrete and the non-linear characteristics of concrete in tension and compression.

The moment-curvature relationship obtained can predict curvature and deflection beyond the service load range to the ultimate load.

1.2 Aim and Objective

The aim of this research work is to determine theoretically and experimentally the relationship between moment and curvature of reinforced concrete beams taking into account the contribution to stiffness of tensile concrete.

To achieve this aim, the following objectives are set to be pursued.

i) To develop analytical formulae needed for calculating the moments and curvatures. The effect of tensile concrete stiffness is accounted for by using a stress-strain curve for concrete in tension which include a descending branch to account for the effect of progressive cracking and the corresponding decrease in the level of tension in the concrete between the cracks. The curve is approximated into simple shapes namely: rectangle and then triangle having the same slope as the curve for compression at zero stress.

ii) To write a computer program used to solve the formulae to obtain the values of moments and curvatures and to compare the results obtained with previous experiments and theories.

iii) To investigate and confirm through laboratory experiments using rectangular beams, the validity of the theoretical results obtained.

1.3 Scope and Limitations

Moment-Curvature relationship obtained in this research work is limited to rectangular beams.

Flanged cross-section is used to develop all the formulae used in this work. No effort was made to consider other various cases concerning flanged beam. However, only the case for rectangle was solved.

For instance, the positions of neutral axis relative to the flange was not considered. The location of the "ultimate strain" whether within or outside the cross-section was also not considered.

1.4 METHODOLOGY

The work was divided into two main parts namely: the theoretical determination of the moments and curvatures and the laboratory experiments to confirm the theoretical results. The theoretical aspect started with the review of available and relevant literature on the state of the art on the chosen topic. The formulae needed for calculating the moments and curvatures were developed taking into consideration the non-linearities of concrete in both tension and compression.

The formulae needed for calculating the moments and curvatures were developed taking into consideration the non-linearities of concrete in both tension and compression. The stress-strain curve of concrete in compression was assumed to be a second degree parabola. In attempt to obtain the best fit for tensile stress-strain curve of concrete that will give accurate moment-curvature relationship, the tensile stress-strain curve of concrete was approximated to a rectangle in the first trial. The result of this approximation was found to be unsatisfactory.

So another trial was made using bilinear approximation for the stress-strain curve of tensile concrete. These assumptions led to a third degree equation to determine the position of neutral axis according to equilibrium of internal forces.
A computer programme was written to solve the third degree equation to obtain the depth of neutral axis. Having the position of neutral axis, it was possible to calculate the moments and curvatures for an assumed value of the tensile steel strain. In this way and for increasing values of strain in tensile reinforcement, the moment-curvature diagram of the cross section was obtained.

The theoretical results obtained were compared with the experimental results obtained by previous investigators. There was remarkable agreement.
The second part of the work was devoted to laboratory experiments. A total of six reinforced concrete beams were cast and tested. Three of the beams has cross-sectional dimensions of 100mm by 300mm. The remaining three has cross-sectional dimension of 300mm by 100mm. The beams were cast using timber forms. Deformed bars were used for tensile reinforcement for all the beams. The variables are the percentage of reinforcement and diameter of bars for the tensile reinforcement. All the beams were vibrated using kango hammer and left overnight

before they were stripped and left for curing.

Wet jute bags were used for curing the beams. The beams were covered with the bags and watered every morning for 28 days.

Two beams were cast at a time. For each pair, three cubes and three cylinders were cast. The cubes and the cylinders were cured under the same condition as the beams. The cubes were crushed a day prior to testing of the beams to determine the strength of the concrete. In like manner, the cylinders were tested to determine the modulus of elasticity of concrete. The beams were tested at the rate of one beam per day.

Loads were applied using two hydraulic jacks as described in the experimental programme. Cracks were observed with the naked eyes only. The following measurements were taken for each beam at each stage of loadings:

1) Tensile strain at the level of tensile reinforcement with the aid of electrical strain gauges of gauge length 6mm. The gauges were mounted in pairs on the extreme reinforcements in the area of constant bending moment.

2) Concrete strain on the surface of the beams in the region of constant bending moment. Stainless steel discs were glued on the top of the beams using epoxy resin at a gauge distance of 200mm. Stainless steel discs were also glued at 25mm from top and bottom of the beam depth and 75mm from each other at the same gauge distance.

The strains at various levels of the beam depth was measured on one side of the beam using "Demecs" strain gauge as the load was being increased.

3) The deflection of the beam in the region of constant bending moment over a length of 2000mm. This measurement was performed using dial gauges mounted at 500mm interval along the beam length.

The experimental results were analyzed and compared with the theory. There was remarkably good agreement between them. The results obtained theoretically and experimentally were compared and presented graphically in figures 5.19-5.14. The closeness in the values indicate that the theory and the experiment are in good agreement.

A considerably simplified theory for the evaluation of deflection of reinforced concrete beam in a cracked state was proposed in this work. The theory took into account the contribution of concrete in the tensile zone to the stiffness of the cross-section.

CHAPTER-TWO

LITERATURE REVIEW

2.1 The Shape of Stress-Strain Diagram of Concrete:

The instantaneous axial deformation of concrete specimen under load can be described by the stress-strain diagram. For many years, the stress-strain relationship for concrete was generally assumed linear for stresses up to concrete strength, then dropping abruptly to zero stress indicating failure. Many researchers like Richant et al. (1929), Berg et al. (1950), Jones (1952) and Hognestad et al. (1955) have the implied that the shape of the stress-strain curve is related to irreversible cracking of concrete.

Hsu (1963) and Popovics (1969) derived the shape of stress-strain diagram based on the theory of progressive internal cracking. The curve starts with a nearly linear portion that stretches to about 30 per cent of the ultimate load. Beyond this point, the curve deviates gradually from the straight line to the horizontal and then having reached a peak, it ends in a descending tail. Figure 2.1 shows a typical stress-strain curve in compression. This curve corresponds to the results obtained by Brock (1962) and Barnard (1964) in uniaxial compression using stiff constant strain rate testing machine. Balavadze (1959) obtained a similar result from axial tension test of reinforced concrete specimens.

Shah and Winter (1966) noted that in the case of short-time loading, the stress-strain diagram is more curved for concrete than the comparable mortar which, on the other hand, has a more curved diagram than the comparable paste of the same water-cement ratio. Crack propagation usually starts on the interfaces between aggregates and mortar, and then penetrates the mortar causing progressive breakdown and discontinuity in the internal structures of the concrete.

In accordance with this mechanism, Gilkey (1961) reported that for the same mix proportion and identical water-cement ratio, the compressive strength of concrete decreases with increasing size of coarse aggregates in the concrete. He noted that variances in water-cement ratio, curing and age introduces little difference in relative deformations. This however, appears conflicting. Barnard (1964) collaborated this fact. He however added that the size of specimen, location of gauge length for strain measurement are among the important factors that affect the shape of the stress-strain curve of concrete.

2.1.1 Numerical Approximations of Stress-Strain Curves

For many years researchers have tried to adequately represent the stress-strain relationship of concrete using mathematical curves and expressions. Until recently, there has been insufficient experimental or analytical information on the shape of the stress-strain curve beyond the peak stress. Kotsovos (1983) reported that the descending portion of the concrete stress-strain relationship depends very much on the testing technique used.

Accurate knowledge of the descending branch of the concrete stress-strain relationship especially in tension is necessary for us because of its sensitive influence on the shape of moment-curvature curve.

Several investigators have developed empirical expressions mainly from boundary conditions and curve fitting for the numerical approximation of the ascending and descending branches of the stress-strain diagram of concrete. It should be mentioned that the stress-strain relationships obtained from concentric compression are not identical with similar relations obtained by flexure or eccentrically loaded specimens. The peak points of stress-strain curves for eccentric loading are located at higher strains as well as higher stresses than the peak points of corresponding curves for concentric compression.

Some of these formulae taken from literature are summarized as shown in Table 2.1.

Table 2.1 FORMULA FOR THE ASCENDING BRANCH OF STRESS-STRAIN DIAGRAM OF CONCRETE

Source	Formula for axial stress σ_c	Equation No	Inference
Bach	$\sigma_c = C_1 \varepsilon_c^n$	(2.1)	Implies that E_{bo} is infinite
Saenz	$\sigma_c = E_{bo}\varepsilon_c \left[1 + \left(\frac{3E_s}{E_{bo}-2}\right)\left(\frac{\varepsilon_c}{\varepsilon'_c}\right) + \left(1 - \frac{2E_s}{E_{bo}}\right)\left(\frac{\varepsilon_c}{\varepsilon'_c}\right)^2\right]$	(2.2)	
Saenz	$\sigma_c = \frac{E_{bo}\varepsilon_c}{1 + \left(\frac{E_{bo}}{E_s} - 2\right).\frac{\varepsilon_c}{\varepsilon'_c} + \left(\frac{\varepsilon_c}{\varepsilon'_c}\right)^2}$	(2.3)	
European Concrete Committee	$\sigma_c = E_{bo}\varepsilon_c\left(1 - \frac{\varepsilon_c}{2\varepsilon'_c}\right)$	(2.4)	Implies that $\frac{E_{bo}}{E_s} = 2$
Sturman, et al	$\sigma_c = C_2\varepsilon_c(1 + C_3\varepsilon_c^{n-1})$	(2.5)	Implies that $\frac{E_{bo}}{E_s} = \frac{n}{(n-1)}$
Desayi and Kristnan	$\sigma_c = \frac{E_s\varepsilon_c}{1 + \left(\frac{\varepsilon_c}{\varepsilon'_c}\right)^2}$	(2.6)	Implies that $\frac{E_{bo}}{E_s} = 2$
Tulin and Gerstle	$\sigma_c = \frac{E_{bo}\varepsilon_c}{C_4 + \left(\frac{\varepsilon_c}{\varepsilon'_c}\right)^n}$	(2.7)	Implies that $\frac{E_{bo}}{E_s} = C_4 + 1$
Smith and Young	$\sigma_c = E_{bo} e^{\frac{\varepsilon_c}{\varepsilon'_c}}$	(2.8)	Implies that $\frac{E_{bo}}{E_s} = e$

Figure 2.2 compares some of the formula presented in Table 2.1 in terms of relative stress $\frac{\sigma_c}{f'_c}$ and relative strain $\frac{\varepsilon_c}{\varepsilon'_c}$. It can be seen that the curvature of the various diagrams differ considerably. This property can be used for the selection of a suitable stress-strain formula for any given area.

Expressions for the stress-strain diagram of concrete that have mathematical form different from those in Table 2.1 have been proposed by many scientists. They include the following:

Alexander (1965) for the complete stress-strain curve (both ascending and descending branches) proposed:

$$\sigma_c = \frac{B'_1 \cdot \varepsilon_c}{[(\varepsilon_c + B'_2)^2 + B'_3]} - B'_4 \varepsilon_c \quad .... \qquad (2.9)$$

Sinha et al. (1964) proposed the following equation

$$\sigma_c = \left(\frac{A'_1}{X}\right)(\varepsilon_c - X)^2 + A'_2 \quad .... \qquad (2.10)$$

Kriz and Lee (1960) for the purpose of obtaining complete stress-strain curve of concrete in flexure proposed the following expression:

$$\sigma_c^2 + A'_3 \varepsilon_c^2 + A'_4 \sigma_c \varepsilon_c + A'_5 \sigma_c + A'_6 \varepsilon + c = 0 \qquad (2.11)$$

Wang et al. (1978) obtained the following expression for complete stress-strain curve in axial compression:

$$Y = \frac{A'_7 X' + B'_5 X'^{(2)}}{1 + C'_5 X' + D' X'^{(2)}} \qquad (2.12)$$

where $Y = \frac{\sigma_c}{f'_c}$; $X' = \frac{\varepsilon_c}{\varepsilon'_o}$ (2.13)

$E = \frac{f'_c}{\varepsilon'_c}$ = secant modulus of elasticity at peak stress.

X= parameter that defines the number of load repetitions, and strength of concrete.

σ_c= concrete compressive stress.

f'_c= compressive strength of concrete

ε_c= concrete compressive strain

ε'_c= concrete compressive strain at maximum stress.

A'_1 ..... A'_7, B'_1 ..... B'_4, C'_1 ..... C'_5, D' and n } experimental parameters in the equations for stress-diagrams that depend on the composition of concrete, age, curing and testing conditions, etc.

A commonly used expression was proposed by Hognestad (1955)
It consists of two parts: a second degree parabola for the ascending part and a straight line for the descending part.
Figure 2.3 shows Hognestad's stress-strain curve for concrete. In this study, the stress-strain relation of concrete in compression is assumed to be a second degree parabola. This is shown in Figure 2.4.

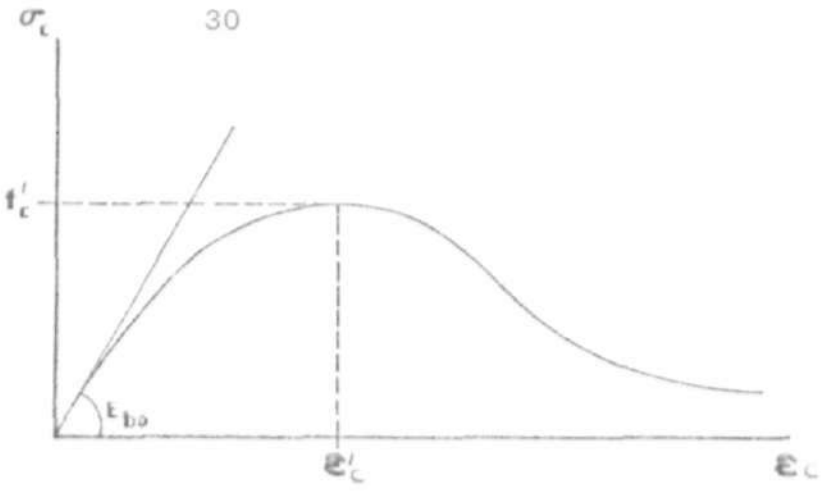


Fig. 2.1 Typical stress-strain curve for concrete in compression.

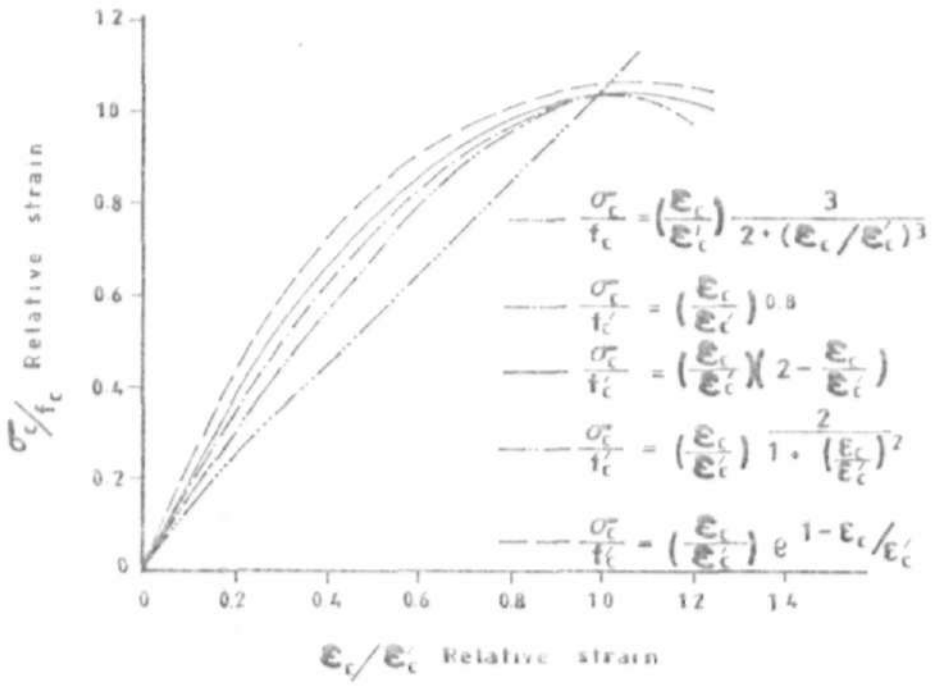


Fig. 2.2. Comparison of several formulae for stress-strain diagram of concrete.

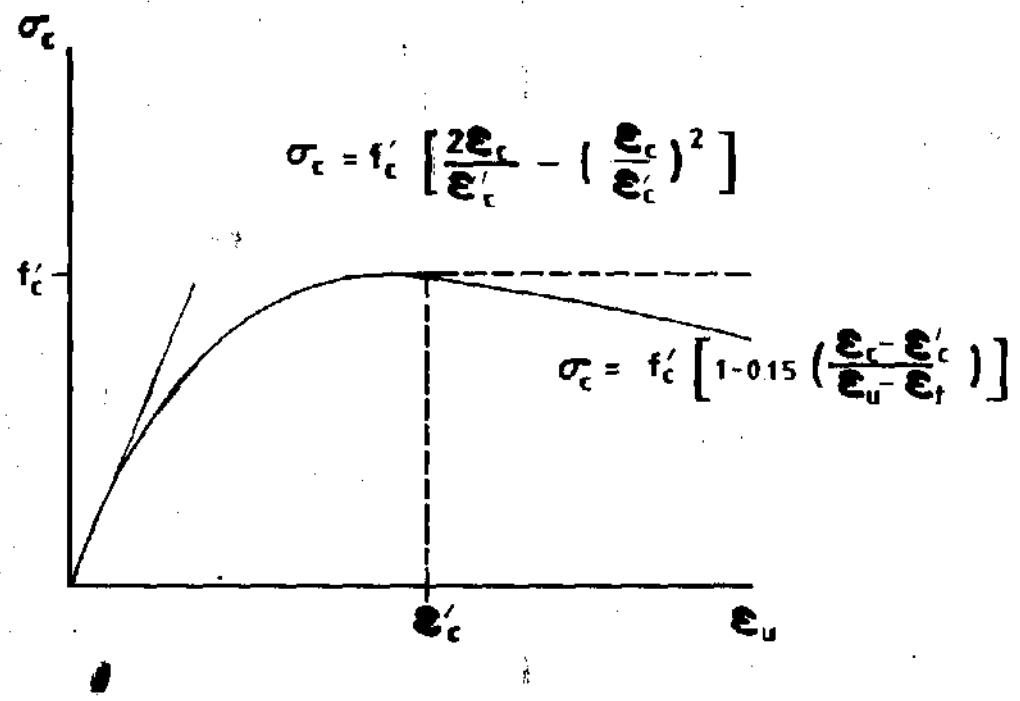


Fig. 2.3. Hognestad stress-strain curve

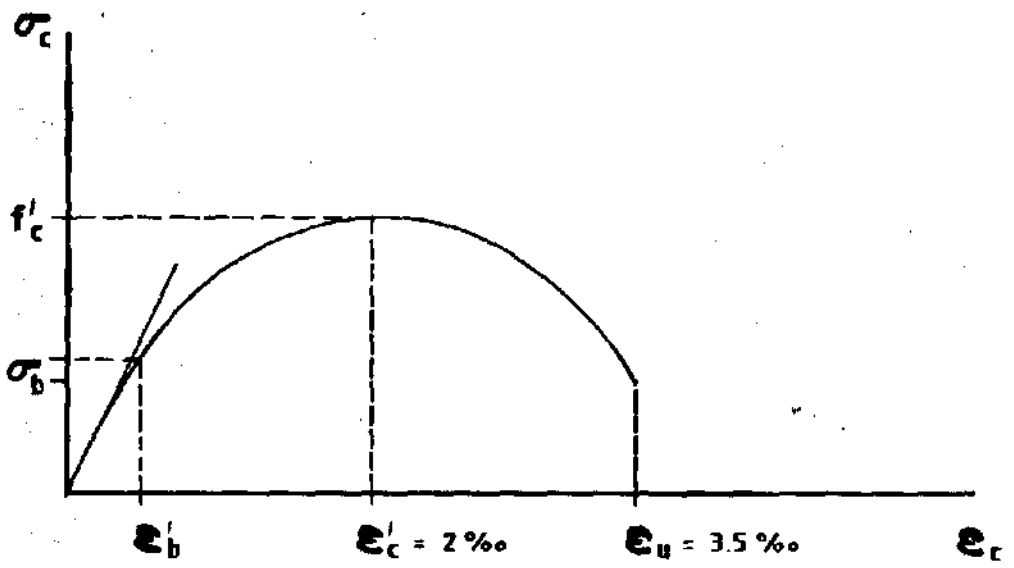


Fig. 2.4. Assumed concrete compressive stress-strain curve.

2.1.2 Tensile Stress-Strain Relationship of Concrete

As mentioned earlier, tensile stress-strain diagram is very important especially the descending branch, because of its influence on the shape of moment-curvature diagrams.

Tensile stress-strain diagram with a descending branch significantly improves the accuracy of calculated deflections compared with deflections calculated from diagrams in which stiffness contribution in tension is neglected.

The shape of concrete stress-strain diagram in tension depends very much on the testing procedure used. McNeedy and Lash (1963) stated that "the term tensile strength and stress-strain relationship in tension have no absolute meanings, but must be expressed in terms of the specific test procedure used".

Three kinds of tests have been used for testing plain concrete in tension: direct tension test, flexural test, and the splitting test. Among the three methods, only direct tension test can provide the complete stress-strain diagram beyond the elastic behaviour of concrete.

When plain concrete is tested in direct tension using a testing machine in which the strain rate cannot be controlled, a linear diagram with a brittle failure is usually obtained. Nonetheless, the non-linear behaviour of plain concrete in tension has been observed experimentally.

Hugh and Chapman (1966), and Evans and Marathe (1968) used modified testing machine to obtain stress-strain diagrams in tension with ascending and descending branches similar to those obtained in compression.

Recent experiments in stiff testing machines by Ahmad and Shah (1982), Carriera and Chu (1986), Gopalaratnam and Surrendra (1985), Shah and Sankar (1987) have shown that the stress-strain diagram of concrete in tension is non-linear and has well defined ascending and descending branches. The curve is also influenced by concrete shrinkage, micro-cracking, concrete strength and reinforcement distribution etc. Clark (1979) established that the stiffness effect of tensile concrete is dependent on the percentage of steel, diameter of reinforcement bars, bond stress, concrete strength and the distribution of reinforcement. Prakhya and Morley (1990) in analyzing the work of Clark (1979), found out that even at strain corresponding to steel yielding, concrete still exhibits 20 to 55 per cent of its maximum tensile capacity. Gilbert et al. (1978) noted that if the effect of tensile concrete is neglected in the calculation of flexural stiffness, deflection may be overestimated by 100 per cent particularly in the serviceability range of loads.

Therefore, the tensile stress-strain relationship used here is taken to be the same as obtained in direct tension tests, and also the same as that which provides good representation of various fracture tests data for concrete. Figure 2.5 shows a typical stress-strain curve for concrete in tension.

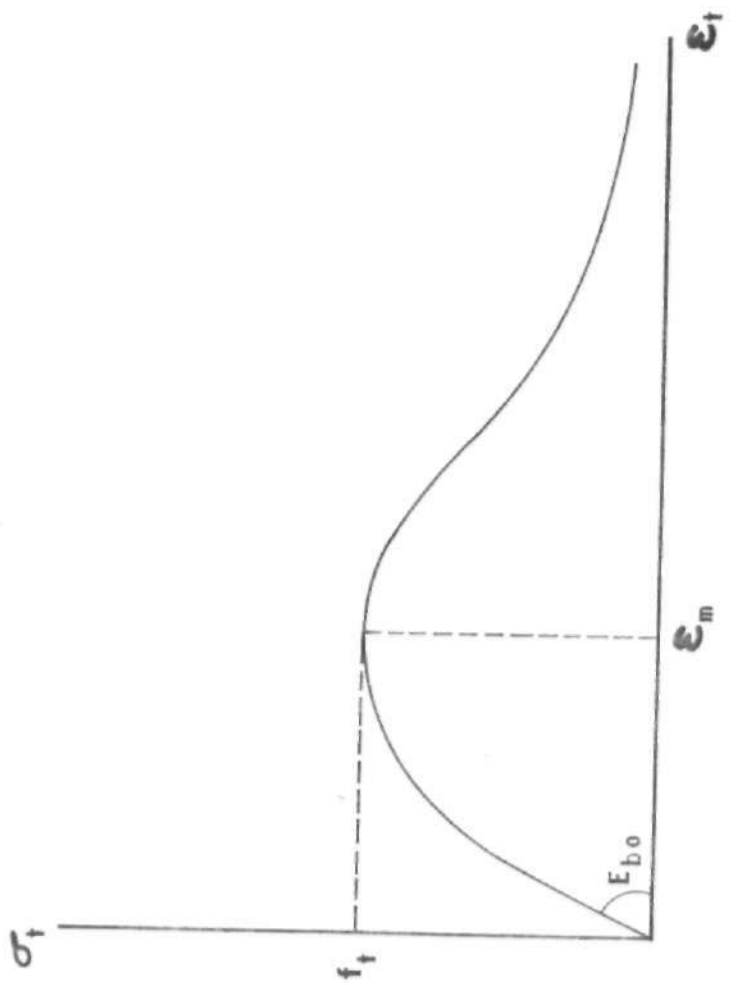


Fig. 2.5. Typical concrete tensile stress-strain curve

2.1.3 Simplified Stress-Strain Curves of Concrete for Obtaining Moment-Curvature Relationship.

Many authors have used several simplifications of the stress-strain curve of concrete in tension to simulate the effect of tensile concrete on the moment-curvature relationship of reinforced concrete sections.

Vebo and Ghali (1977) took into account the contribution of tension stiffening in increasing the average stiffness of reinforced concrete slab compared to the stiffness of a section at which a crack is formed. In their work, the stiffening effect is simulated by approximating the stress-strain relation of concrete in tension as shown in Figure 2.6. The parameters defining the curve are given as follows:

$$\varepsilon_m = 1.2 \frac{f_t}{E_{bo}} \quad \text{.... (2.14a)}$$

$$\varepsilon_1 = 2.1 \frac{f_t}{E_{bo}} \quad \text{.... (2.14b)}$$

$$\varepsilon_{ut} = 11.1 \frac{f_t}{E_{bo}} \quad \text{.... (2.14c)}$$

Where: f_t= tensile strength of concrete

E_{bo}= modulus of elasticity of concrete at the origin of the concrete stress-strain diagram.

ε_{ut}= ultimate tensile strain in concrete

ε_m= concrete tensile strain at maximum stress

Bazant and Oh (1984) approximated the tensile stress-strain curve of concrete into bilinear relationship characterised as follows:

i) For $\varepsilon_t \leq \varepsilon_m$; $\sigma_t = E_o \times \varepsilon_t$ (2.14)

ii) For $\varepsilon_m < \varepsilon_t \leq \varepsilon_u$; $\sigma_t = f_t - (\varepsilon_t - \varepsilon_m)(-E_t)$ (2.15)

iii) For $\varepsilon_t > \varepsilon_u$; $\sigma_t = 0$ (2.16)

The value of E_t is given as follows:

$$E_t = \frac{-70E_{bo}}{57 + f_t} \qquad (2.17)$$

Where E_t- tangent strain-softening modulus.

Carrera and Chu (1986) used a nonlinear stress-strain diagram both in tension and compression to evaluate the moment-curvature relationship of reinforced concrete beams.

Expressions used to describe the complete stress-strain diagram in both tension and compression including ascending and descending branches are given as follows:

$$\sigma_c = \frac{\beta f'_c \left(\frac{\varepsilon_c}{\varepsilon'_c}\right)}{\beta - 1 + \left(\frac{\varepsilon_c}{\varepsilon'_c}\right)^{\beta}} \qquad (2.18)$$

and $$\sigma_t = \frac{\beta f_t\left(\frac{\varepsilon_t}{\varepsilon_m}\right)}{\beta - 1 + \left(\frac{\varepsilon_t}{\varepsilon_m}\right)^{\beta}} \qquad (2.19)$$

where β is the shape factor.

ε_t- concrete tensile strain

σ_c- concrete compressive stress

σ_t- concrete tensile stress.

E_o- modulus of elasticity of steel reinforcement

ε_c- concrete compressive strain.

ε'_c- concrete compressive strain at maximum stress.

Prakhya and Morley (1990) studied the parameters that affects the shaped of the non-linear descending branch of tensile stress-strain curve. They compared the complete stress-strain curve of reinforced concrete in tension to a simple non linear equation similar to that used by Carreira and Chu for plain concrete as follows:

$$\sigma_t = f_t\left(\frac{\varepsilon_{at}}{\varepsilon_m}\right) \text{ if } \frac{\varepsilon_t}{\varepsilon_m} \le 1 \qquad (2.20)$$

$$= \frac{\beta f_t\left(\frac{\varepsilon_t}{\varepsilon_m}\right)}{\beta_t - 1 + \left(\frac{\varepsilon_t}{\varepsilon_m}\right)^{\beta t}} \text{ if } \frac{\varepsilon_t}{\varepsilon_m} > 1 \qquad (2.21)$$

where β_t is related to the diameter of bar, percentage of reinforcement and cover to the reinforcement.

For various values of β_t, the different shapes of relative stress and strain are shown in Figure 2.8.

Based on their findings, Prakhya and Morley used a non-linear approximation to account for the tensile concrete for the purpose of obtaining the moment-curvature relationship.

Maria Kaminska and Artem Czkwianianc (1993) used the approximation shown in figure 2.10 to represent the stress-strain curve of concrete in tension for the purpose of obtaining the moment-curvature relationship.

The compression zone is characterized by the following expressions:

$$\sigma_c = \frac{\beta f_c \left(\frac{\varepsilon_c}{\varepsilon'_c}\right)}{\beta - 1 + \left(\frac{\varepsilon_c}{\varepsilon'_c}\right)^{\beta}} \quad \ldots\ldots \quad (2.21a)$$

where $\beta = \frac{1}{1 - \frac{f'_t}{\varepsilon_c} E_{bo}}$ .... (2.21b)

It should be noted that mere simplification of the tensile stress-strain curve in order to account for the stiffness contribution of tensile concrete does not ensure satisfactory results. The tensile strain corresponding to the maximum tensile stress of concrete and the ultimate strain at which there remains any significant tension stiffening

are among the sensitive parameters that affect the shape of the moment-curvature relationship. In this research work, these parameters were craefully chosen and adjusted until the best fit to experimental results of previous researchers were obtained.

The extent of linear tension-softening is defined by the parameter α,

where $\varepsilon_{ut} = \alpha\varepsilon_m$, and ε_{ut} = ultimate tensile strain in concrete,

ε_m = concrete compressive strain at maximum compressive stress.

Different values of α have been specified by various investigators.

Damjanic and Owen (1984) proposed the value of α between 5 to 10

for shear type cracking and 20 to 25 for flexural cracking. Bazant and Oh (1984) suggested a value given by an empirical expression:

$$\alpha = \frac{E_{to}}{E_t} + 1 \qquad (2.22)$$

where $E_t = \dfrac{0.483E_{to}}{0.393 + f_t}$ (2.23)

E_t - tangent strain-softening modulus

E_{to} - modulus of elasticity of concrete.

f_t - tensile strength of concrete.

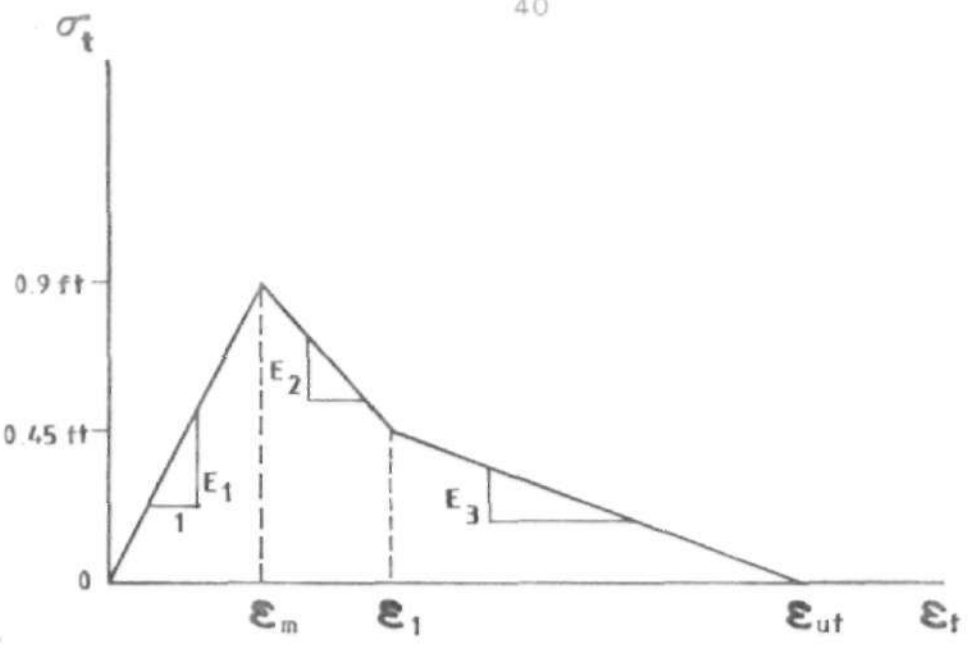


Fig. 2.6. Approximation of tensile stress-strain curve by Vebo and Ghali .

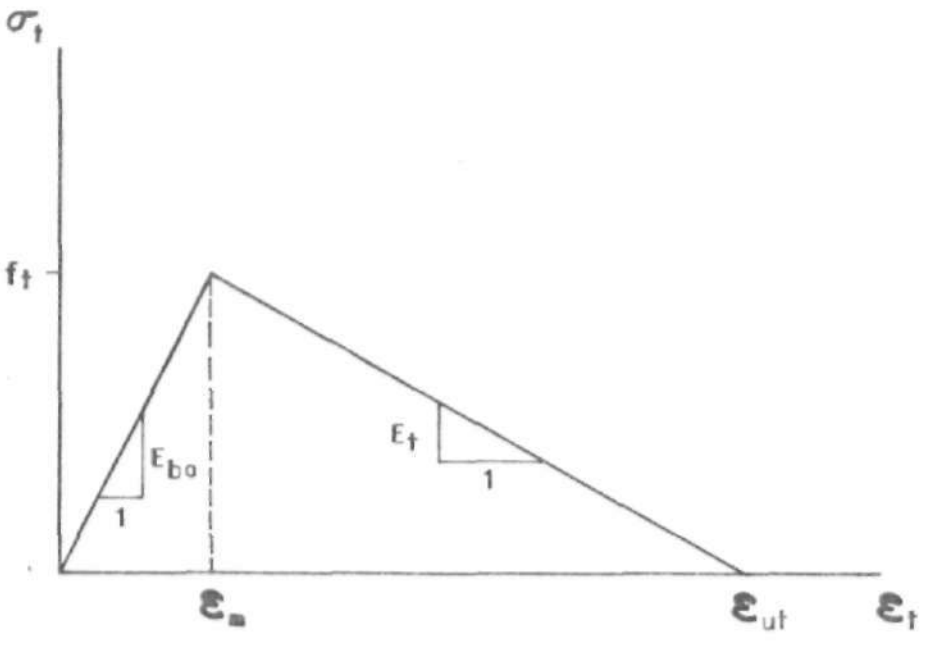


Fig. 2.7. Approximation of tensile stress-strain curve by Bazant and Oh.

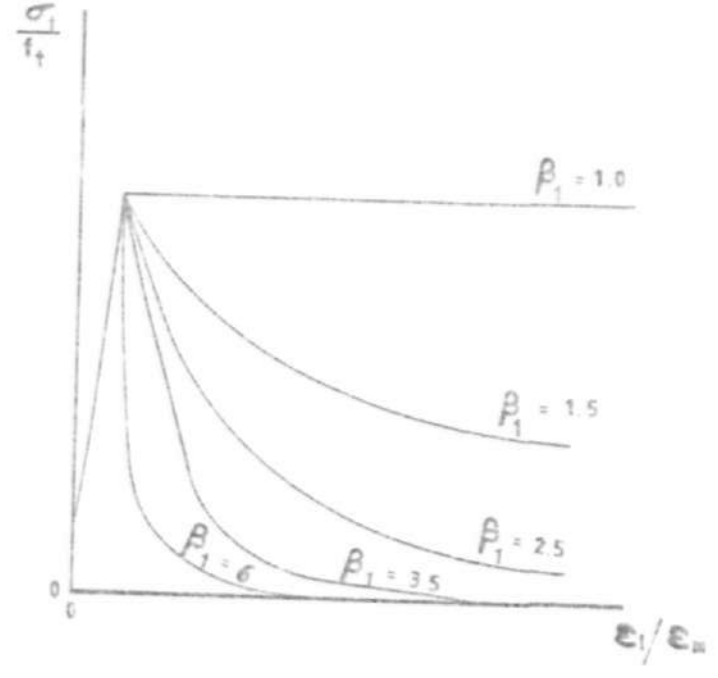


Fig. 2.8. Representive tensile concrete stress-strain curves of concrete component by Prakhya and Morley.

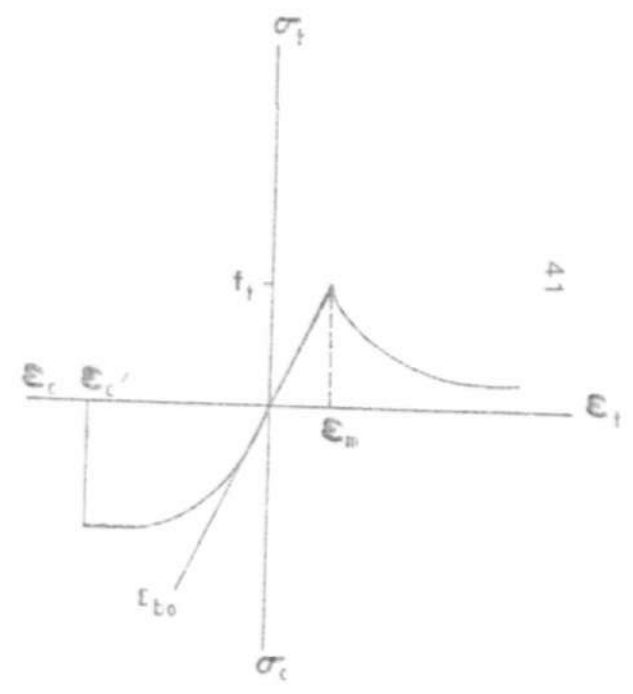


Fig. 2.9. Stress-strain relationship adopted by Prakhya and Morley.

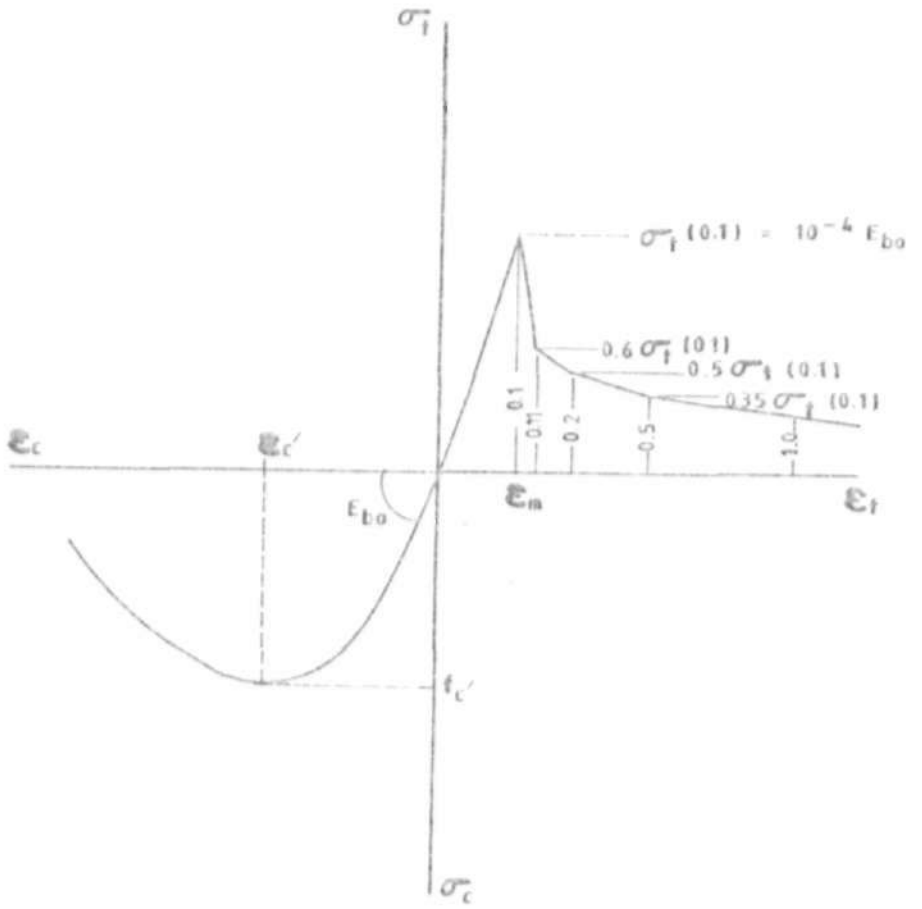


Fig. 2.10. Stress-strain relationship used by Kaminska and Czkwianiane (1993).

2.1.4 Concluding Remark on Stress-Strain Relationship

Having carefully analyzed the state of the art of concrete stress-strain relationship, one can safely remark as follows: that all the analytical equations and the various mathematical shapes used to represent the stress-strain curves of concrete are complicated and difficult to use for any analytical and practical purposes. For this reason, several simplifications have been used to represent the stress-strain curves both in tension and compression as has been shown in the earlier examples.

Therefore, for the purpose of this research work, the stress-strain curve of concrete in compression is assumed a second degree parabola (Figure 2.4). The tensile stress-strain relationship is simplified as a rectangle in the first trial, then a triangle: Figures 3.2 and 3.3.

2.2 Moment-Curvature Relationship

The real stiffness of cracked cross-section is in fact an average of the properties between the uncracked and fully cracked concrete between the cracks. This phenomenon as mentioned earlier is attributed to the fact that concrete does not crack suddenly and completely but undergoes progressive microcracking. This description is shown in Figure 2.11. As early as 1917 in Germany, Bach and Graf conducted extensive experimental investigations on reinforced concrete beams for the purpose of obtaining the relationship between moment and curvature.

Monnier (1970) investigated the moment-curvature relationship both theoretically and experimentally. In his theoretical considerations, he assumed concrete to have zero tensile capacity which results in underestimation of the flexural stiffness. He derived empirical expressions for calculating the depth of neutral axis of cracked cross-section hence moment-curvature relationship.

The expression which is based on parabolic stress-strain curve of concrete in compression is as follows:

$$-K_x^3\left(3 + \frac{\varepsilon_{ac}}{\varepsilon'_c}\right) + 3K_x^2(1 - 2n_o\omega) + 12K_x n_o\omega - 6n_o\omega - 0 \qquad (2.24)$$

where $n_o = \frac{E_s}{E_{bo}}$ and $E_s = \frac{\varepsilon'_c}{2\sigma_s}$ (2.25)

K_x - constant which defines the depth to the neutral axis.

ε_{ac} - strain at the commencement of yielding of tensile reinforcement

n_o - modular ratio.

ω - tensile steel ratio.

The stress and strain distribution adopted by Monnier is shown in Figure 2.12. Equation 2.24 is a third degree equation in ' K_x ' which was fully solved in Chapter Three of this work.

The moment-curvature curve was idealized into trilinear curve by Monnier (1970) in order to obtain expression for the flexural stiffness of the cracked section $(EI)_g$. See Figure 2.13. From the Figure, we can write that:

$$(EI)_g = \frac{M_y - M_{cr}}{\frac{M_y}{(EI)_{gc}} - \frac{M_{cr}}{(EI)_o}} \qquad (2.26)$$

Monnier also proposed empirical expressions for calculating the stiffness in the uncracked state $(EI)_o$ and the cracking moment M_{cr}.

$$(EI)_o = E_{bo} I_{bo} \qquad (2.27)$$

where $E_{bo} = (\frac{1}{3}\sigma'\omega + 200).10^5 \ kN/mm^2$ (2.28)

$$M_{cr} = f_t W_{bo} \qquad (2.29)$$

where $f_t = \frac{1}{2}\left(\frac{1}{20}f'_{cu} + 10\right) \ kg/cm^2$ (2.30)

The stiffness of the fully cracked section follows from the relation:

$$(EI)_{gc} = \frac{M_y}{\kappa_y} = \frac{M_y}{\frac{\varepsilon_{cc}}{h(1 - K_x)}} \qquad (2.31)$$

$$M_y = \omega\, \sigma_{sy}\, B_o\, h^2 \left[1 - \frac{4 - \frac{\varepsilon'_b}{\varepsilon'_c}}{4\left(3 - \frac{\varepsilon'_b}{\varepsilon'_c}\right)} \cdot K_x \right] \qquad (2.32)$$

$$(EI)_{cr} = \omega\, E_s\, B_o\, h^3\, (1 - K_x) \left[1 - \frac{4 - \frac{\varepsilon'_b}{\varepsilon'_c}}{4(3 - \frac{\varepsilon'_b}{\varepsilon'_c})} \right] \qquad (2.33)$$

where M_y- yield moment

I_{bo}- moment of inertia of uncracked cross-section

M_{cr}- cracking moment

W_{bo}- section modulus of uncracked cross-section

$(EI)_{cr}$- bending stiffness of fully cracked section

σ_{sy}- yield stress of tensile reinforcement

κ_y- yield curvature

h- effective height of the beam

f_w cube strength of concrete.

In Monnier's experimental investigations, nine reinforced concrete beams of cross-sectional dimensions 250mm by 290mm were tested. Reinforcement percentage was varied from 0.22 per cent to 1.5 per cent. Results obtained from his measurements were compared with his theory. Good agreement was achieved. It was however difficult to adopt without verifications the results of his measurements because they were present with very small scales.

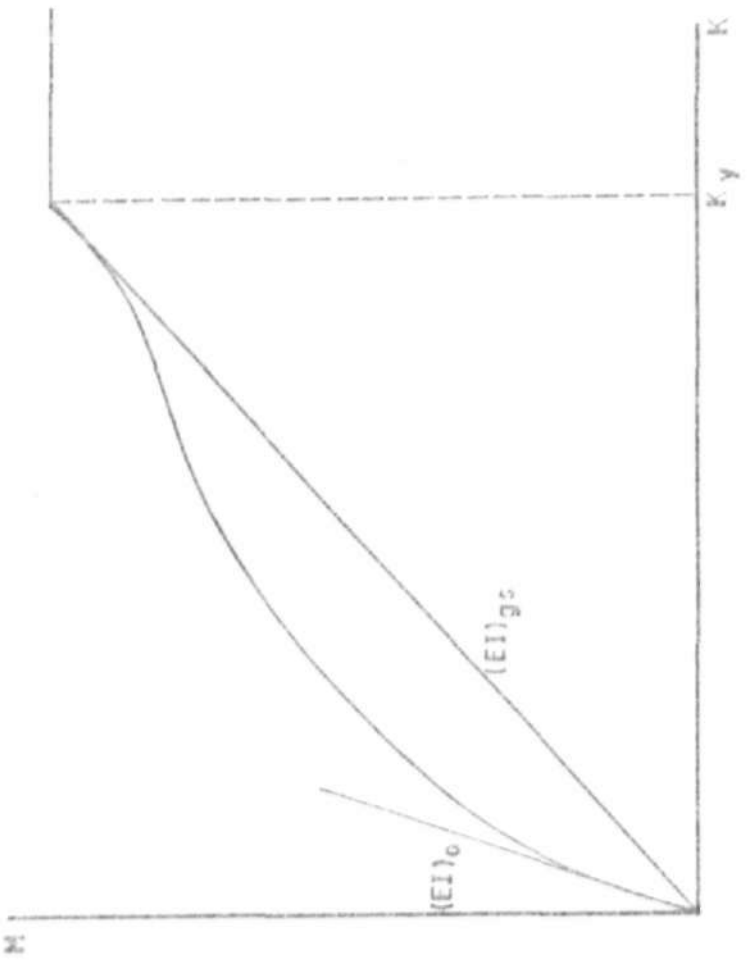


Fig. 2.11 Typical M-K curve showing influnce of tensile concrete .

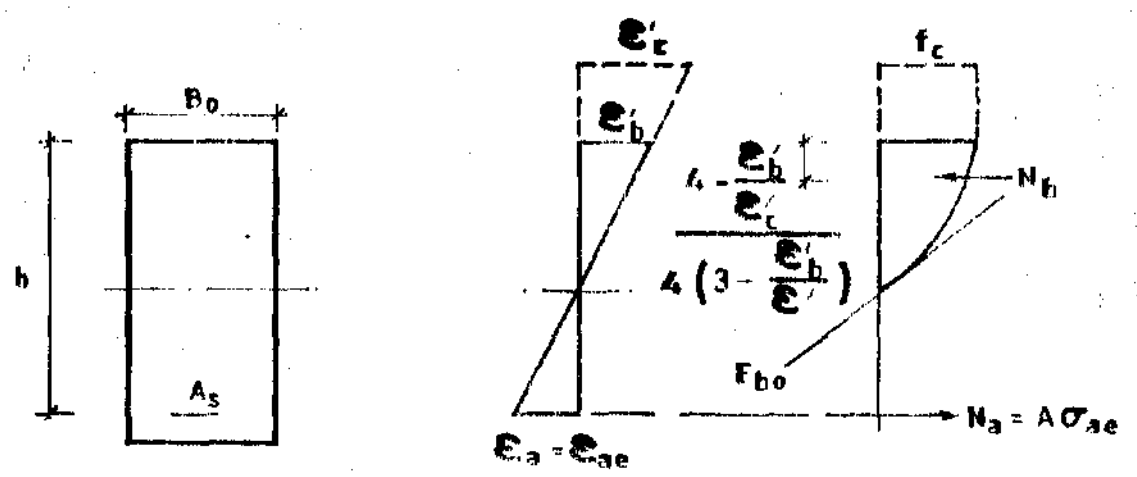


Fig. 2.12 Strain and stress distribution adopted by Monnier .

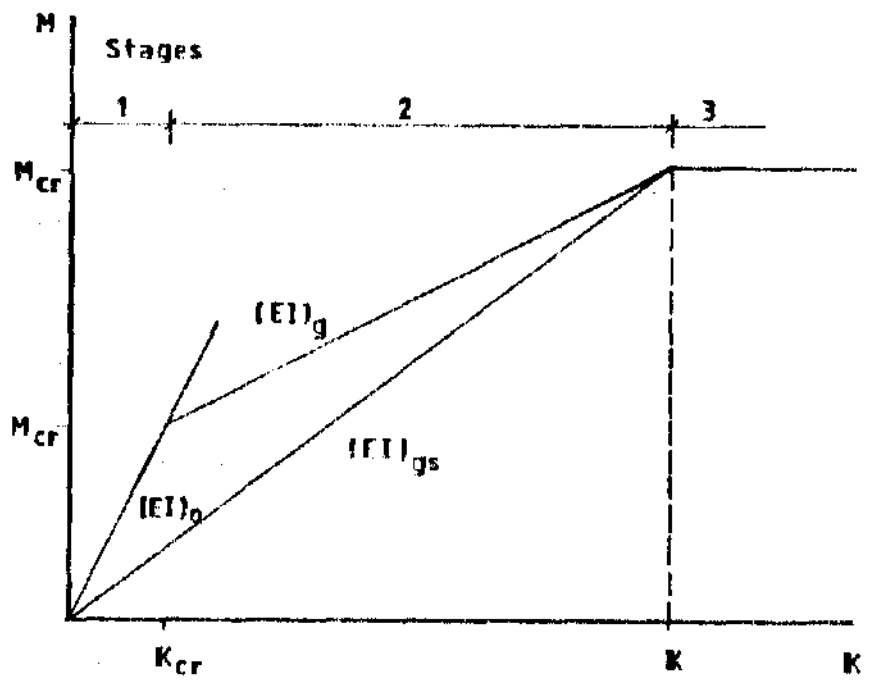


Fig. 2.13 Monnier's idealized M-K diagram.

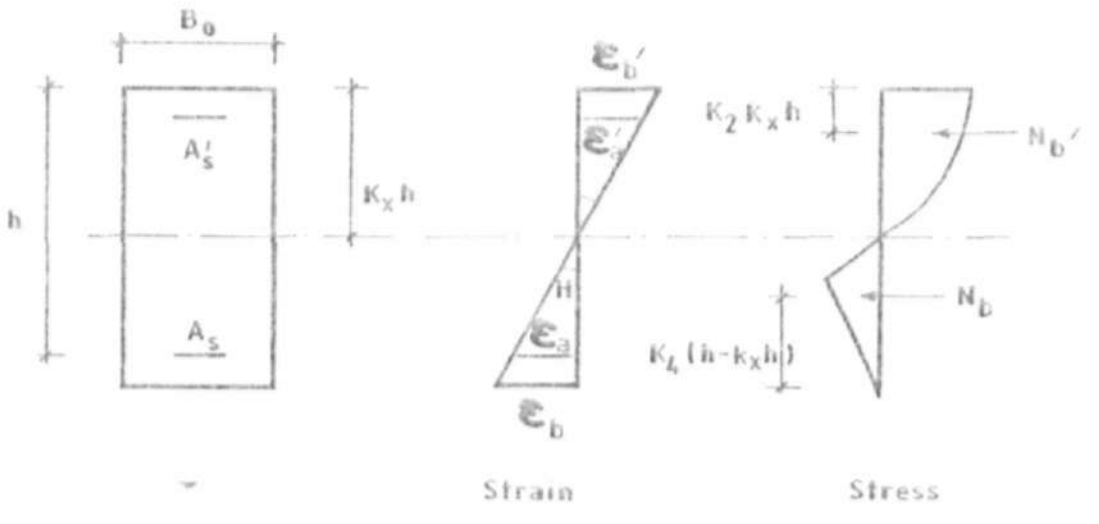


Fig. 2.14. Stress-strain distribution adopted by Bazant and Oh.

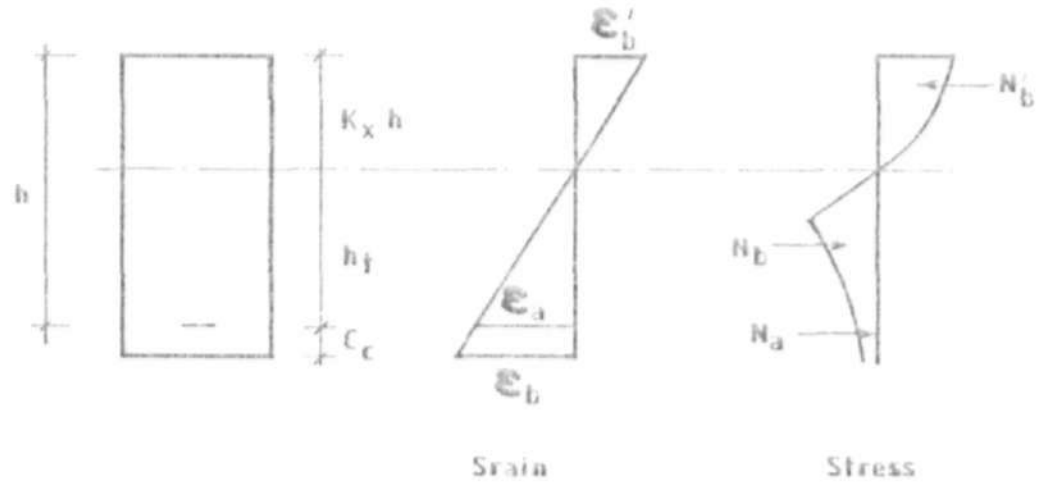


Fig. 2.15. Stress-strain distribution adopted by Prakhya and Morley.

Bazant and Oh (1984) obtained moment-curvature theoretical relationship for rectangular beams. The tensile stress-strain curve was approximated as shown in Figure 2.7 for the purpose of accounting for the stiffness contribution of tensile concrete.

The stress-strain distribution adopted for calculating the moment and curvature is shown in Figure 2.14.

From conditions of equilibrium, moment due to stress block about the neutral axis may be written as follows:

$$M = K_1 f_c B_o K_x h \left(\frac{h}{2} - K_2 K_x h\right) + \sum_{i=1}^{2} \sigma_{si} Ai \left(\frac{h}{2} - di\right)$$

$$+ K_3 f_t B_o (h - K_x h) \cdot \left[\frac{h}{2} - K_4 (h - K_x h)\right] \qquad (2.34)$$

where $K_1 = \int_0^{\varepsilon'_b} \frac{\sigma_c \, d\varepsilon_c}{f_t \varepsilon'_b}$, and (2.35)

$d\varepsilon_c$ - infinitesimal compressive strain

ε'_b - concrete strain at extreme compressive fibre

f_c - concrete compressive strength

B_o - breath of the beam

f_t, ε_c *and* h - are as previously defined.

$$K_2 = 1 - \frac{\int_0^{\varepsilon'_b} \varepsilon_c \sigma_c \, d\varepsilon_c}{\varepsilon'_b \int_0^{\varepsilon'_b} \sigma_c \, d\varepsilon_c} \qquad (2.36)$$

$$K_3 = \frac{\int_0^{e'_b} \sigma_c . de_c}{f_r e'_b} \qquad (2.37)$$

$$K_4 = 1 - \frac{\int_0^{e'_b} e_c . de_c}{e'_b \int_0^{e'_b} \sigma_c . de_c} \qquad (2.38)$$

Knowing the stress-strain curve of concrete in compression, values of K_1, K_2, K_3 and K_4 can be obtained. The curvature of the neutral axis is given by the formula

$$\kappa = \frac{e'_b}{K_x h} \qquad (2.39)$$

Bazant and Oh (1984) compared the results of their theory with the tests by Sinha, Gerstle and Turlin (1964). The theory was found to be in good agreement.

Prakhya and Morley (1990) used the same procedure as Carriera and Chu (1986). Both of them used non-linear approximation of tensile stress-strain curve for the purpose of accounting for the stiffness contribution of tensile concrete.

The stress and strain distribution for calculating the moment-curvature relationship is as shown in Figure 2.14. From equilibrium of forces we may write that:

$$N'_b + N_b + N_a = 0 \tag{2.40}$$

Taking moment about neutral axis we have:

$$M_{cc} + M_{ct} + M_a - M_x = 0 \tag{2.41}$$

$$N'_b = \sigma'_{bu} B_o K_x h \gamma_c; \quad \gamma_c = \frac{1}{\eta_c} \int_0^{\varepsilon'_b} \sigma_c \varepsilon_c d\varepsilon_c \tag{2.42}$$

$$N_b = f_t B_o (h_t + c_o) \gamma_t; \quad \gamma_t = \frac{1}{\eta_t} \int_0^{\varepsilon'_b} \sigma_t \varepsilon_c d\varepsilon_c \tag{2.43}$$

$$N_a = \sigma_a(\varepsilon_a) A_s; \quad M_a = N_a(h - K_x h) \tag{2.44}$$

$$M_{cc} = \sigma_{bu} B_o (K_x h)^2 \xi_c; \quad \xi_c = \left(\frac{1}{\eta_c}\right)^2 \int_0^{\varepsilon'_b} \varepsilon_c \sigma_c d\varepsilon_c \tag{2.45}$$

$$M_{ct} = f_t B_o (h_t + c_o)^2 \xi_t; \quad \xi_t = \left(\frac{1}{\eta_t}\right)^2 \int_0^{\varepsilon'_b} \varepsilon_c \sigma_c d\varepsilon_c \tag{2.46}$$

where: $\eta_c = \dfrac{\varepsilon'_b}{\varepsilon'_c}$

and $\eta_t = \dfrac{\varepsilon_b}{\varepsilon_m}$ (2.47)

M_a- moment due to tensile steel about the neutral axis

M_{cc}- moment due to compressive concrete

M_{ct}- moment due to tensile concrete

N_b *and* N'_b- resultant tensile and compressive force in concrete respectively

N_a- resultant steel tensile force

By iterating numerically, the values of ε_b , γ_c and γ_t are calculated. Values of N'_b and N_b are computed using equations (2.42) and (2.43). These values are substituted in equation (2.49) from which K_x is evaluated. Having found K_x , the value of curvature may be calculated using the equation:

$$\kappa = \frac{\varepsilon'_b}{K_x h} = \frac{\varepsilon_b}{h(1 - K_x)} \qquad (2.48)$$

Where:

ε'_b , ε_b , K_x and h are as previously defined.

The two-zone non-linear model proposed by Prakhya and Morley (1990) seek to use the actual behaviour of concrete in both tension and compression to obtain a precise moment-curvature relationship. This was however not the case. The accuracy of the results they obtained was not higher than those of other investigators with simpler approximations. Moreover, there is no direct solution to the non-linear equation which was used to represent the stress distribution in the section. Solutions were found only through numerical procedure using successive approximations.

Alwis (1990) like Monnier used the trilinear curve to represent the moment-curvature relationship whereby the uncracked, cracked and yield behaviours are depicted as linear segments. Behaviour after yielding of tensile reinforcement was assumed to be perfectly plastic; as

a result, only two co-ordinate points are required to define the curve, Figure 2.16.

Idealization, however, does not reflect the true nature of moment-curvature curve. As mentioned earlier, the first branch of the curve is related to the uncracked concrete. At the cracking moment M_{cr} ,

the influence of crack formation becomes noticeable.

Since micro cracking is a continuous process, no exact value of bending moment can be assigned to its formation hence the first branch smoothly shades into the second branch. The main advantage of the trilinear moment-curvature relationship is its simplicity when compared to deflection analysis using numerical methods.

Alwis compared the moment-curvature curves derived using Branson's (1967) formula and that obtained by Bazant and Oh previously mentioned with those produced by the trilinear model. He observed good agreement among these models, especially in the serviceability range of loads.

An empirical formula for calculating the effective bending stiffness of cracked reinforced concrete sections under service loads was proposed by Branson (1963, 1977). The formula was found to conform adequately to the various test results also published by Branson (1983). The formula which has been endorsed by ACI Committee 318-83 for estimating deflection is as follows:

$$(EI)_{eff} = (EI)_{ge} + [(EI)_{o} - (EI)_{ge}]\left(\frac{M_{cr}}{M}\right)^{3} \qquad (2.49)$$

where:

$(EI)_{ef}$ - effective stiffness of the cross-section

M - applied bending moment

M_{cr} - cracking moment

$(EI)_{cr}$ - bending stiffness of fully cracked section

$(EI)_{e}$ - bending stiffness of uncracked section

This is the most widely accepted of all the approximate methods for computing deflections of cracked members under service loads.
A bilinear moment-curvature curve for use in estimating service load deflections of reinforced concrete slabs was proposed by Rasheidat (1986). In his model, the tangent stiffness of the section after cracking is assumed equal to the stiffness of the fully cracked section. The model however, is not intended for beams or at higher load levels.

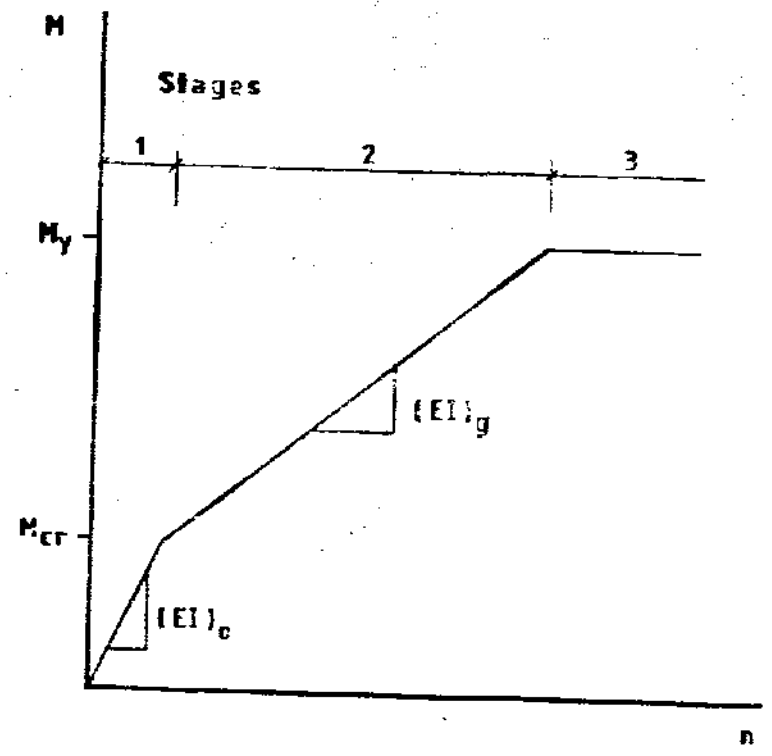


Fig. 2.16. Trilinear approximation of moment-curvature relationship by ALWIS.

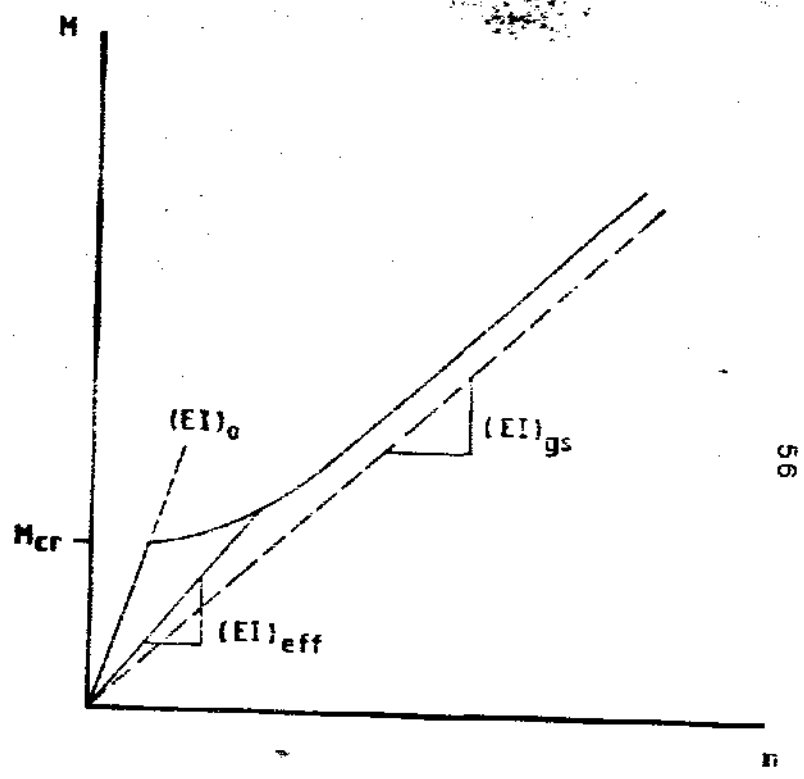


Fig. 2.17. Branson's moment-curvature relationship for calculating Ieff.

2.2.1 Codes Provisions for Beam Deflections

The Nigerian Standard Code of Practice NCP1 1973 Part I gives three methods of calculating instantaneous deflections in Sections 3.10.1 to 3.10.3

I) The application of Elastic Theory using second moments of area, based on the area of concrete in compression, together with the transformed areas of reinforcement.

ii) The application of Elastic Theory using an effective second moment of area as defined below:

$$I_{eff} = \left(\frac{M_{cr}}{M_{max}}\right)^3 I_g + 1 - \frac{(M_{cr})^3}{M_{max}} \qquad (2.50)$$

where $M_{cr} = \frac{f_r I_g}{y_t}$ (2.51)

I_{eff} = Effective Second Moment of Area

M_{cr} = Moment of Cracking

M_{max} = Maximum Bending Moment

I_g = Gross Second Moment of Area

f_r = Modulus of Rapture

y_t = Distance from centroidal axis to top fibre of beam

iii) The application of a rigorous theory based on appropriate moment-curvature relationships.

The first method is quite appropriate for uncracked cross-sections. The third method is exactly what the current research is all about.
Concerning the second method however, the following remarks can be made. The formula consists of three components, the units of which are not the same. While the first component is in the unit of stiffness, the third component is in the unit of moment squared. In view of this, the components are not "addable".
Moreover, the formula does not contain any variable moment, since the applied variable bending moment, M is not reflected in the formula. The cracking moment, M_{cr} and the maximum bending moment M_{max} are constant values, hence the I_{eff} as given by the formula is just for a particular point on the beam. It might be that the authors of the Nigerian Standard Code of Practice intended to quote the Branson's formula, but with these shortcomings, it is far from it.
The provisions for calculating beam deflections are stated in the CP 110: Part 1: 1972 Section 3.3.8. This Code generally recommends that deflection of any part of the structure should not adversely affect the appearance or efficiency of the structure. The permissible deflections in beams are given in terms of span/effective depth ratios.

These ratios are themselves modified by factors which are dependent upon the percentage of compression steel, the percentage of tension steel and its state of stress under working load. Initial design for stiffness is not possible on this basis.

CHAPTER-THREE

3.0 Theoretical Considerations

3.1 Assumptions

In order to develop the formula required for flexural stiffness (moment-curvature relationship) of reinforced concrete section, the following assumptions were made:

1. Plane sections initially normal to zero strain surface remain plane and normal to it at any bending stage.
2. Strain distribution across reinforcing bars is considered uniform and equal to the strain corresponding to the centroid of each bar.
3. Perfect adhesion exists between the concrete and steel reinforcement. Deformation of the materials does not break the bond between them.
4. The complete stress-strain relationships of the concrete and steel reinforcement in tension and in compression are known. The stress-strain relationship of concrete in compression is assumed a second degree parabola. This is as shown in Figure 2.4.
   The tensile stress-strain relationship is shown in Figure 2.5.

The stress-strain relationship for steel is assumed to be linearly elasto-plastic (without strain hardening). This assumption is made for the purpose of this research work.

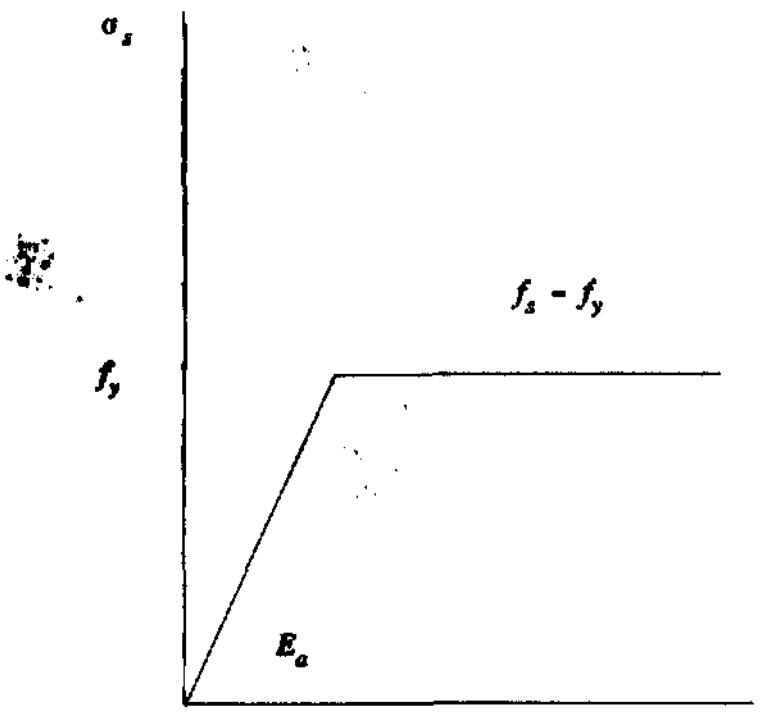


Figure 3.1 Idealized stress-strain diagram for reinforcing steel

Contribution to stiffness by concrete in the tensile zone was taken into account. This was done using the stress-strain curve of concrete in tension which includes strain-softening to account for the effect of progressive cracking and the decrease in tension in the concrete in-between cracks. To realise this, the stress-strain curve is approximated into simple shapes: the first trial was a rectangle, and then a triangle having the same shape as the curve for compression concrete at zero stress. In Figures 3.2 and 3.3 are shown the rectangular and triangular approximations.

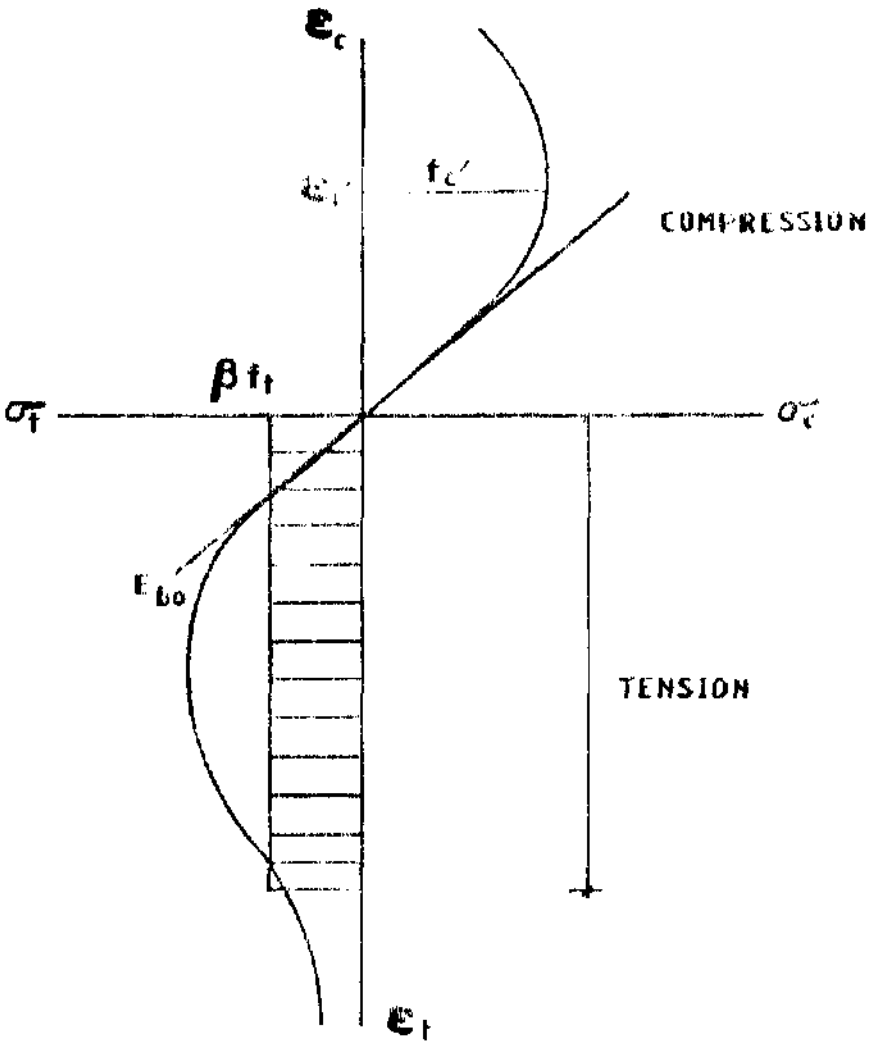


Fig. 3.2. Stress-strain curve of concrete showing rectangular approximation of tensile zone

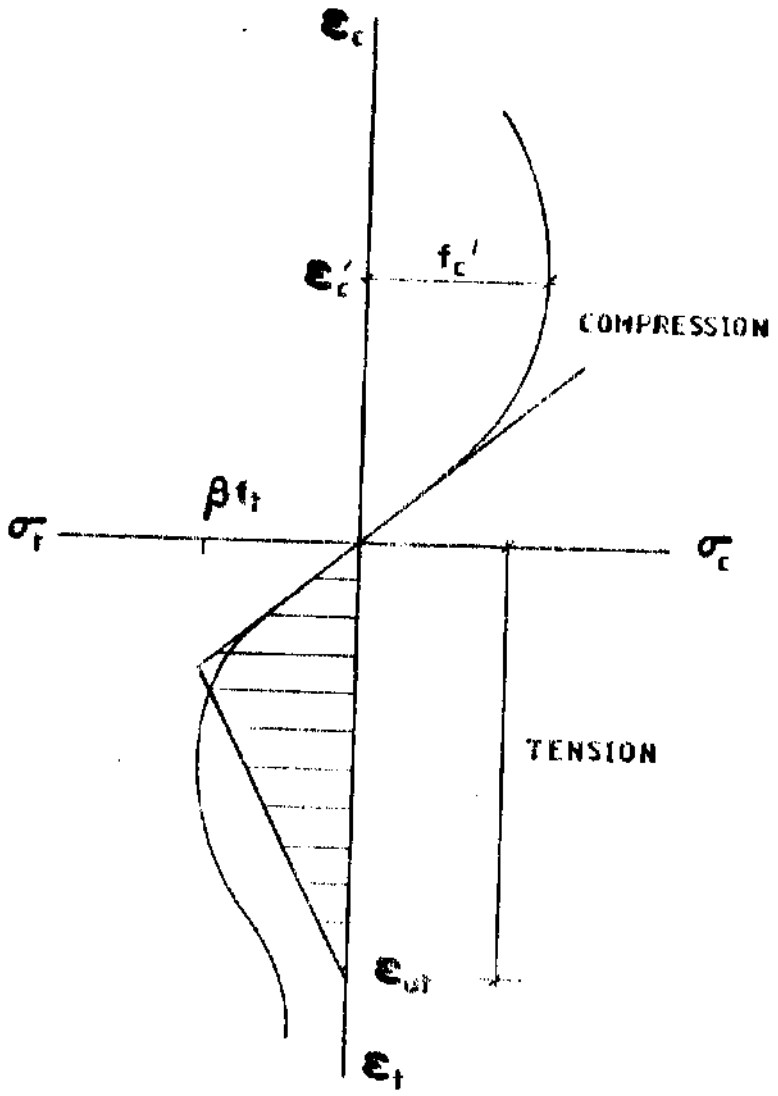


Fig. 3.3. Stress-strain curve of concrete showing triangular approximation of tensite zone.

3.2 Derivation of Formulae for Calculating Moment-Curvature Relationship

The formulae derived are based on the equations already obtained by Monnier (1970). He developed expressions for calculating the neutral axis depth, the resisting bending moments and the curvatures. In his work, however, the contribution to stiffness of tensile concrete was neglected.

The formulae were derived for a general case: a cross-section of a flanged beam with both tensile and compression reinforcement. The steel strain is given a value and from relations between the deformations and from equilibrium of forces, the depth of the neutral axis can be found. After the determination of the neutral axis depth, it is possible to calculate all strains, stresses, moment and curvature.

In this way, and for increasing values of steel strain, the moment-curvature relationship of a cracked reinforced concrete beam is obtained.

3.2.1 Formulae for Calculating M-x Relationship Neglecting the Contribution of Tensile Concrete

From Figure 3.4, since the deformations are directly proportional to their distances from the neutral axis we can write that:

a) $$e'_c = e_a \cdot \frac{K_x}{1 - K_x} \quad \text{or} \quad \frac{e'_b}{e'_c} = \frac{e_a}{e'_c} \cdot \frac{K_x}{1 - K_x} \qquad (3.1)$$

b) $$\frac{\varepsilon_{bh}}{\varepsilon'_c} = \frac{\varepsilon_a}{\varepsilon'_c}.\frac{K_x - K_{ho}}{1 - K_x} = \frac{\varepsilon'_b}{\varepsilon'_c}.\frac{K_x - K_{ho}}{K_x} \quad (3.2)$$

c) $$\varepsilon'_a = \varepsilon_a.\frac{K_x - K'_d}{1 - K_x} = \varepsilon'_b.\frac{K_x - K'_d}{K_x} \quad (3.3)$$

where:

$$K'_d = \frac{K'_d.h}{h} \quad (3.4)$$

$$K_x = \frac{K_x.h}{h} \quad (3.5)$$

$$K_{ho} = \frac{K_{ho}.h}{h} \quad (3.6)$$

Concrete compressive stress:

$$\frac{N_b}{B_o\,h} = \frac{1}{3}.\frac{\varepsilon_a}{\varepsilon'_c}.\frac{K_x}{1 - K_x}.\left(3 - \frac{\varepsilon_a}{\varepsilon'_c}.\frac{K_x}{1 - K_x}\right).K_x.f'_c$$

$$-\frac{a}{3}.\frac{\varepsilon_a}{\varepsilon_c}.\frac{K_x - K_{ho}}{1 - K_x}.\left(3 - \frac{\varepsilon_a}{\varepsilon'_c}.\frac{K_x - K_{ho}}{1 - K_x}\right)$$

$$.(K_x - K_{ho}).(1 - K_{ho}).f'_c \quad (3.7)$$

$a = 0$ if $K_x \leq K_{ho}$ (3.8a)

$a = 1$ if $K_x > K_{ho}$ (3.8b)

Where K'_d- constant which defines cover to compressive reiforcement

K_x- constant which defines the depth to the neutral axis of the beam

K_{ho}- constant which defines the flange depth of the beam

As a consequence of parabolic stress-strain diagram, we have

r - i i . (3.10)

Substituting equation (3.9) in (3.8) and re-arranging we obtain:

$$\frac{K}{*_{„} *} \quad \frac{a_{.}}{fc/1 \quad - Kf} \quad [-((3 \cdot r_{„}) - o(l - *J(3 \cdot r,»J\$$$$+ 3[1 - «(1 - KJil \cdot JTJ2 \cdot rjnJC?$$$$\cdot 3 \; a \; JCJ1 - Kj\2 + KJ1 \; t \; r_a)|Jt,$$$$- « < (1 - KJ(? + *_{to} . rj[\qquad (3.11)$$

Compressive force in top reinforcement

Assuming the steel grades of the tensile and compressive reinforcement are the same and using equation (3.3) we have:

$$-JL-Vo \quad \frac{N*_m \quad . \quad n - l \; K - K_d}{Bh \quad * \quad ir \quad 1 - K} * \qquad (3.12)$$

where:

$$»_{rt} - \frac{£_*}{—} \quad \text{and}$$

n_0 - modular ratio

E_a **and** *Efo* - modulus of elasticity of steel and concrete respectively

N_a *and* N'_a - resultant steel tensile and compressive force

K_{br} - constant which defines the breath of beam web

ω' - compressive steel ratio

σ_{ac} *and* B_o - are as previously defined

This equation is valid only if $\varepsilon_a < \varepsilon_{ac'}$. The other case, $\varepsilon'_a \geq \varepsilon_{ac}$ will not normally occur before the tensile reinforcement yield and under that circumstance, where both tensile and compressive reinforcement yield:

$$\frac{N'_a}{B_o\, h} = \omega'.\frac{n_o - 1}{n_o}.\sigma_{ac} \qquad (3.13)$$

The equations (3.12) and (3.13) are summarised in one equation as follows:

$$\frac{N'_a}{B_o\, h} = \frac{\sigma_a}{6n_o(1 - K_x)^2}\left[\frac{\omega'(n_o - 1)(K_x - K_d).6n_o(1 - K_x)^2}{n_o.(1 - K_x)}\right] \qquad (3.14)$$

$$\frac{N'_a}{B_o\, h} = \frac{\sigma_a}{6n_o(1 - K_x)^2}\left[6(n_o - 1)\omega'\left\{l_1K_x^2 + l_2K_x^2(1 - K_d) - l_3K_d\right\}\right] \qquad (3.15)$$

In which $l_1 = l_2 = l_3$ *if* $\varepsilon'_a < \varepsilon_{au}$ and

$$\left.\begin{aligned} l_1 &= -1 \\ l_2 &= -\frac{2}{1 + K_d} \end{aligned}\right\} \text{if} \quad \varepsilon'_a \geq \varepsilon_{au}$$

$$\left.\begin{aligned} l_3 &= -\frac{1}{K_d} \end{aligned}\right\} \text{in that case} \quad \sigma_a = \sigma_{au} \qquad (3.16)$$

Tensile force in bottom reinforcement

This force is equal to:

$$\frac{N_a}{B_o\, h} = \omega \sigma_a \qquad (3.17)$$

Providing the same denominator as in equation (3.15) we obtain:

$$\frac{N_a}{B_o\, h} = \frac{\sigma_a}{6n_o(1 - K_x)^2}.\left\{6n_o(1 - 2K_x + K_x^2)\omega\right\} \qquad (3.18)$$

Equilibrium of forces

From addition of equations (3.11), (3.14), and (3.18); that is $N'_b + N'_a - N_a = 0$ and re-arranging we obtain:

$$\begin{aligned} &-\{(3 + r_a) - a(1 - K_{bu})(3 + r_a)\}K_x^3 \\ &+ [3[1 - a(1 - K_{bu})\{1 + K_{ho}(2 + r_a)\}] - 6(n_o - 1)l_1\omega' - 6n_o\omega]K_x^2 \\ &+[3aK_{ho}(1 - K_{bu})\{2 + K_{ho}(1 + r_a)\} + 6(n_o - 1)(1 + K_d)l_3\omega' + 12n_o\omega]K_x \\ &- [aK_{ho}^2(1 - K_{bu})(3 + K_{ho}r_a) + 6(n_o - 1)K_d l_3\omega' + 6n_o\omega] = 0 \end{aligned} \qquad (3.19)$$

With the right solution for K_x; $r_d = \frac{\varepsilon'_b}{\varepsilon'_c}$ can be found using equation (3.1).

The actual curvature is given by the ratio:

$$\kappa = \frac{\varepsilon_b}{K_x.h} = \frac{\varepsilon_a}{h(1 - K_x)} \qquad (3.20)$$

3.2.4 Resisting Bending Moment

The bending moment is obtained from moment equilibrium with respect to tensile reinforcement

$$\frac{M_c}{B_o\, h^2} = \frac{\sigma_a}{6n_o(1 - K_x)^2}\Bigg[(3 - r_d)K_x^2\left\{1 - \frac{4 - r_d}{4(3 - r_d)}.K_x\right\}$$

$$- a(3 - r_d\frac{K_x - K_{ho}}{K_x}).(K_x - K_{ho})^2.(1 - K_{bf})$$

$$.\left\{(1 - K_{ho}) - \frac{4 - r_d\frac{K_x - K_{ho}}{K_x}}{4\left(3 - r_d\frac{K_x - K_{ho}}{K_x}\right)}.(K_x - K_{ho})\right\}$$

$$+ 6m\omega'(n_o - 1)(K_x - K_d)(1 - K_d)\Bigg] \qquad (3.21)$$

in which $m = 1$ *if* $\varepsilon'_a < \varepsilon_{ae}$ *and* $m = \frac{1 - K_x}{K_x - K_d}$ *if* $\varepsilon'_a \geq \varepsilon_{ae}$

Where:

M_c- bending moment in the cross-section neglecting tensile concrete

N'_b- resultant concrete compressive force

ε_b, ε'_b- concrete strain at extreme tensile and compressive fibres respectively

ε'_c- concrete compressive strain at maximum stress.

ε_a *and* ε'_a- strain in tensile and compression reinforcement respectively

ε_{ac}- yield strain of tensile reinforcement

Equation (3.21) can be simplified as:

$$M_c = \frac{\sigma_a}{24n_o(1 - K_x)K_x}\{[(3 - r_d) - (4 - r_d)K_x]K_x^3 - (1 - K_{bo})(K_x - K_{ho})^2.[4(1 - K_{ho}).\{3K_x - r_d(K_x - K_{ho})\} - \{4K_x - r_d(K_x - K_{ho})\}(K_x - K_{ho})] + 24m\omega'(n_o - 1)(K_x - K_d)K_x(1 - K_d)] \quad (3.22)$$

Equation (3.19) is a third degree equation in K_x . It can be re-written as follows:

$$-AK_x^3 + BK_x^2 + CK_x + D = 0 \quad (3.23)$$

where

$$A = [(3 + r_d) - a(1 - K_{bo})(3 + r_d)] \quad (3.24)$$

$$B = 3[1 - a(1 - K_{bo})\{1 + K_{ho}(2 + r_d)\}] - 6(n_o - 1)l_1\omega - 6n_o\omega] \quad (3.25)$$

$$C = [3aK_{ho}(1-K_{bo})\{2+K_{ho}(1+r_d)\} + 6(n_o-1)(1+K_d)l_2\omega' + 12n_o\omega] \quad (3.26)$$

$$D = [aK_{ho}^2(1-K_{bo})(3+K_{ho}.r_d) + 6(n_o-1)K_dl_3\omega' + 6n_o\omega] \quad (3.27)$$

The result obtained for the moment curvature relationship is a straight line through the origin which represents the moment-curvature relationship of fully cracked section, ie. neglecting the stiffness contribution of tensile concrete.

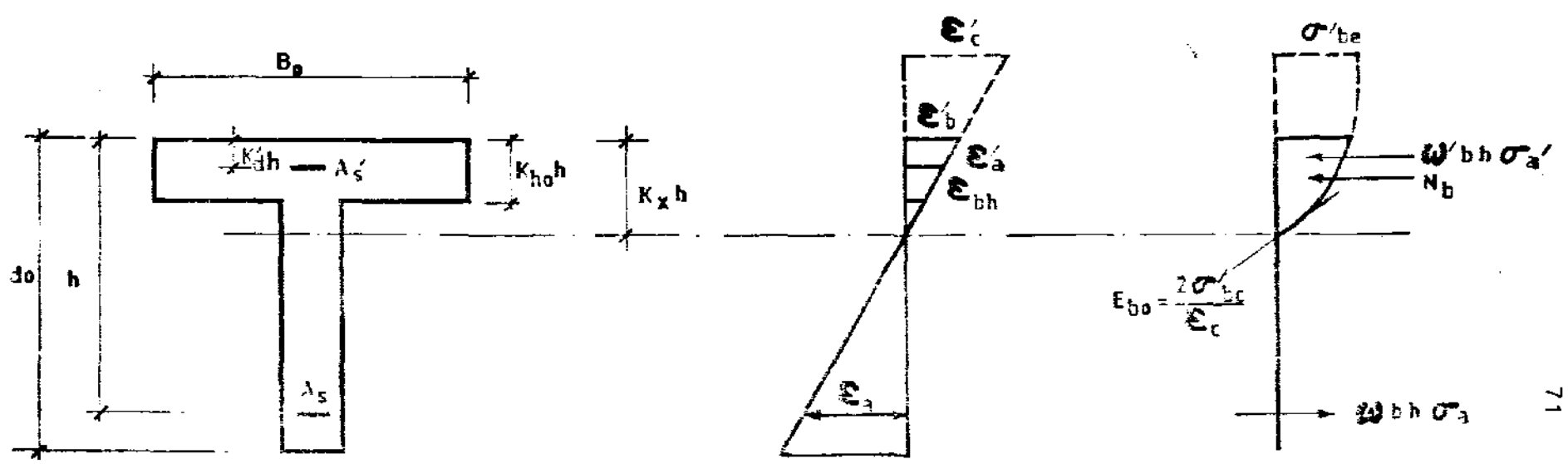


Fig. 3.4. Stress and strain distribution used for calculating M-K relationship without considering tensile concrete.

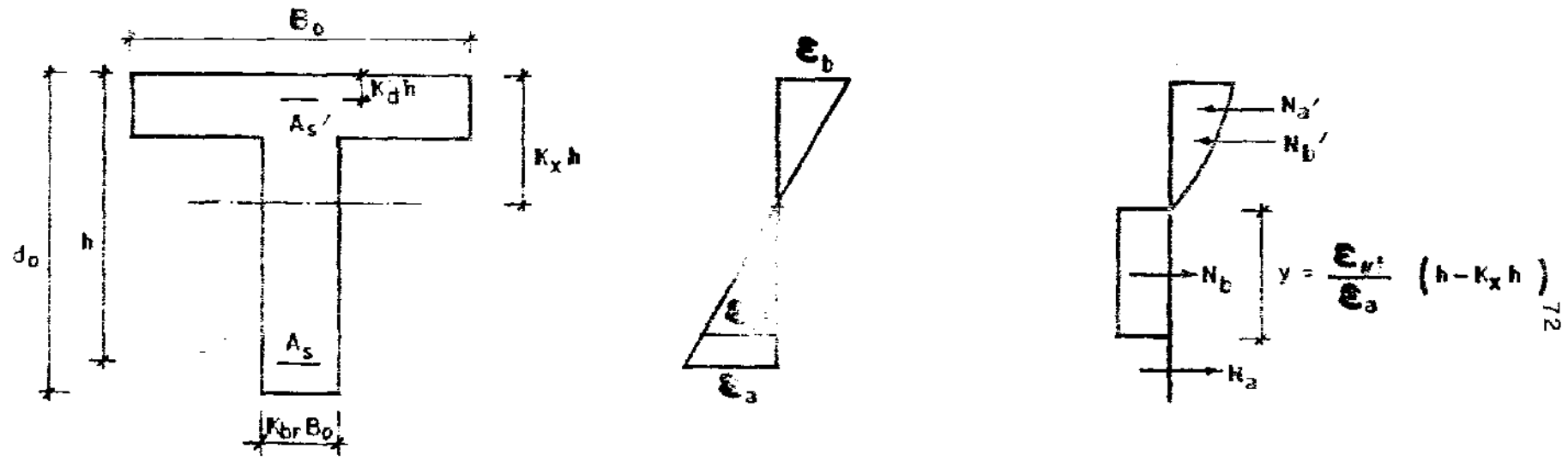


Fig. 3.5. Rectangular approximation (ultimate strain within the cross-section)

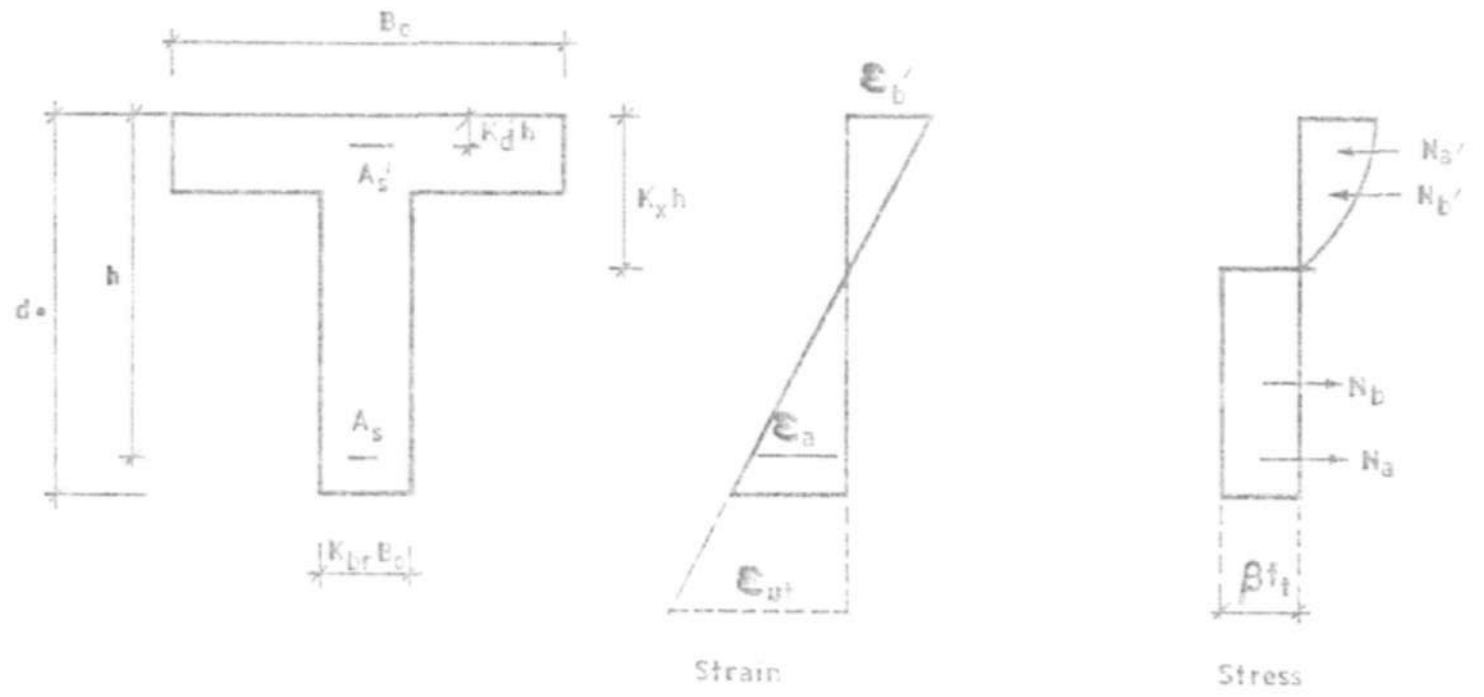


Fig. 3.6. Rectangular approximation (ultimate strain outside the cross-section).

3.2.2 Consideration of Tensile Concrete Using Rectangular Approximation

Using this approximation, two cases were considered.

a) The "ultimate strain" of concrete in tension is assumed to be reached within the cross-section (Figure 3.4).

b) The "ultimate strain" of concrete in tension is assumed to be reached outside the cross-section (Figure 3.5).

It is important to state here that ultimate strain and tensile strength of concrete adopted here are not the real values. They are values carefully chosen using the experimental data of previous investigators as a basis. These values are adjusted until the best fit to experimental curves were obtained.

3.2.2.1 Ultimate strain within the cross-section

From Figure 3.4 we can write that:

$$y = \frac{\varepsilon_{ut}}{\varepsilon_a}.(h - K_x.h) \qquad (3.28)$$

Force due to tensile concrete:

$$\frac{N_b}{B_o h} = f_t.K_{br}.(1 - K_x).\frac{\varepsilon_{ut}}{\varepsilon_a} \qquad (3.29)$$

To conform to Monnier's expression, equation (3.29) is multiplied and divided by the expression $\dfrac{\sigma_a}{6\, n_e\, (1 - K_x)^2}$:

The expression becomes

$$\frac{N_b}{B_o h} = \frac{\sigma_a}{6n_o(1 - K_x)^2}\left\{\frac{f_t \frac{\varepsilon_{ut}}{\varepsilon_a}(1 - K_x)K_{br}.6n_o(1 - K_x)^2}{\sigma_a}\right\} \qquad (3.30)$$

$$= \frac{\sigma_a}{6n_o(1 - K_x)^2}\left\{\frac{6.n_o f_t \frac{\varepsilon_{ut}}{\varepsilon_a}K_{br}.(1 - 3K_x + 3K_x^2 - K_x^3)}{\sigma_a}\right\} \qquad (3.31)$$

The coefficients of the third degree equation for this case (tension concrete) are as follows:

$$A_{(1)} = -6.n_o \frac{f_t}{\sigma_a}.\frac{\varepsilon_{ut}}{\varepsilon_a}.K_{br} \qquad (3.32)$$

$$B_{(1)} = +18.n_o \frac{f_t}{\sigma_a}.\frac{\varepsilon_{ut}}{\varepsilon_a}.K_{br} \qquad (3.33)$$

$$C_{(1)} = -18.n_o \frac{f_t}{\sigma_a}.\frac{\varepsilon_{ut}}{\varepsilon_a}.K_{br} \qquad (3.34)$$

$$D_{(1)} = +6.n_o \frac{f_t}{\sigma_a}.\frac{\varepsilon_{ut}}{\varepsilon_a}.K_{br} \qquad (3.35)$$

Equilibrium of forces:

$N'_a + N'_b - N_a - N_b = 0$ From here we find that:

$$A = -\left\{(3 + r_a) - \alpha(1 - K_{br})(3 + r_a)\right\} + 6n_o \frac{f_t}{\sigma_a}.\frac{\varepsilon_{ut}}{\varepsilon_a}.K_{br} \qquad (3.36)$$

$$B = 3[1 - a(1 - K_{br})\{1 - K_{ho}(2 + r_a)\}] - 6(n_o - 1)l_1\omega' + 6n_o\,\omega - 18n_o\frac{f_t}{\sigma_a}.\frac{\varepsilon_{ut}}{\varepsilon_a}.K_{br} \quad (3.37)$$

$$C = 3aK_{ho}(1 - K_{br})\{2 + K_{ho}(1 + r_a)\} + 6(n_o - 1)(1 + K_d)l_2\omega' + 12n_o\,\omega + 18n_o\frac{f_t}{\sigma_a}.\frac{\varepsilon_{ut}}{\varepsilon_a}.K_{br} \quad (3.38)$$

$$D = -[aK_{ho}^2(1 - K_{br})(3 + K_{ho}\,.\,r_a) + 6(n_o - 1)K_d.l_3.\omega' + 6n_o\,\omega + 6n_o\frac{f_t}{\sigma_a}.K_{br} \quad (3.39)$$

Resisting bending moment due to tensile concrete with respect to tensile reinforcement:

$$M_t = f_t K_{br}.B_o.\frac{\varepsilon_{ut}}{\varepsilon_a}.h(1 - K_x).h(1 - K_x).(1 - 0.5\frac{\varepsilon_{ut}}{\varepsilon_a}) \quad (3.40)$$

To conform to Monnier's expression, equation (3.40)

is multiplied and divided by: $\dfrac{\sigma_a}{24n_o(1-K_x)K_x}$

$$\frac{M_t}{B_o h^2} = \frac{\sigma_a}{24n_o(1 - K_x)K_x}\left\{\frac{f_t K_{br}\frac{\varepsilon_{ut}}{\varepsilon_a}(1-K_x)^2(1-0.5\frac{\varepsilon_{ut}}{\varepsilon_a}24n_o(1-K_x)K_x}{\sigma_a}\right\} \quad (3.41)$$

$$= \frac{\sigma_a}{24n_o(1 - K_x)K_x}\left\{\frac{24f_t}{\sigma_a}.\frac{\varepsilon_{ut}}{\varepsilon_a}.K_{br}.(1-K_x)^3.K_x.(1-0.5\frac{\varepsilon_{ut}}{\varepsilon_a})\right\} \quad (3.42)$$

Resisting moment in the cross-section including tensile concrete with respect to tensile reinforcement becomes:

$$\frac{M_c}{B_o h^2} = \frac{\sigma_a}{24n_o(1 - K_x)K_x}\Big[\{4(3 - r_d) - (4 - r_d)K_x\}K_x^3$$

$$- a(1 - K_{br})(K_x - K_{ho})^2\ [4(1-K_{ho})\{3K_x - r_d\ (K_x-K_{ho})\}$$

$$- 4\ K_x - r_d\ (K_x - K_{ho})\}(K_x - K_{ho})]$$

$$+ 24\ m\ \omega'\ (n_o - 1)(K_x - K_d)\ K_x\ (1 - K_d)]$$

$$- 24.\frac{f_t}{\sigma_a}.\frac{\varepsilon_{ut}}{\varepsilon_a}.K_{br}.(1 - K_x)^3.K_x(1 - 0.5\frac{\varepsilon_{ut}}{\varepsilon_a})\Big] \quad (3.43)$$

.2.2.2 Ultimate Strain Outside the Cross-Section

$$N_b = f_t.(d_o - K_x h).K_{br}.B_o \quad (3.44)$$

$$\frac{N_b}{B_o h} = \frac{f_t}{h}.(d_o - K_x h).K_{br} \quad (3.45)$$

To conform to Monnier's expression, equation (3.45)

Is multiplied and divided by: $\frac{\sigma_a}{6n_o(1-K_x)^2}$,

Therefore

$$\frac{N_b}{B_o h} = \frac{\sigma_a}{6n_o(1 - K_x)^2}\left\{\frac{\frac{f_t}{h}.(d_o - K_{xh}).K_{br}.6n_o(1 - K_x)^2}{\sigma_a}\right\} \quad (3.46)$$

$$- \frac{\sigma_a}{6n_o(1 - K_x)^2}\left[6n_o\frac{f_t}{\sigma_a h}.K_{br}.\{d_o - (2d_o+h)K_x+(d_o+2h)K_x^2-K_x^3h\}\right] \quad (3.47)$$

The coefficients of the third degree equation for this case (tension concrete) are as follows:

$$A_{(2)} = -6\, n_o \frac{f_t}{\sigma_a} . K_{br} \quad (3.48)$$

$$B_{(2)} = +6\, n_o \frac{f_t}{\sigma_a h} . K_{br}\,(d_o + 2h) \quad (3.49)$$

$$C_{(2)} = -6\, n_o \frac{f_t}{\sigma_a h} . K_{br}\,(2d_o + h) \quad (3.50)$$

$$D_{(2)} = -6\, n_o \frac{f_t}{\sigma_a h} . K_{br} . d_o \quad (3.51)$$

Equilibrium of forces in the cross-section:

$N'_a + N'_b - N_a - N_b = 0$. From here we find that:

$$A = -\{(3 + r_a) - a(1 - K_{br})(3 + r_a)\} + 6n_o\frac{f_t}{\sigma_a}.K_{br} \quad (3.52)$$

$$B = 3\left[1 - a(1 - K_{br})\{1 - K_{ho}(2 + r_a)\}\right] - 6(n_o - 1)l_1\omega' - 6n_o\omega$$

$$- 6\, n_o \frac{f_t}{\sigma_a.h} . K_{br}\,(d_o + 2h) \quad (3.53)$$

$$C = 3aK_{ho}(1 - K_{br})\{2 + K_{ho}(1 + r_a)\} + 6(n_o - 1)(1 + K_d)l_2\omega'$$

$$+ 12n_o\,\omega + 6\, n_o\frac{f_t}{\sigma_a.h}.K_{br}(2d_o + h) \quad (3.54)$$

$$D = -\left[aK_{ho}^2(1 - K_{br})(3 + K_{ho}.r_a) + 6(n_o - 1)K_d.l_3.\omega' - 6n_o\omega\right]$$

$$- 6\, n_o \frac{f_t}{\sigma_a.h} . K_{br} . d_o \quad (3.55)$$

Resisting moment due to tensile concrete with respect to the tensile reinforcement:

$$M_t = f_t(d_o - K_x h)K_{br}.B_o.\{\frac{1}{2}(d_o - K_x h) - (d_o - h)\} \quad (3.56)$$

To conform to Monnier's expression equation (3.56) is multiplied and divided by $\frac{\sigma_a}{24n_o(1-K_x)K_x}$: Therefore

$$\frac{M_t}{B_o h^2} = \frac{\sigma_a}{24n_o(1 - K_x)K_x}\left[\frac{\frac{f_t}{B_o h^2}.K_{br}.B_o(d_o - K_x h).\{\frac{1}{2}(d_o - K_x h) - (d_o - h)}{\sigma_a}\right] \quad (3.57)$$

$$- \frac{\sigma_a}{24n_o(1 - K_x)K_x}\left[\frac{f_t}{B_o h^2}.K_{br}.24n_o(1-K_x)K_x.(d_o - K_x h)\right.$$

$$\left.\cdot\left\{\frac{1}{2}(d_o - K_x h) - (d_o - h)\right\}\right] \quad (3.58)$$

Resisting moment including tensile concrete with respect to tensile reinforcement:

$$\frac{M_c}{B_o h^2} = \frac{\sigma_a}{24n_o(1 - K_x)K_x}\left[\{4(3 - r_d) - (4 - r_d)K_x\}K_x\right.$$

$$- a(1 - K_{br})(K_x - K_{ho})^2\,[4(1-K_{ho})\{3K_x - r_d\,(K_x - K_{ho})\}$$

$$- \{4\,K_x - r_d\,(K_x - K_{ho})\}(K_x - K_{ho})]$$

$$\left. + 24\,m\,\omega'\,(n_o - 1)(K_x - K_d)\,K_x\,(1 - K_d)\right] - \frac{f_t}{\sigma_a.h^2}.K_{br}$$

$$. 24.n_o.(1 - K_x).K_x(d_o - K_x h).\left\{\frac{1}{2}(d_o - K_x h) - (d_o - h)\right\} \quad (3.59)$$

A computer program was written to solve these equations and to obtain the moments and the corresponding curvatures and the various positions of neutral axis. The results are presented in Chapter Four. The result of this approximation was found to be unsatisfactory. So another trial was made using triangular approximation of the tensile stress-strain curve.

3.2.3 Consideration of Tensile Concrete Using Triangular Approximation of Tensile Stress-Strain Curve

Three stages in the deformation of flexural member under load were considered using this approximation. The stress and strain distribution in these stages are shown in Figure 3.6.

In Stage I, the bending moment is less than the cracking moment and the concrete is therefore uncracked. The concrete in tension zone effectively contributes to resist the external moment and the strains are quite small. The stress distribution is assumed perfectly elastic.

In Stage II, with increase in bending moment, outermost tensile fibre of concrete will attain its tensile strength; cracks are developed. The stress distribution is assumed a trapezium.

In Stage III, with further increase in bending moment, cracks has developed and extended close to the neutral axis. Part of the tensile concrete no longer contribute to the resistance of external bending moment. The stress distribution is assumed a small triangle.

3.2.3.1 Stage I

From Figure 3.8 we can write that:

$$\frac{\sigma_b}{d_o - K_x.h} = \frac{f_t}{y} \qquad (3.60)$$

Substituting for the value of y in equation (3.59) we have:

$$\sigma_b = \frac{f_t.(d_o - K_x.h)}{\frac{\varepsilon_m}{\varepsilon_b}.(d_o - K_x.h)} = f_t\frac{\varepsilon_b}{\varepsilon_m} \qquad (3.61)$$

$$\varepsilon_b = \frac{d_o - K_x.h}{h - K_x.h}.\varepsilon_a \qquad (3.62)$$

Force due to tensile stress block:

$$N_b = \frac{1}{2}\sigma_b.K_{br}.B_o(d_o - K_x.h) \qquad (3.63)$$

Substituting equations (3.59) and (3.61) in equation (3.63) we have:

$$\frac{N_b}{B_o h} = \frac{1}{2h}f_t.K_{br}.(d_o - K_x.h).\frac{(d_o - K_x.h)}{h(1 - K_x)}.\frac{\varepsilon_a}{\varepsilon_m} \qquad (3.64)$$

To conform to Monnier's expression, equation (3.63) is multiplied and

divided by $\dfrac{\sigma_a}{6\, n_o(1-K_x)^2}$:

Therefore

$$\frac{N_b}{B_o h} = \frac{\sigma_a}{6n_o(1-K_x)^2}\left\{\frac{\frac{1}{2h^2(1-K_x)} f_t K_{br}(d_o - K_x h)^2 . \frac{\varepsilon_a}{\varepsilon_m} . 6n_o(1-K_x)^2}{\sigma_a}\right\} \tag{3.65}$$

$$- \frac{\sigma_a}{6n_o(1-K_x)^2}\left[3n_o . \frac{f_t}{\sigma_a h^2} . K_{br} . \frac{\varepsilon_a}{\varepsilon_m}\left\{d_o^2 - (2d_o h + d_o^2)K_x\right.\right.$$

$$\left.\left. + (h^2 + 2d_o h)\, K_x^2 - K_x^3 . h^2\right\}\right] \tag{3.66}$$

The coefficients of the third degree equation for this stage (tension concrete) are as follows:

$$A^{(1)} = -3.n_o \frac{f_t}{\sigma_a} . K_{br} \frac{\varepsilon_a}{\varepsilon_m} \tag{3.67}$$

$$B^{(1)} = -3.n_o \frac{f_t}{\sigma_a} . K_{br} \frac{\varepsilon_a}{\varepsilon_m}\left(1 + \frac{2d_o}{h}\right) \tag{3.68}$$

$$C^{(1)} = -3.n_o \frac{f_t}{\sigma_a} . K_{br} \frac{\varepsilon_a}{\varepsilon_m} . \frac{d_o}{h^2} . (2h + d_o) \tag{3.69}$$

$$D^{(1)} = -3.n_o \frac{f_t}{\sigma_a} . K_{br} \frac{\varepsilon_a}{\varepsilon_m} . \frac{d_o^2}{h^2} \tag{3.70}$$

Where: N_b- resultant concrete tensile force

σ_b- *concrete stress at the extreme tensile fibre*

d_o- depth of the beam

N_a , N_b' , ε_m, ε_a *and* σ_a are as previously defined

Equilibrium of forces (Stage I) including tensile concrete:

$N'_a + N'_b - N_a - N_b = 0$ From here we find that:

$$A = -\left\{(3 + r_a) - a(1 - K_{br})(3 + r_a) + 3n_o\frac{f_t}{\sigma_a}K_{br}.\frac{\varepsilon_a}{\varepsilon_m}\right\} \qquad (3.71)$$

$$B = 3[1 - a(1 - K_{br})\{1 - K_{ho}(2 + r_a)\}] - 6(n_o - 1)l_1\omega'$$

$$- 6n_o\,\omega - 3n_o\frac{f_t}{\sigma_a}.K_{br}\frac{\varepsilon_a}{\varepsilon_m}.\left(1 + \frac{2d_o}{h}\right) \qquad (3.72)$$

$$C = 3aK_{ho}(1 - K_{br})\{2 + K_{ho}(1 + r_a)\} + 6(n_o - 1)(1 + K_d)l_2\omega'$$

$$+ 12n_o\,\omega + 3n_o\frac{f_t}{\sigma_a}.K_{br}\,\frac{\varepsilon_m}{\varepsilon_a}.\frac{d_o}{h^2}.(2h + d_o) \qquad (3.73)$$

$$D = -[aK_{ho}^2(1 - K_{br})(3 + K_{ho}\,.\,r_a) + 6(n_o - 1)K_d.l_3.\omega'$$

$$+ 6n_o\,\omega] - 3n_o\frac{f_t}{\sigma_a}.K_{br}\,\frac{\varepsilon_a}{\varepsilon_m}.\frac{d_o^2}{h^2} \qquad (3.74)$$

Resisting bending moment (Stage I) due to tensile concrete with respect to tensile reinforcement:

$$M_t = \frac{1}{2}f_t.\frac{\varepsilon_b}{\varepsilon_m}.K_{br}.B_o(d_o - K_x.h)\left\{\frac{1}{3}(d_o - K_x h) - (d_o - h)\right\}$$

$$- f_t\frac{\varepsilon_b}{\varepsilon_m}.K_{br}.B_o(d_o - K_x.h)\left\{\frac{1}{6}(d_o - K_x h) - \frac{1}{2}(d_o - h)\right\} \qquad (3.75)$$

To conform to Monnier's expression, equation (3.75) is multiplied and divided by $\dfrac{\sigma_a}{24\,n_o(1 - K_x)K_x}$:

Therefore;

$$\frac{M_t}{B_o h^2} = \frac{\sigma_a}{24n_o(1 - K_x)K_x}.\frac{1}{\sigma_a.B_o h^2}\left[f_t\frac{\varepsilon_b}{\varepsilon_m}.K_{br}B_o(d_o - K_x h)\right.$$

$$\left. .\,24n_o(1 - K_x)K_x\left\{\frac{1}{6}(d_o - K_x h) - \frac{1}{2}(d_o - K_x h)\right\}\right] \qquad (3.76)$$

$$-\frac{\sigma_a}{24n_o(1-K_x)K_x}\left[24n_o\frac{f_t}{\sigma_a h^2}\cdot\frac{\varepsilon_b}{\varepsilon_m}.K_{br}.(d_o-K_x h).(1-K_x)K_x\right.$$

$$\left.\cdot\left\{\frac{1}{6}(d_o-K_x h)-\frac{1}{2}(d_o-K_x h)\right\}\right] \qquad (3.77)$$

Resisting bending moment including tensile concrete with respect to tensile reinforcement:

$$\frac{M_c}{B_o h^2} = \frac{\sigma_a}{24n_o(1-K_x)K_x}\left[\{4(3-r_d)-(4-r_d)K_x\}\,K_x^3\right.$$

$$-\alpha(1-K_{br})(K_x-K_{ho})^2\,[4(1-K_{ho})\{3K_x-r_d\,(K_x-K_{ho})\}$$

$$-\{4K_x-r_d\,(K_x-K_{ho})\}(K_x-K_{ho})\,]$$

$$\left.+\,24\,m\,\omega'\,(n_o-1)(K_x-K_d)\,K_x\,(1-K_d)\,\right]$$

$$-\,24.n_o\frac{f_t}{\sigma_a h^3}.K_{br}.\frac{\varepsilon_a}{\varepsilon_m}(d_o-K_x h)^2K_x\left\{\frac{1}{6}(d_o-K_x h)-\frac{1}{2}(d_o-h)\right\} \qquad (3.78)$$

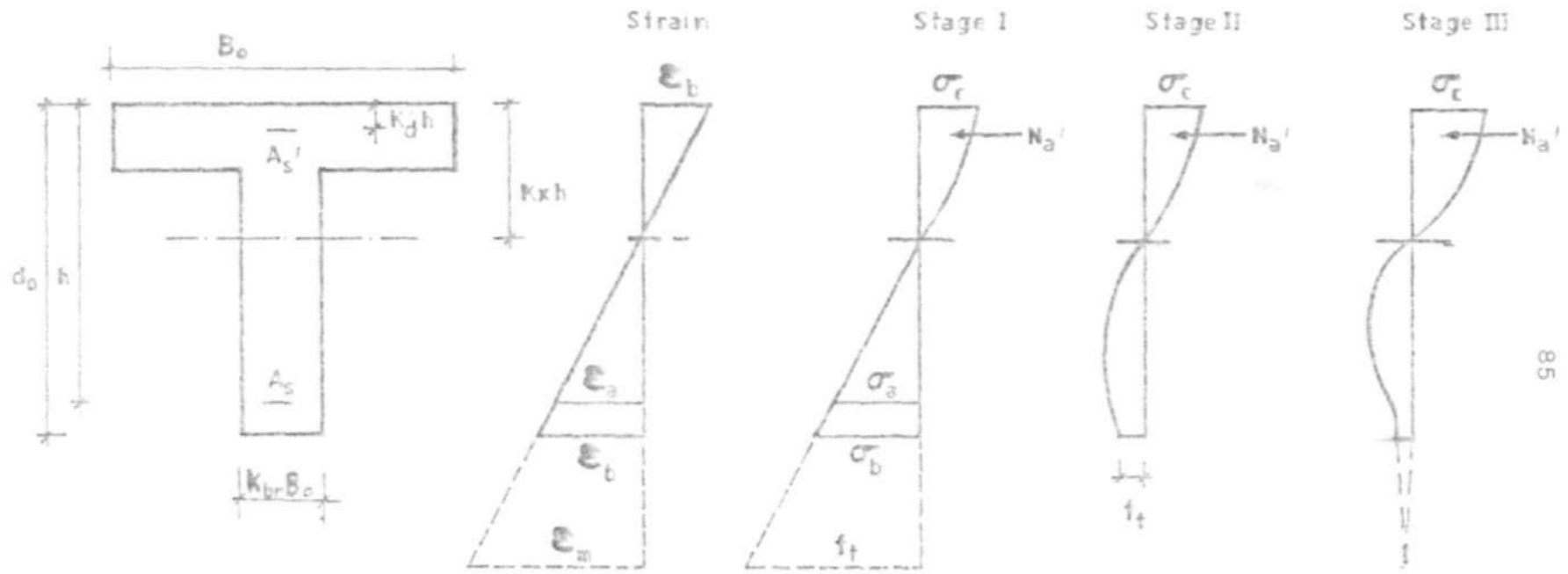


Fig 3.7. Stresses and Strains distribution showing the deformative stages used in the triangular approximation.

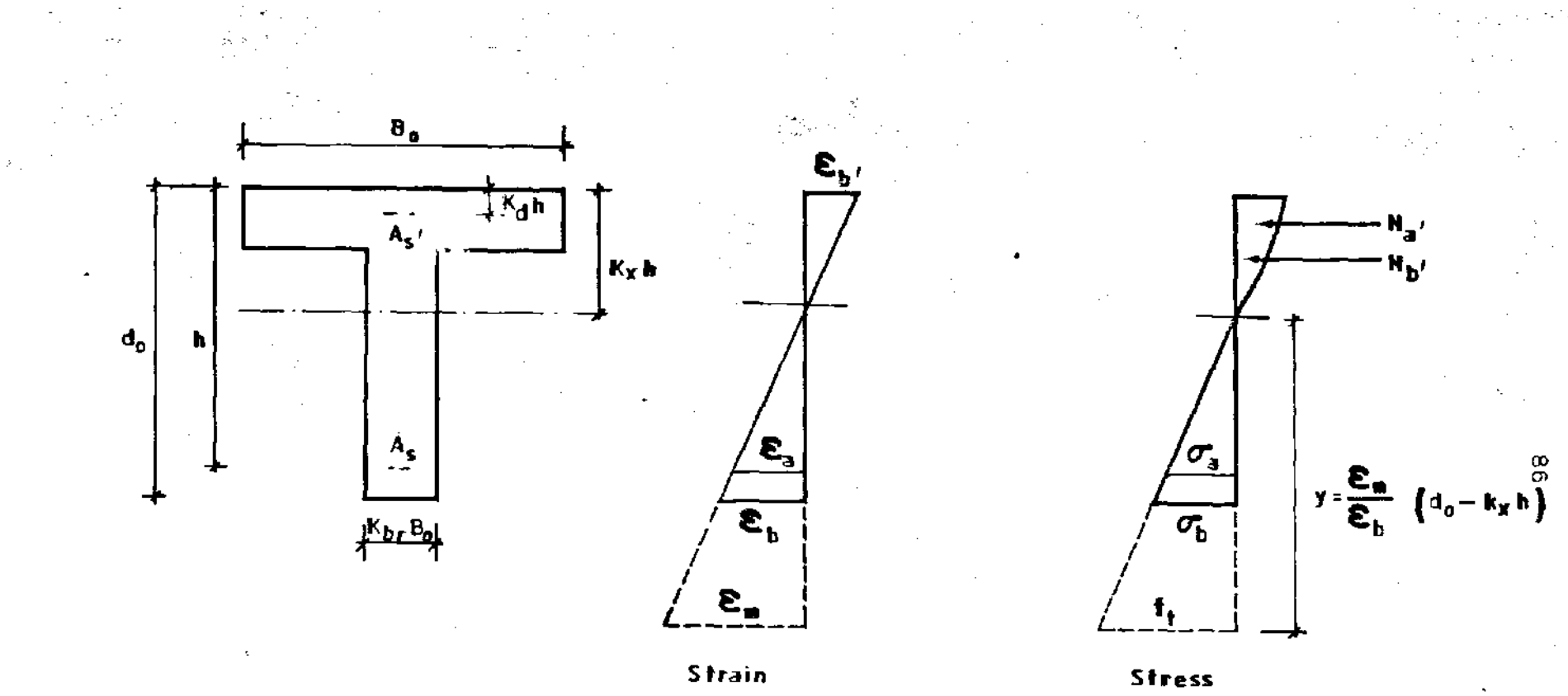


Fig. 3.8. Stress and Strain distribution for stage I.

3.2.3.2 Second Stage

In this stage, the stress distribution is approximated to a trapezium. In order to calculate the forces due to stress block, the trapezium is divided into three triangles. Forces due to these triangles are designated N_{b1}, N_{b2}, N_{b3} (see Figure 3.8).

From Figure 3.8, we can write that:

$$\frac{\varepsilon_{ut}}{y} = \frac{\varepsilon_b}{(d_o - K_x h)} \Rightarrow y = \frac{\varepsilon_{ut}}{\varepsilon_b}(d_o - K_x h) \qquad (3.79)$$

$$\frac{\varepsilon_m}{x} = \frac{\varepsilon_b}{(d_o - K_x h)} \Rightarrow x = \frac{\varepsilon_m}{\varepsilon_b}(d_o - K_x h) \qquad (3.80)$$

$$\sigma_b = \frac{f_t(\varepsilon_{ut} - \varepsilon_b)}{(\varepsilon_{ut} - \varepsilon_m)} \qquad (3.81)$$

Force due to stress block (first triangle)

$$N_{b1} = 0.5 f_t \,.\, x \,.\, K_{br} B_o = 0.5 f_t \frac{\varepsilon_m}{\varepsilon_b}(d_o - K_x h).K_{br} B_o \qquad (3.82)$$

Substituting the value of equation (3.61) in equation (3.82) we obtain

$$N_{b1} = 0.5 f_t \,.\, (d_o - K_x h) \,.\, K_{br} \,.\, B_o \,.\frac{\varepsilon_m (h - K_x h)}{\varepsilon_a (d_o - K_x h)} \qquad (3.83)$$

To conform to Monnier's expression equation (3.83) is multiplied and divided by: $\dfrac{\sigma_a}{6n_o(1-K_x)^2}$

Therefore;

$$\frac{N_{b1}}{B_o h} = \frac{\sigma_a}{6n_o(1-K_x)^2}\left\{\frac{0.5f_t K_{br}.\frac{\varepsilon_m}{\varepsilon_a}.(1-K_x).6n_o(1-K_x)^3}{\sigma_a}\right\} \quad (3.84)$$

$$= \frac{\sigma_a}{6n_o(1-K_x)^2}\left\{3n_o\frac{f_t}{\sigma_a}.K_{br}.\frac{\varepsilon_m}{\varepsilon_a}.(1-3K_x+3K_x^2-K_x^3)\right\} \quad (3.85)$$

The coefficients of the third degree equation for the first triangle are as follows:

$$A_{(2)}^{(1)} = -3\,n_o \cdot \frac{f_t}{\sigma_a} \cdot K_{br} \cdot \frac{\varepsilon_m}{\varepsilon_a} \quad (3.86)$$

$$B_{(2)}^{(1)} = +9\,n_o \cdot \frac{f_t}{\sigma_a} \cdot K_{br} \cdot \frac{\varepsilon_m}{\varepsilon_a} \quad (3.87)$$

$$C_{(2)}^{(1)} = -9\,n_o \cdot \frac{f_t}{\sigma_a} \cdot K_{br} \cdot \frac{\varepsilon_m}{\varepsilon_a} \quad (3.88)$$

$$D_{(2)}^{(1)} = +3\,n_o \cdot \frac{f_t}{\sigma_a} \cdot K_{br} \cdot \frac{\varepsilon_m}{\varepsilon_a} \quad (3.89)$$

Force due to stress block (second triangle)

$$N_{b2} = 0.5f_t \cdot K_{br}.B_o\,\{(d_o - K_x h) - x\} \quad (3.90)$$

Substituting the value of equation (3.80), we have:

$$N_{b2} = 0.5f_t\left[(d_o - K_x.h) - \frac{\varepsilon_m(h-K_x.h)}{\varepsilon_a(d_o - K_x.h)}.(d_o-K_x.h)\right] \quad (3.91)$$

$$\frac{N_{b2}}{B_o.h} = 0.5\frac{f_t}{h}\left[(d_o - K_x.h) - \frac{\varepsilon_m}{\varepsilon_a}(h - K_x.h)\right].K_{br} \quad (3.92)$$

To conform to Monnier's expression equation (3.92) is multiplied and divided by: $\dfrac{\sigma_a}{6n_o(1 - K_x)^2}$

$$\frac{N_{b2}}{B_o.h} = \frac{\sigma_a}{6n_o(1-K_x)^2}\left[0.5\frac{f_t}{h}K_{br}\{(d_o-K_x.h)-\frac{\varepsilon_m}{\varepsilon_a}(h-K_x.h)\}\frac{6n_o(1-K_x)}{\sigma_a}\right] \quad (3.93)$$

$$= \frac{3.n_o.f_t.K_{br}}{\sigma_a.h}\left\{-K_x^3.h+\frac{\varepsilon_m}{\varepsilon_a}.K_x^3.h+K_x^2(d_o+2h)\right.$$

$$\left. - 3.\frac{\varepsilon_m}{\varepsilon_a}.K_x^2.h - K_x(2d_o+h) + 3.\frac{\varepsilon_m}{\varepsilon_a}.K_x.h + d_o-\frac{\varepsilon_m}{\varepsilon_a}.h\right\} \quad (3.94)$$

The coefficients of the third degree equations for the second triangle are as follows:

$$A_{(2)}^{(2)} = \frac{3\ n_o\ .\ f_t K_{br}}{\sigma_a}\left(1 - \frac{\varepsilon_m}{\varepsilon_a}\right) \quad (3.95)$$

$$B_{(2)}^{(2)} = \frac{3\ n_o\ .\ f_t\ K_{br}}{\sigma_a}\left\{\left(\frac{d_o}{h}+2\right) - 3.\frac{\varepsilon_m}{\varepsilon_a}\right\} \quad (3.96)$$

$$C_{(2)}^{(2)} = \frac{3\ n_o\ .\ f_t K_{br}}{\sigma_a}\left\{\left(\frac{2.d_o\ +\ 1}{h}\right) - 3.\frac{\varepsilon_m}{\varepsilon_a}\right\} \quad (3.97)$$

$$D_{(2)}^{(2)} = \frac{3\ n_o\ .\ f_t\ K_{br}}{\sigma_a}\left(\frac{d_o}{h} - \frac{\varepsilon_m}{\varepsilon_a}\right) \quad (3.98)$$

Force due to stress block (third triangle)

$$N_{b3} = \frac{\sigma_b}{2}.\{(d_o - K_x.h) - x\}.K_{br}.B_o \quad (3.99)$$

Substituting the values for equations (3.80) and (3.81), we have:

$$N_{b3} = \frac{\sigma_b}{2}\left\{(d_o-K_x.h)-\frac{\varepsilon_m}{\varepsilon_a}.\frac{(h-K_x.h)}{(d_o-K_x.h)}.(d_o-K_x.h)\right\}.K_{br}.B_o \quad (3.100)$$

$$- \frac{\sigma_b}{2}\ K_{br}.B_o\{(d_o-K_x.h)-\frac{\varepsilon_m}{\varepsilon_a}.(h-K_x.h)\}$$

$$= \frac{0.5f_r(\varepsilon_{ut}-\varepsilon_b)}{(\varepsilon_{ut}-\varepsilon_m)}.K_{br}.B_o\{(d_o-K_x.h)-\frac{\varepsilon_m}{\varepsilon_{a_t}}.(h-K_x h)\} \qquad (3.101)$$

Substituting the value for equation (3.62), we obtain:

$$N_{b3} = \left\{\varepsilon_{ut}-\frac{(d_o-K_x.h)}{(h-K_x h)}.\varepsilon_a\right\}.\{(d_o-K_x h)$$

$$-\frac{\varepsilon_m}{\varepsilon_a}.(h-K_x h)\Big\}.\frac{0.5f_r K_{br}.B_o}{(\varepsilon_{ut}-\varepsilon_m)}$$

$$=\left[\varepsilon_{ut}(d_o-K_x h)-\frac{\varepsilon_a(d_o-K_x h)^2}{(h-K_x h)}-\frac{\varepsilon_{ut}.\varepsilon_m}{\varepsilon_a}.(h-K_x h)\right.$$

$$\left.+\varepsilon_m.(d_o-K_x h)\right]\frac{0.5\,f_t\,K_{br}}{\varepsilon_{ut}-\varepsilon_m} \qquad (3.102)$$

Expanding and simplifying equation (3.102) yields:

$$\frac{N_{b3}}{B_o.h} = \left[\varepsilon_{ut}(d_o-K_x h)(h-K_x h)-\varepsilon_a^2(d_o-K_x h)^2\right.$$

$$\left.-\varepsilon_{ut}\varepsilon_m.h^2(1-K_x)^2+\varepsilon_a.\varepsilon_m(d_o-K_x h).h(1-K_x)\right]$$

$$.\left[\frac{0.5f_t K_{br}.6n_o(1-K_x)^2}{(\varepsilon_{ut}-\varepsilon_m).\varepsilon_a.\sigma_a.(1-K_x)h^2}\right] \qquad (3.103)$$

$$=[\varepsilon_{ut}\varepsilon_a.h(d_o-2d_oK_x+d_oK_x^2-K_x h+2K_x^2h-K_x^3h)$$

$$-\varepsilon_a^2(d_o^2-2d_oK_x h+K_x^2h^2-d_o^2K_x+2d_oK_x^2h-K_x^3h^2)$$

$$-\varepsilon_{ut}.\varepsilon_m.h^2(1-3K_x+3K_x^2-K_x^3)+\varepsilon_a\varepsilon_m h(d_o-2d_oK_x+d_oK_x^2-K_x h$$

$$+2K_x^2.h-K_x^3.h\}\frac{3n_o\,f_t\,K_{br}}{(\varepsilon_{ut}-\varepsilon_m).\sigma_a.h^2.\varepsilon_a} \qquad (3.104)$$

$$- \left[\varepsilon_{ut}.\varepsilon_a.h\{d_o - K_x(2d_o+h) + K_x^2(d_o+2h) - K_x^3 h\}\right.$$

$$- \varepsilon_a^2\{d_o^2 - K_x.d_o(2h+d_o) + K_x^2\, h(h + 2d_o) - K_x^3 h^2\}$$

$$- \varepsilon_{ut}.\varepsilon_m h^2(1-3K_x+3K_x^2-K_x^3) + \varepsilon_a\varepsilon_m h\{d_o - K_x(2d_o + h)$$

$$\left. + K_x^2(d_o + 2h) - K_x^3.h\}\right]\frac{3n_o f_t K_{br}}{(\varepsilon_{ut} - \varepsilon_m).\sigma_a.h^2.\varepsilon_a} \qquad (3.105)$$

The coefficients of the third degree equation for the third triangle are as follows:

$$A_{(2)}^{(3)} = \frac{3\, n_o \cdot f_t K_{br}}{(\varepsilon_{ut}-\varepsilon_a)\sigma_a}.\left\{- \varepsilon_{ut} + \varepsilon_a + \frac{\varepsilon_{ut}.\varepsilon_m}{\varepsilon_a} - \varepsilon_m\right\} \qquad (3.106)$$

$$B_{(2)}^{(3)} = \frac{3n_o f_t K_{br}}{(\varepsilon_{ut}-\varepsilon_a)\sigma_a}.\left\{\varepsilon_{ut}\left(\frac{d_o}{h}+2\right) - \varepsilon_a\left(1+2\frac{d_o}{h}\right) - \frac{3\varepsilon_a+\varepsilon_m}{\varepsilon_a} + \varepsilon_m\left(\frac{d_o}{h}+2\right)\right\} \qquad (3.107)$$

$$C_{(2)}^{(3)} = \frac{3n_o f_t K_{br}}{(\varepsilon_{ut}-\varepsilon_a)\sigma_a}.\left\{- \varepsilon_{ut}\left(\frac{2d_o}{h} + 1\right) + \varepsilon_a(2h + d_o).\frac{d_o}{h^2}\right.$$

$$\left. + \frac{3.\varepsilon_{ut}.\varepsilon_m}{\varepsilon_a} - \varepsilon_m\left(\frac{2d_o}{h} + 1\right)\right\} \qquad (3.108)$$

$$D_{(2)}^{(3)} = \frac{3n_o f_t K_{br}}{(\varepsilon_{ut}-\varepsilon_a)\sigma_a}.\left[\varepsilon_{ut}.\frac{d_o^2}{h^2} - \frac{\varepsilon_{ut}.\varepsilon_m}{\varepsilon_a} + \varepsilon_m.\frac{d_o}{h}\right] \qquad (3.109)$$

Addition of forces due to stress block in triangles 1, 2 and 3 in order to obtain the sum for each coefficient of the third degree equation:

$$A_{(2)}^{(1)} + A_{(2)}^{(2)} + A_{(2)}^{(3)} = - 3\, n_o \cdot \frac{f_t}{\sigma_a}.K_{br} + \frac{3n_o f_t}{(\varepsilon_{ut}-\varepsilon_m)\sigma_a}.K_{br}.$$

$$\left\{- \varepsilon_{ut} + \varepsilon_a + \frac{\varepsilon_{ut}.\varepsilon_m}{\varepsilon_a} - \varepsilon_m\right\} \qquad (3.110)$$

$$B_{(2)}^{(1)} + B_{(2)}^{(2)} + B_{(2)}^{(3)} - 3n_o.\frac{f_t}{\sigma_a}.K_{br}\left(\frac{d_o}{h}+2\right)+\frac{3n_o f_t}{(\varepsilon_{ut}-\varepsilon_m)\sigma_a}.K_{br}.$$

$$\left\{\varepsilon_{ut}\left(\frac{d_o}{h}+2\right)-\varepsilon_a\left(1+\frac{2d_o}{h}\right) - \frac{3\varepsilon_{ut}.\varepsilon_m}{\varepsilon_a} + \varepsilon_m\left(\frac{d_o}{h}+2\right)\right\} \qquad (3.111)$$

$$C_{(2)}^{(1)} + C_{(2)}^{(2)} + C_{(2)}^{(3)} - -3n_o.\frac{f_t}{\sigma_a}.K_{br}\left(\frac{2d_o}{h}+1\right)+\frac{3n_o.f_t}{(\varepsilon_{ut}-\varepsilon_m)\sigma_a}.K_{br}.$$

$$\left\{-\varepsilon_{ut}\left(\frac{2d_o}{h}+1\right)-\varepsilon_a(2h+d_o)\frac{d_o}{h^2} + \frac{3\varepsilon_{ut}.\varepsilon_m}{\varepsilon_a}-\varepsilon_m\left(\frac{2d_o}{h}+1\right)\right\} \qquad (3.112)$$

$$D_{(2)}^{(1)} + D_{(2)}^{(2)} + D_{(2)}^{(3)} - 3n_o.\frac{f_t}{\sigma_a}.K_{br}.\frac{d_o}{h}+\frac{3n_o.f_t}{(\varepsilon_{ut}-\varepsilon_m)\sigma_a}.K_{br}.$$

$$\left\{\varepsilon_{ut}\frac{d_o}{h} - \varepsilon_a\frac{d_o^2}{h^2} - \frac{\varepsilon_{ut}.\varepsilon_m}{\varepsilon_a} + \varepsilon_m.\frac{d_o}{h}\right\} \qquad (3.113)$$

Equilibrium of forces including tensile concrete:

$N'_a + N'_b - N_a - N_b = 0$ From here we find that:

$$A = -\left[\{(3 + r_a) - a(1 - K_{br})(3 + r_a)\} + 3n_o\frac{f_t}{\sigma_a}.K_{br}\right.$$

$$\left.+\frac{3n_o.f_t}{(\varepsilon_{ut}-\varepsilon_m)\sigma_a}.K_{br}\left\{-\varepsilon_{ut} + \varepsilon_a + \frac{\varepsilon_{ut}.\varepsilon_m}{\varepsilon_a} - \varepsilon_m\right\}\right] \qquad (3.114)$$

$$B = 3[1 - a(1 - K_{br})\{1 - K_{ho}(2 + r_a)\}] - 6(n_o - 1)I_1\omega'$$

$$+ 6n_o\,\omega - 3n_o\frac{f_t}{\sigma_a}\left(\frac{d_o}{h}+2\right) + 3n_o\frac{f_t}{\varepsilon_{ut}-\varepsilon_m)\sigma_a}$$

$$.\left\{\varepsilon_{ut}\left(\frac{d_o}{h}+2\right)-\varepsilon_a\left(1+\frac{2d_o}{h}\right) - \frac{3\varepsilon_{ut}.\varepsilon_m}{\varepsilon_a} + \varepsilon_m\left(\frac{d_o}{h}+2\right)\right\} \qquad (3.115)$$

$$C = 3aK_{ho}(1 - K_{br})\{2 + K_{ho}(1 + r_a)\} + 6(n_o - 1)(1 - K_a)l_3\omega' + 12n_o\,\omega + 3n_o\frac{f_t}{\sigma_a}.K_{br}\left(\frac{2d_o}{h}+1\right) + 3n_o\frac{f_t}{(\varepsilon_{ut}-\varepsilon_m)\sigma_a}.K_{br}\cdot\left\{-\varepsilon_{ut}\left(\frac{2d_o}{h}+1\right)-\varepsilon_a(2h+d_o)\frac{d_o}{h^2} + \frac{3\varepsilon_{ut}.\varepsilon_m}{\varepsilon_a}-\varepsilon_m\left(\frac{2d_o}{h}+1\right)\right\} \quad (3.116)$$

$$D = -[aK_{ho}^2(1-K_{br})(3+K_{ho}.r_a) + 6(n_o-1)K_a.l_2.\omega'+6n_o\omega] - 3n_o\frac{f_t}{\sigma_a}.K_{br}\frac{d_o}{h} + \frac{3n_o f_t K_{br}}{(\varepsilon_{ut} - \varepsilon_m)\sigma_a}\cdot\left\{\varepsilon_{ut}\frac{d_o}{h} - \varepsilon_a\frac{d_o^2}{h^2} - \frac{\varepsilon_{ut}.\varepsilon_m}{\varepsilon_a} + \varepsilon_m.\frac{d_o}{h}\right\} \quad (3.117)$$

Moment due to stress block (first triangle) with respect to tensile reinforcement:

$$M_{(2)}^{(1)} = 0.5f_t.K_{br}.B_o.x\left\{(h - K_x.h)-\frac{2}{3}x\right\} \quad (3.118)$$

Substituting the value of equation (3.80) we obtain:

$$M_{(2)}^{(1)} = 0.5f_t.K_{br}.B_o.\frac{\varepsilon_m}{\varepsilon_b}(d_o - K_x.h)(h - K_x.h) - \frac{1}{3}f_t.K_{br}.B_o.\left(\frac{\varepsilon_m}{\varepsilon_b}\right)^2.(d_o - K_x.h)^2 - f_t.K_{br}.B_o.\frac{\varepsilon_m}{\varepsilon_b}(d_o-K_x.h)\left[\frac{1}{2}(h-K_x.h)-\frac{1}{3}\frac{\varepsilon_m}{\varepsilon_b}(d_o-K_x.h)\right] \quad (3.119)$$

To conform equation (3.119) to Monnier's expression, we multiply and divide by: $\dfrac{\sigma_a}{24n_o(1 - K_x)K_x}$.

Therefore

$$\frac{M_{(2)}^{(1)}}{B_o h^2} = \frac{\sigma_a}{24n_o(1-K_x)K_x}\cdot\frac{1}{\sigma_a B_o h^2}\left[f_t K_{br} B_o \frac{\varepsilon_m}{\varepsilon_b}(d_o - K_x h)\right.$$

$$\left. 24n_o(1-K_x)K_x\left\{\frac{1}{2}(h-K_x h)-\frac{1}{3}\frac{\varepsilon_m}{\varepsilon_b}(d_o-K_x h)\right\}\right]$$

$$-\frac{\sigma_a}{24n_o(1-K_x)K_x}\left[24n_o\frac{f_t}{\sigma_a h^2}K_{br}\frac{\varepsilon_m}{\varepsilon_b}(d_o-K_x h)K_x\right.$$

$$\left.\left\{\frac{1}{2}(h-K_x h)-\frac{1}{3}\frac{\varepsilon_m}{\varepsilon_b}(d_o-K_x h)\right\}\right] \qquad (3.120)$$

Moment due to stress block (second triangle) with respect to tensile reinforcement:

$$M_{(2)}^{(2)} = 0.5 f_t K_{br} B_o \{(d_o - K_x h) - x\}.$$

$$\left[\frac{2}{3}\{(d_o - K_x h) - x\} - (d_o - h)\right] \qquad (3.121)$$

$$= 0.5 f_t K_{br} B_o (d_o - K_x h)\left(1-\frac{\varepsilon_m}{\varepsilon_b}\right).$$

$$\left[\frac{2}{3}(d_o - K_x h)\left(1 - \frac{\varepsilon_m}{\varepsilon_b}\right) - (d_o - h)\right]$$

$$-\frac{1}{3} f_t K_{br} B_o (d_o - K_x h)^2\left(1-\frac{\varepsilon_m}{\varepsilon_b}\right)^2.$$

$$-\frac{1}{2} f_t K_{br} B_o (d_o - K_x h)\left(1 - \frac{\varepsilon_m}{\varepsilon_b}\right).(d_o - h)$$

$$-f_t K_{br} B_o (d_o - K_x h)\left(1-\frac{\varepsilon_m}{\varepsilon_b}\right).$$

$$\left[\frac{1}{3}(d_o - K_x h)\left(1 - \frac{\varepsilon_m}{\varepsilon_b}\right) - \frac{1}{2}(d_o - h)\right] \qquad (3.122)$$

To conform to Monnier's expression equation (3.122) is multiplied and divided by: $\dfrac{\sigma_a}{24n_o(1-K_x)K_x}$

$$\frac{M_{(2)}^{(2)}}{B_o h^2} = \frac{\sigma_a}{24n_o(1-K_x)K_x}\cdot\frac{1}{\sigma_a B_o h^2}\left[f_t K_{br} B_o (d_o - K_x h)\left(1-\frac{\varepsilon_m}{\varepsilon_b}\right)\right.$$

$$\left. 24n_o(1-K_x)K_x\left\{\frac{1}{3}(d_o-K_x h)\left(1-\frac{\varepsilon_m}{\varepsilon_b}\right)-\frac{1}{2}(d_o-K_x h)\right\}\right. \qquad (3.123)$$

$$-\frac{\sigma_a}{24n_o(1-K_x)K_x}\left[24n_o\frac{f_t}{\sigma_a h^2}K_{br}(d_o-K_x h)\left(1-\frac{\varepsilon_m}{\varepsilon_b}\right)(1-K_x)K_x\right.$$

$$\left.\left[\frac{1}{3}(d_o-K_x h)\left(1-\frac{\varepsilon_m}{\varepsilon_b}\right)-\frac{1}{2}(d_o-K_x h)\right]\right. \qquad (3.124)$$

Moment due to stress block (third triangle) with respect to the tensile reinforcement:

$$M_{(2)}^{(3)} = \frac{\sigma_b}{2}K_{br}B_o\{(d_o-K_x h)-x\}\left[\frac{1}{3}\{(d_o-K_x h)-x\}-(d_o-h)\right] \qquad (3.125)$$

$$-\frac{\sigma_b}{2}K_{br}B_o\left\{(d_o-K_x h)-\frac{\varepsilon_m}{\varepsilon_b}(d_o-K_x h)\right\}\cdot$$

$$\left[\frac{1}{3}\left\{(d_o-K_x h)-\frac{\varepsilon_m}{\varepsilon_b}(d_o-K_x h)\right\}-(d_o-h)\right] \qquad (3.126)$$

Substituting the value of equation (3.81), in equation (3.126) we obtain:

$$\frac{f_t(\varepsilon_{ut}-\varepsilon_b)}{2(\varepsilon_{ut}-\varepsilon_m)}K_{br}B_o(d_o-K_x h)\left(1-\frac{\varepsilon_m}{\varepsilon_b}\right)\cdot$$

$$\left[\frac{1}{3}(d_o-K_x h)\left(1-\frac{\varepsilon_m}{\varepsilon_b}\right)-(d_o-h)\right] \qquad (3.127)$$

To conform to Monnier's expression, equation (3.127) is multiplied and divided by: $\dfrac{\sigma_a}{24n_o(1-K_x)K_x}$

Therefore

$$\frac{M_{(2)}^{(3)}}{B_o h^2} = \frac{\sigma_a}{24n_o(1-K_x)K_x}\cdot\frac{1}{\sigma_a B_o h^2}\left[\frac{f_t(\varepsilon_m - \varepsilon_b)}{2(\varepsilon_m - \varepsilon_m)}.K_{br}.B_o.\right.$$

$$.(d_o - K_x h).\left(1 - \frac{\varepsilon_m}{\varepsilon_b}\right)\left\{\frac{1}{3}(d_o - K_x h)\left(1 - \frac{\varepsilon_m}{\varepsilon_b}\right)\right.$$

$$\left.\left. - (d_o - h)\right\} . 24n_o(1 - K_x)K_x\right] \qquad (3.128)$$

$$- \frac{\sigma_a}{24n_o(1-K_x)K_x}\left[12n_o f_t \frac{(\varepsilon_m - \varepsilon_b)}{\sigma_a . h^2(\varepsilon_m - \varepsilon_m)}.K_{br}.(d_o - K_x h).\right.$$

$$\left.(1-K_x)K_x\left\{\frac{1}{3}(d_o - K_x h)\left(1 - \frac{\varepsilon_m}{\varepsilon_b}\right) - (d_o - h)\right\}\right] \qquad (3.129)$$

Sum of the moments in triangular stress blocks 1, 2 and 3 gives

$$M_t = \frac{\sigma_a}{24n_o(1-K_x)K_x}\left[24n_o.\frac{f_t}{\sigma_a . h^2}.K_{br}.\frac{\varepsilon_m}{\varepsilon_b}.(d_o - K_x h).\right.$$

$$(1-K_x)K_x.\left\{\frac{1}{2}(h - K_x h) - \frac{1}{3}\frac{\varepsilon_m}{\varepsilon_b}.(d_o - K_x h)\right\}$$

$$+ \frac{24n_o f_t . K_{br}}{\sigma_a . h^2}.(d_o - K_x h)\left(1 - \frac{\varepsilon_m}{\varepsilon_b}\right)(1 - K_x).K_x.$$

$$\left\{\frac{1}{3}(d_o - K_x h)\left(1 - \frac{\varepsilon_m}{\varepsilon_b}\right) - \frac{1}{2}(d_o - h)\right\}$$

$$+ 12n_o \frac{f_t(\varepsilon_m - \varepsilon_b)}{\sigma_a . h^2(\varepsilon_m - \varepsilon_m)}.K_{br}.(d_o - K_x h)\left(1 - \frac{\varepsilon_m}{\varepsilon_b}\right).$$

$$\left.. (1-K_x).K_x\left\{\frac{1}{3}(d_o - K_x h)\left(1 - \frac{\varepsilon_m}{\varepsilon_b}\right) - (d_o - h)\right\}\right] \qquad (3.130)$$

Resisting moment in the cross-section with respect to the tensile reinforcement:

$$\frac{M}{B_o h^2} = \frac{\sigma_a}{24 n_o (1 - K_x) K_x} \Big[\{4(3 - r_d) - (4 - r_d) K_x\} K_x^3$$

$$- a(1 - K_{ho})(K_x - K_{ho})^2 \{4(1 - K_{ho})\{3K_x - r_d (K_x - K_{ho})\}$$

$$- \{4 K_x - r_d (K_x - K_{ho})\}(K_x - K_{ho}) \}$$

$$+ 24 m \omega' (n_o - 1)(K_x - K_d) K_x (1 - K_d)$$

$$- 24 n_o \frac{f_t}{\sigma_a h^2} K_{br} \frac{\varepsilon_m}{\varepsilon_a} (d_o - K_x h)(1 - K_x) K_x \left\{ \frac{1}{2} (h - K_x h) \right.$$

$$\left. - \frac{1}{3} \frac{\varepsilon_m}{\varepsilon_a} (d_o - K_x h) \right\} + 24 n_o \frac{f_t}{\sigma_a h^2} K_{br} (d_o - K_x h) \left(1 - \frac{\varepsilon_m}{\varepsilon_a} \right)$$

$$(1 - K_x) K_x \left\{ \frac{1}{3} (d_o - K_x h) \left(1 - \frac{\varepsilon_m}{\varepsilon_b} \right) - \frac{1}{2} (d_o - h) \right\}$$

$$+ 12 n_o \frac{f_t}{\sigma_a h^2} \cdot \frac{(\varepsilon_{ut} - \varepsilon_b)}{(\varepsilon_{ut} - \varepsilon_m)} K_{br} (d_o - K_x h)$$

$$\cdot \left(1 - \frac{\varepsilon_m}{\varepsilon_b} \right) (1 - K_x) K_x \left\{ \frac{1}{3} (d_o - K_x h) \left(1 - \frac{\varepsilon_m}{\varepsilon_b} \right) (d_o - h) \right\} \Big] \qquad (3.131)$$

3.2.3.3 Third Stage

From Figure 3.9 we can write that:

$$\frac{x}{\varepsilon_m} = \frac{h - K_x.h}{\varepsilon_a} \Rightarrow x = \frac{\varepsilon_m}{\varepsilon_a}(h - K_x.h) \qquad (3.132)$$

$$\frac{z}{\varepsilon_{ut}} = \frac{h - K_x.h}{\varepsilon_a} \Rightarrow z = \frac{\varepsilon_{ut}}{\varepsilon_a}(h - K_x.h) \qquad (3.133)$$

$$y = z - x = h(1 - K_x)(\frac{\varepsilon_{ut}}{\varepsilon_a} - \frac{\varepsilon_m}{\varepsilon_a}) \qquad (3.134)$$

Force due to stress block:

$$N_b = \frac{1}{2} f_t.K_{br}.B_o.z \quad .... \qquad (3.135)$$

Substituting the value of equation (3.133) in equation (3.135), we obtain:

$$N_b = \frac{1}{2} f_t.K_{br}.B_o.\frac{\varepsilon_{ut}}{\varepsilon_a}(h - K_x.h)$$

$$\frac{N_b}{B_o.h} = \frac{1}{2} f_t.K_{br}.\frac{\varepsilon_{ut}}{\varepsilon_a}(1 - K_x) \quad .... \qquad (3.136)$$

To conform to Monnier's expression, equation (3.136) is multiplied and divided by: $\frac{\sigma_a}{6n_o(1 - K_x)^2}$, Therefore

$$\frac{N_b}{B_o.h} = \frac{\sigma_a}{6n_o(1-K_x)^2}\left[\frac{\frac{f_t}{2}.K_{br}.\frac{\varepsilon_{ut}}{\varepsilon_a}(1 - K_x).6n_o(1-K_x)^2}{\sigma_a}\right] \qquad (3.137)$$

$$= \frac{\sigma_a}{6n_o(1-K_x)^2}\left[3n_o\frac{f_t}{\sigma_a}.K_{br}.\frac{\varepsilon_{ut}}{\varepsilon_a}(1 - 3K_x+3K_x^2-K_x^3)\right] \qquad (3.138)$$

The coefficients of the third degree equation for this stage is as follows:

$$A_{(3)} = -3n_o \frac{f_t}{\sigma_a} . K_{br} . \frac{\varepsilon_{ut}}{\varepsilon_a} \quad .... \quad (3.139)$$

$$B_{(3)} = +9n_o \frac{f_t}{\sigma_a} . K_{br} . \frac{\varepsilon_{ut}}{\varepsilon_a} \quad .... \quad (3.140)$$

$$C_{(3)} = -9n_o \frac{f_t}{\sigma_a} . K_{br} . \frac{\varepsilon_{ut}}{\varepsilon_a} \quad .... \quad (3.141)$$

$$D_{(3)} = +3n_o \frac{f_t}{\sigma_a} . K_{br} . \frac{\varepsilon_{ut}}{\varepsilon_a} \quad .... \quad (3.142)$$

Equilibrium of forces in the cross-section $N'_a + N'_b - N_a - N_b = 0$. From here we find that:

$$A = -\{(3 + r_a) - a(1 - K_{br})(3 + r_a) + 3n_o \frac{f_t}{\sigma_a} K_{br} . \frac{\varepsilon_{ut}}{\varepsilon_a}\} \quad (3.143)$$

$$B = 3[1 - a(1 - K_{br})\{1 + K_{ho}(2 + r_a)\}] - 6(n_o - 1)l_1\omega'$$

$$- 6n_o\ \omega - 9n_o \frac{f_t}{\sigma_a} . K_{br} \frac{\varepsilon_{ut}}{\varepsilon_a} \quad .... \quad (3.144)$$

$$C = 3aK_{ho}(1 - K_{br})\{2 + K_{ho}(1 + r_a)\} + 6(n_o - 1)(1 + K_d)l_2\omega'$$

$$+ 12n_o\ \omega + 9n_o \frac{f_t}{\sigma_a} . K_{br}\ \frac{\varepsilon_{ut}}{\varepsilon_m} \quad (3.145)$$

$$D = -[aK_{ho}^2(1 - K_{br})(3 + K_{ho} . r_a) + 6(n_o - 1)K_d l_3 . \omega'$$

$$+ 6n_o\ \omega + 3n_o \frac{f_t}{\sigma_a} . K_{br}\ \frac{\varepsilon_{ut}}{\varepsilon_a} \quad (3.146)$$

Resisting moment due to stress block (first triangle) with respect to tensile reinforcement:

$$M_{(3)}^{(1)} = \frac{f_t}{2}.K_{br}.B_o.x.\{(h - K_x.h) - \frac{2}{3}x\} \qquad (3.147)$$

Substituting the value of equation (3.132) in equation (3.147), we obtain:

$$M_{(3)}^{(1)} = \frac{f_t}{2}.K_{br}.B_o.\frac{\varepsilon_m}{\varepsilon_a}(h - K_x.h)^2.(1 - \frac{2}{3}\frac{\varepsilon_m}{\varepsilon_a}) \qquad (3.148)$$

To conform to Monnier's expression equation (3.140) is multiplied add divided by: $\frac{\sigma_a}{24n_o(1-K_x)K_x}$: Therefore;

$$\frac{M_{(3)}^{(1)}}{B_o.h^2} = \frac{\sigma_a}{24n_o(1-K_x)K_x}.\frac{1}{\sigma_a}\left[\frac{f_t}{2}.K_{br}.B_o\frac{\varepsilon_m}{\varepsilon_a}(h - K_x.h)^2.\right.$$

$$\left.(1 - \frac{2}{3}.\frac{\varepsilon_m}{\varepsilon_a}) \;.\; 24n_o(1-K_x)K_x\right] \qquad .... \qquad (3.149)$$

$$= \frac{\sigma_a}{24n_o(1-K_x)K_x}\left[12n_o\frac{f_t}{\sigma_a}.K_{br}.\frac{\varepsilon_m}{\varepsilon_a}(1-\frac{2}{3}\frac{\varepsilon_m}{\varepsilon_a})(1-K_x)^3K_x\right] \qquad (3.150)$$

Resisting moment due to stress block (second triangle) with respect to tensile reinforcement:

$$M_{(3)}^{(2)} = \frac{f_t}{2}.K_{br}.B_o.y.\left[(h - K_x.h) - \left(x + \frac{1}{3}y\right)\right] \qquad (3.151)$$

Substituting the values of equations (3.132) and (3.134), we obtain:

$$M_{(3)}^{(2)} = \frac{f_t}{2}.K_{br}.B_o.(h - K_x.h)^2.\left(\frac{\varepsilon_{ut}}{\varepsilon_a} - \frac{\varepsilon_m}{\varepsilon_a}\right).$$

$$\left\{1 - \frac{\varepsilon_m}{\varepsilon_a} - \frac{1}{3}\frac{\varepsilon_{ut}}{\varepsilon_a} + \frac{1}{3}\frac{\varepsilon_m}{\varepsilon_a}\right\} \qquad .... \qquad (3.152)$$

To conform to Monnier's expression, we have:

$$\frac{M_{(3)}^{(2)}}{B_o.h^2} = \frac{\sigma_a}{24n_o(1-K_x)K_x}.\frac{1}{\sigma_a}\left[\frac{f_t}{2}.K_{br}.(1-K_x)^2\left(\frac{\varepsilon_{ut}}{\varepsilon_a} - \frac{\varepsilon_m}{\varepsilon_a}\right).\right.$$

$$\left.\left\{1 - \frac{\varepsilon_m}{\varepsilon_a} - \frac{1}{3}\frac{\varepsilon_{ut}}{\varepsilon_a} + \frac{1}{3}\frac{\varepsilon_m}{\varepsilon_a}\right\} 24n_o(1 - K_x)K_x\right] \qquad (3.153)$$

$$= \frac{\sigma_a}{24n_o(1-K_x)K_x}\left[12n_o\frac{f_t}{\sigma_a}.K_{br}.\frac{(\varepsilon_{ut}-\varepsilon_m)}{\varepsilon_a}.(1-K_x)^3K_x\right.$$

$$\left.\left(1-\frac{1}{3}\frac{\varepsilon_{ut}}{\varepsilon_a}-\frac{2}{3}\frac{\varepsilon_m}{\varepsilon_a}\right)\right] \quad .... \quad (3.154)$$

Sum of the resisting bending moment due to tensile stress block:

$$M_t = M_{(3)}^{(1)} + M_{(3)}^{(2)}$$

$$M_t = \frac{\sigma_a}{24n_o(1-K_x)K_x}\left[12n_o\frac{f_t}{\sigma_a}.K_{br}.\frac{\varepsilon_m}{\varepsilon_a}\left(1-\frac{2}{3}\frac{\varepsilon_m}{\varepsilon_a}\right)(1-K_x)^3K_x\right.$$

$$+ 12n_o\frac{f_t}{\sigma_a}.K_{br}.\frac{\varepsilon_{ut}-\varepsilon_m}{\varepsilon_a}(1-K_x)^3K_x.$$

$$\left.\left(1-\frac{1}{3}\frac{\varepsilon_{ut}}{\varepsilon_a}-\frac{2}{3}\frac{\varepsilon_m}{\varepsilon_a}\right)\right] \quad .... \quad (3.155)$$

Resisting bending moment in the cross-section with respect to tensile reinforcement:

$$M = \frac{\sigma_a}{24n_o(1-K_x)K_x}\left[\{4(3-r_d)-(4-r_d)K_x\}K_x^3\right.$$

$$- a(1-K_{br})(K_x-K_{ho})^2\{4(1-K_{ho})\{3K_x-r_d(K_x-K_{ho})\}$$

$$- \{4K_x-r_d(K_x-K_{ho})^2\}(K_x-K_{ho})\}$$

$$+ 12\,m\,\omega'(n_o-1)(K_x-K_d)K_x(1-K_d)$$

$$- 12.n_o\frac{f_t}{\sigma_a}.K_{br}.\frac{\varepsilon_m}{\varepsilon_a}\left(1-\frac{2}{3}\frac{\varepsilon_a}{\varepsilon_m}\right)(1-K_x)^3K_x$$

$$+ 12.n_o\frac{f_t}{\sigma_a}.K_{br}.\left(\frac{\varepsilon_{ut}-\varepsilon_m}{\varepsilon_a}\right).(1-K_x)^3K_x$$

$$\left.\cdot\left(1-\frac{1}{3}\frac{\varepsilon_{ut}}{\varepsilon_a}-\frac{2}{3}\frac{\varepsilon_m}{\varepsilon_a}\right)\right. \quad (3.156)$$

456148

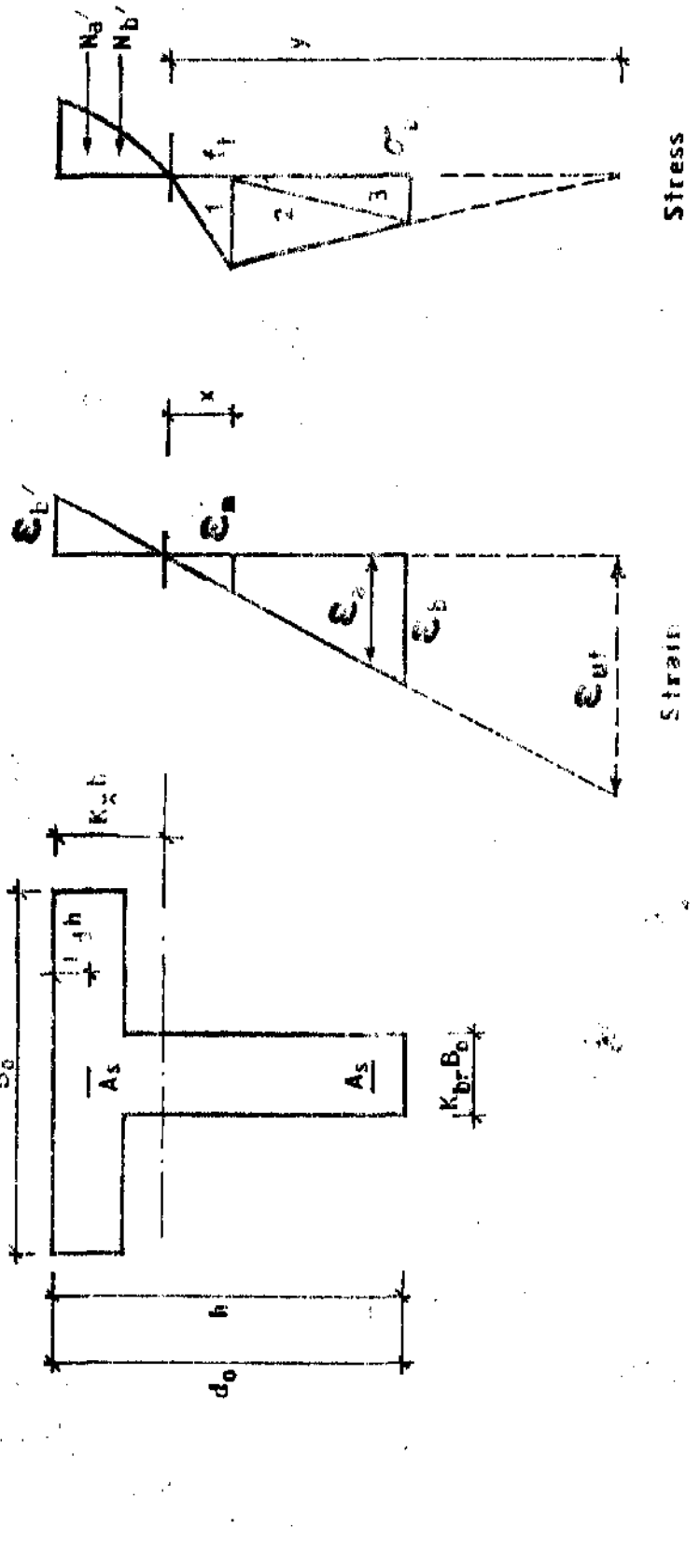


Fig. 3.9 Stress and Strain distribution for stage II

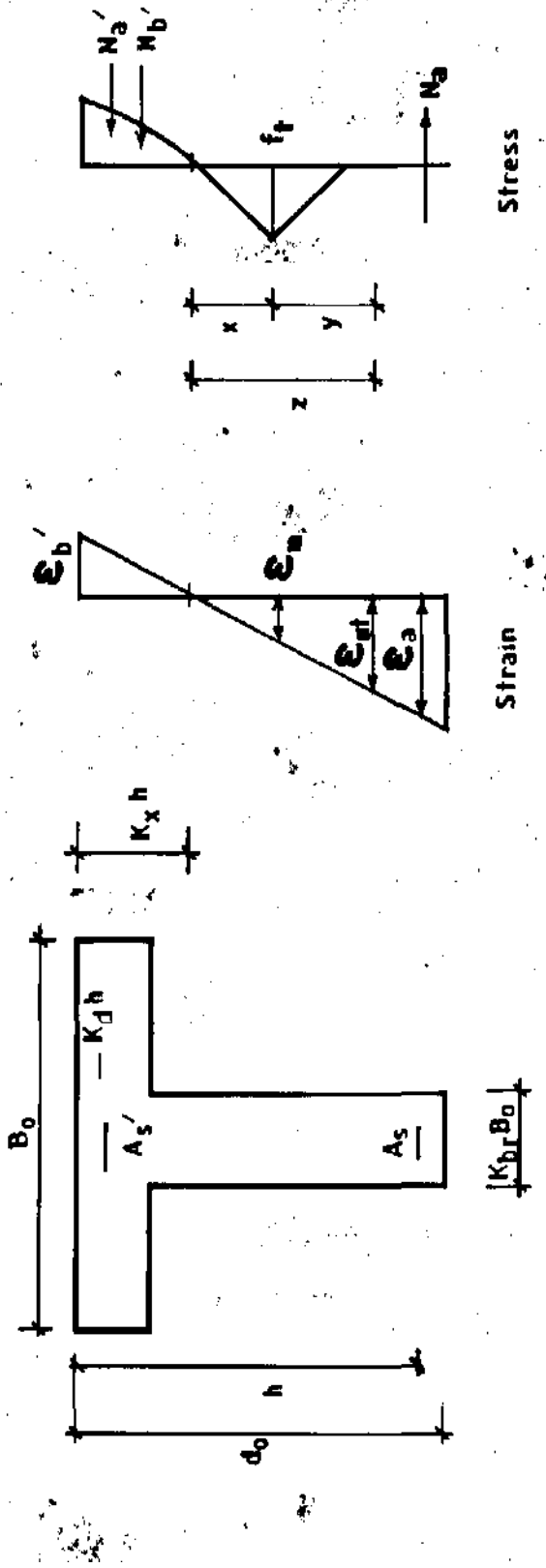
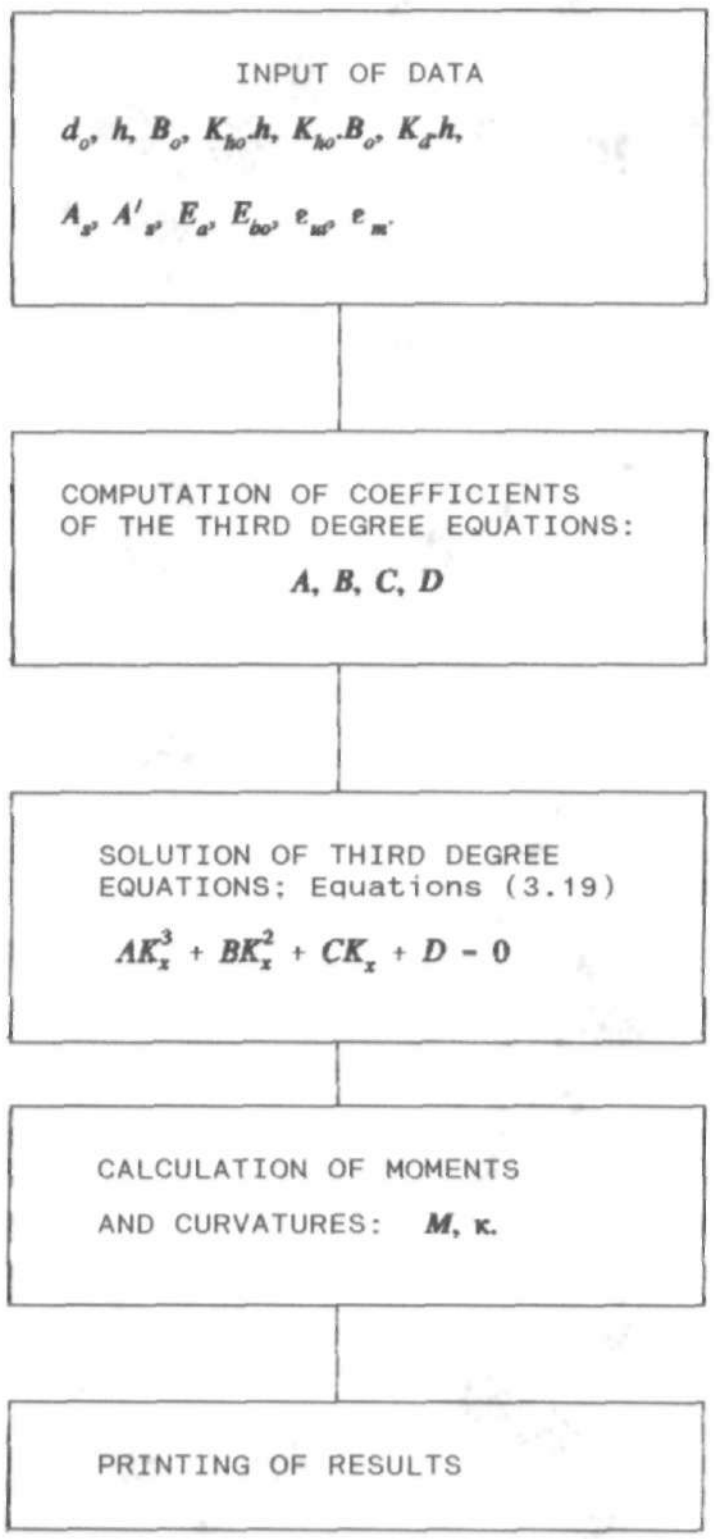


Fig. 3.10. Stress and strain distribution for stage III

3.2.3.4 COMPUTATION OF MOMENT-CURVATURE RELATIONSHIP:

The flow chart below shows the procedure adopted for solving the moment-curvature relationship:



CHAPTER FOUR

4.1 COMPARISON OF RESULTS

In this chapter, the theoretical results obtained by the author was compared with the results obtained experimentally by Monnier (1970). Figure 4.1 showo the moment-curvature curve obtained by the author from the rectangular approximation of the tensile stress-strain curve of concrete compared to the moment-curvature curve obtained experimentally by Monnier (1970). From this result, it is obvious that rectangular approximation of the concrete tensile stress-strain curve is inappropriate.

For this reason, another approximation of the tensile stress-strain curve was made using full triangle, trapezium, and a small triangle. The full triangle represents the first stage of deformation i.e. uncracked cross-section, the trapezium represents the second stage while the small triangle represents the third stage of deformation. These approximations was used to obtain the moment-curvature relation. These results were compared with the experimental results obtained by Monnier (1970) which are presented in figures 4.2 to 4.5. The results were found to be in good agreement.

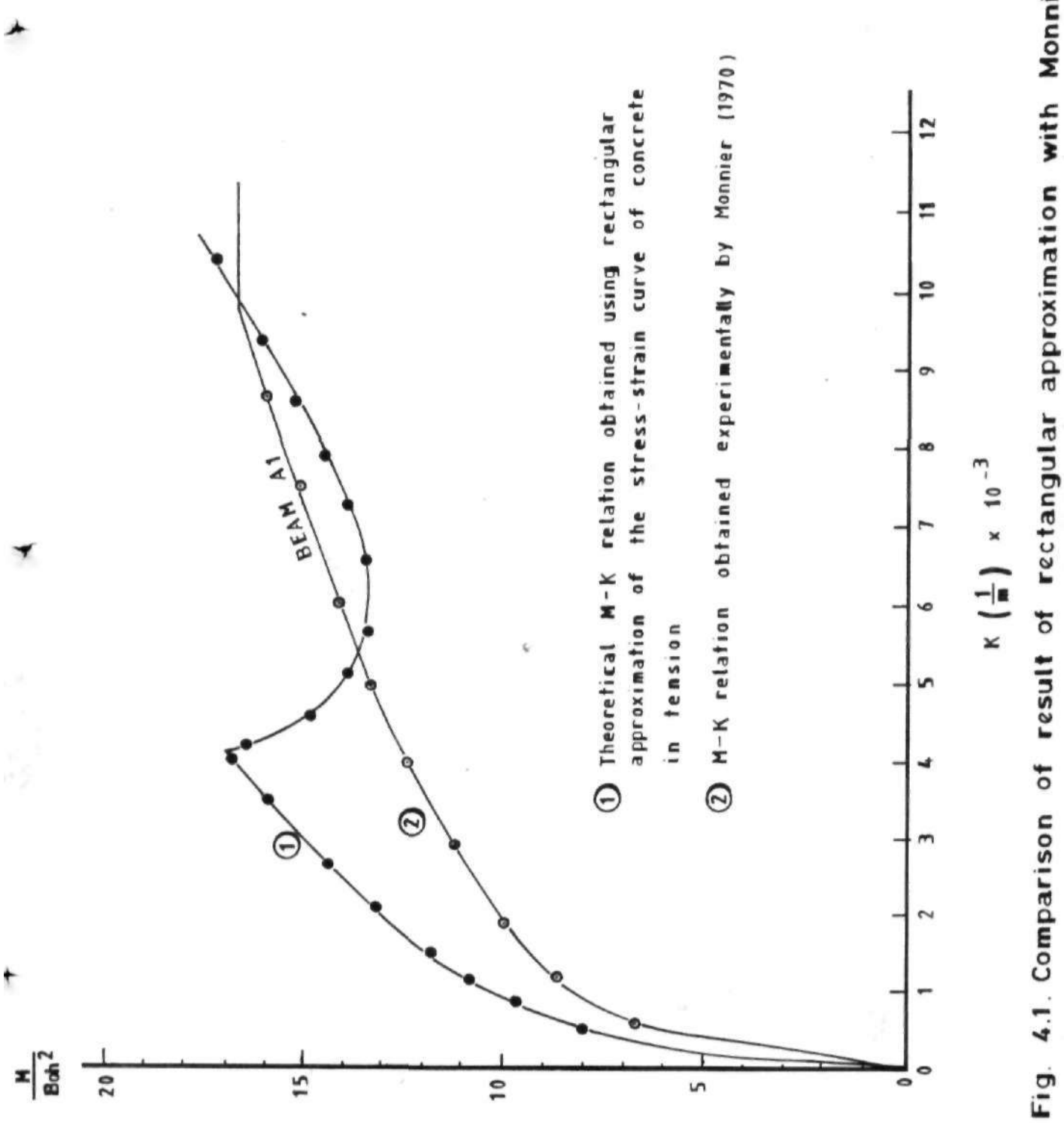
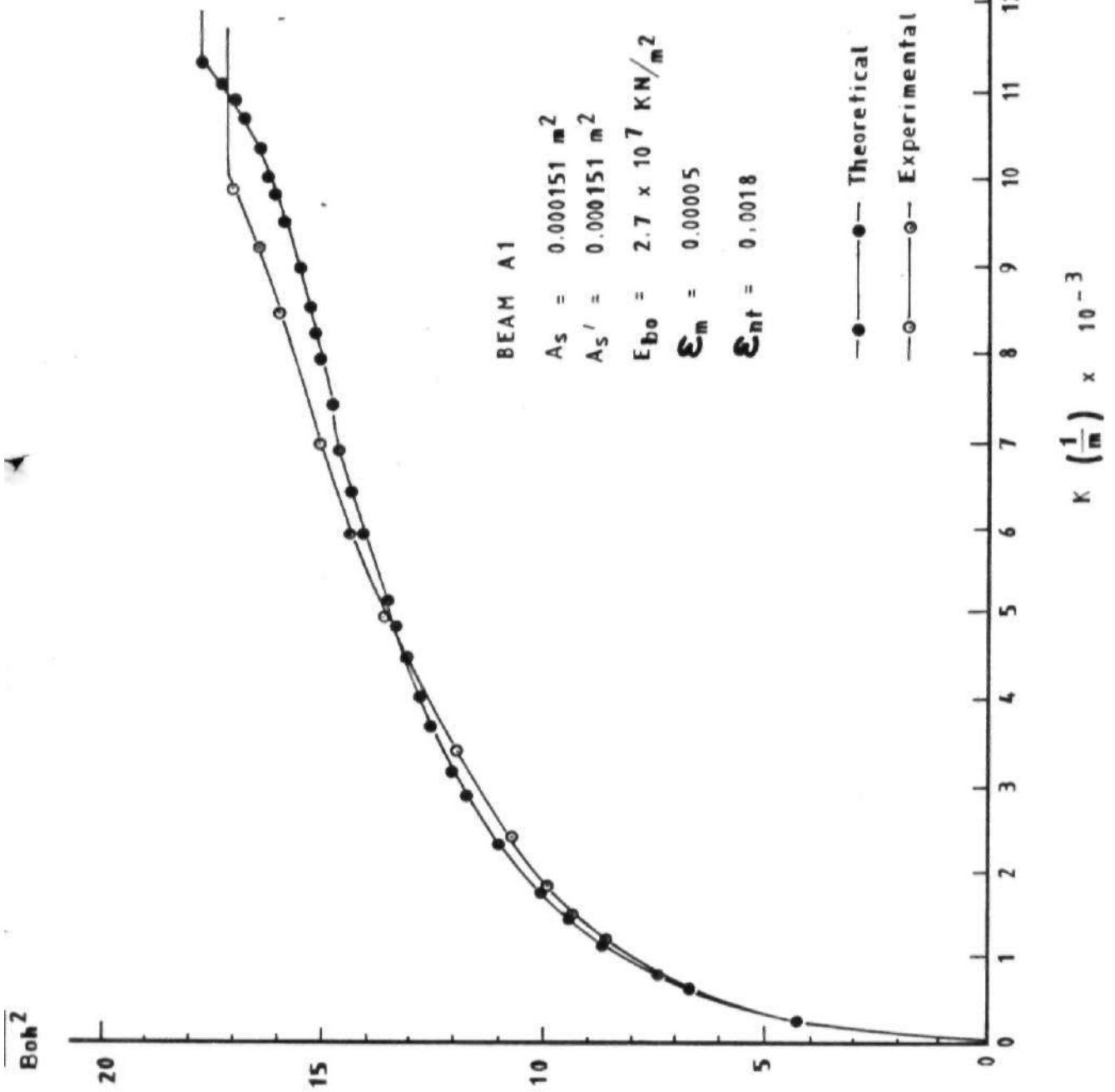


Fig. 4.1. Comparison of result of rectangular approximation with Monnier's result.


BEAM A1
A_s = 0.000151 m^2
A_s' = 0.000151 m^2
E_{bo} = 2.7 x 10^7 KN/m^2
ε_m = 0.00005
ε_{nf} = 0.0018
—●— Theoretical
—○— Experimental
Boh^2
20
15
10
5
0
0 1 2 3 4 5 6 7 8 9 10 11 12 13 14
K $(\frac{1}{m})$ x 10^{-3}

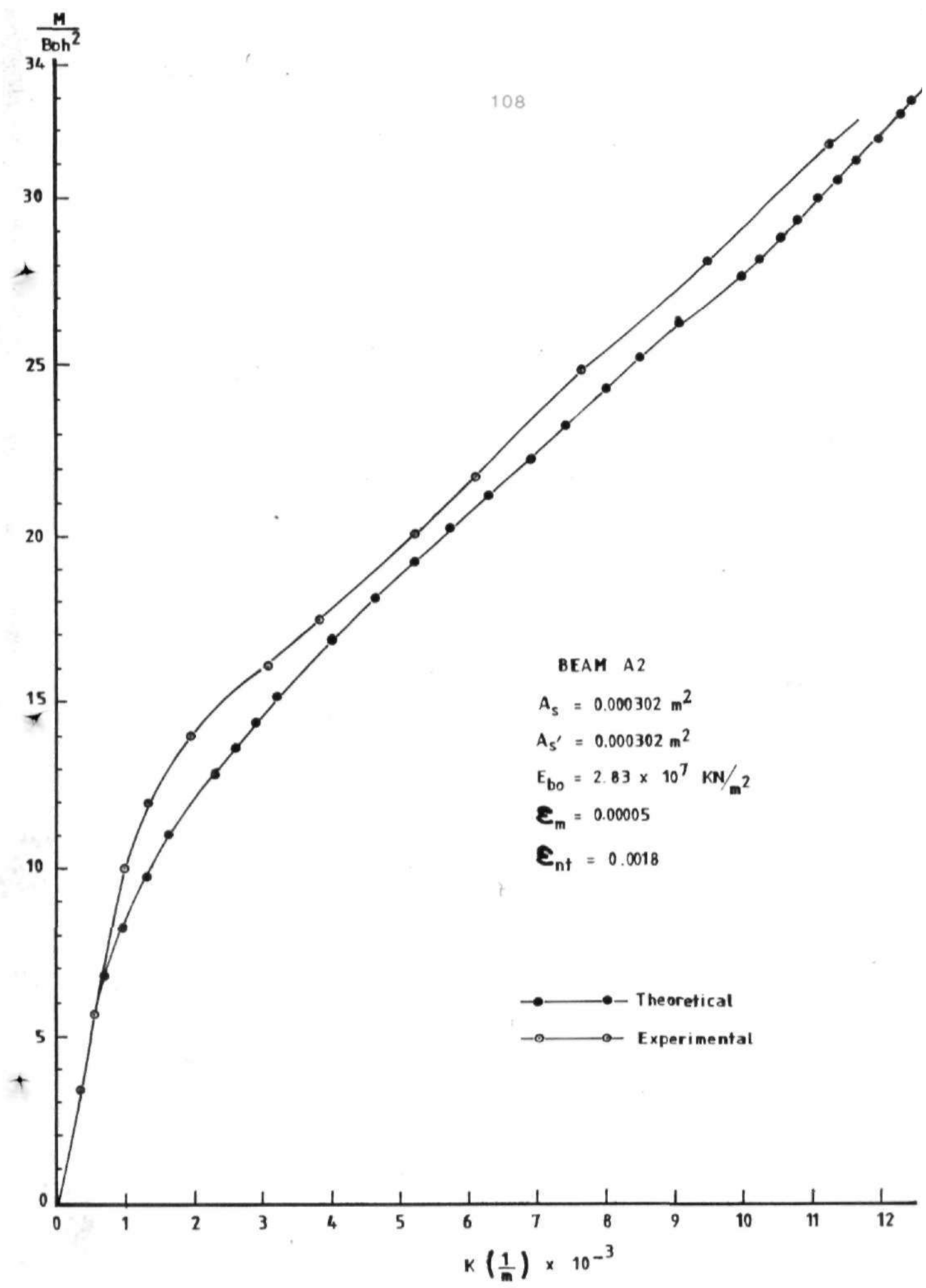


Fig. 4.3. (see fig. 4.1. for the title)

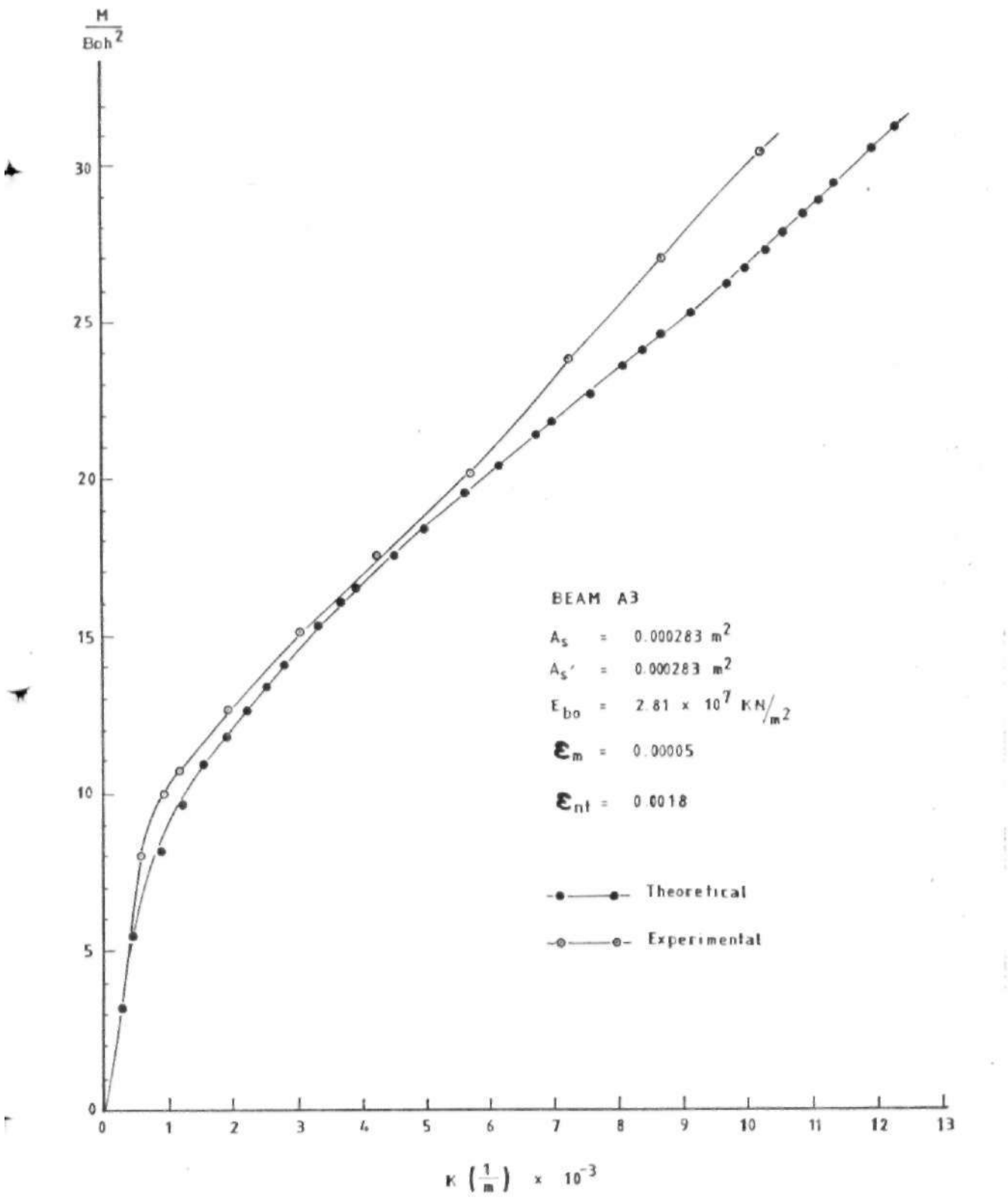

M / Boh²
30
25
20
15
10
5
0
0
1
2
3
4
5
6
7
8
9
10
11
12
13
K (1/m) × 10⁻³
BEAM A3
As = 0.000283 m²
As' = 0.000283 m²
Ebo = 2.81 × 10⁷ KN/m²
εm = 0.00005
εnt = 0.0018
Theoretical
Experimental

Fig. 4.4.

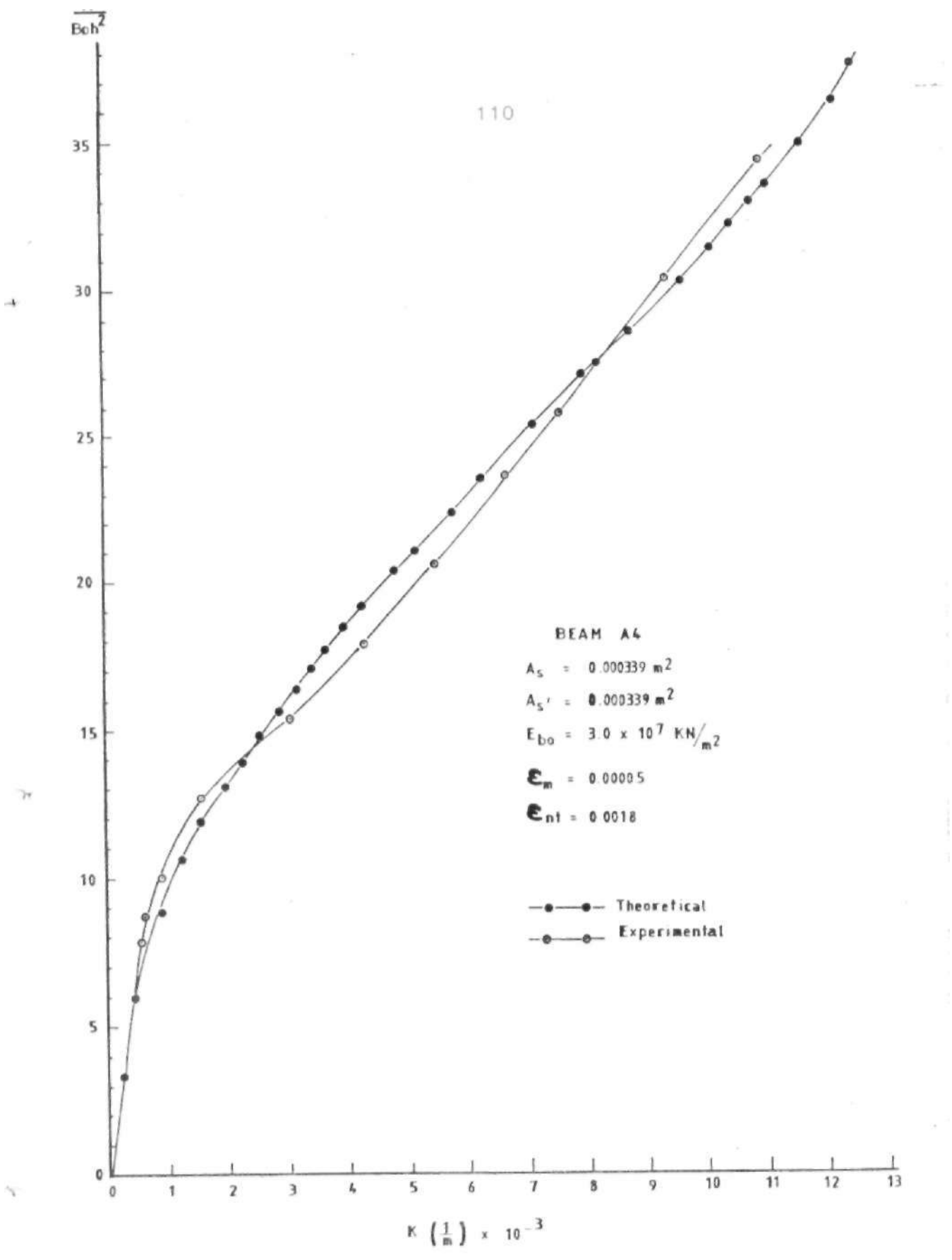

$\overline{Bch^2}$
35
30
25
20
15
10
5
0
0 1 2 3 4 5 6 7 8 9 10 11 12 13
K $\left(\frac{1}{m}\right)$ x 10^{-3}
BEAM A4
A_s = 0.000339 m^2
$A_{s'}$ = 0.000339 m^2
E_{bo} = 3.0 x 10^7 KN/m^2
ε_m = 0.00005
ε_{nf} = 0.0018
Theoretical
Experimental

Fig. 4.5

CHAPTER-FIVE

EXPERIMENTAL PROGRAMME

5.1 CONCRETE MIX:

The concrete mix was not aimed at achieving a particular strength. It was however desired that at least a strength higher than 20 N/mm2 be attained.

The coarse aggregate used for the concrete is the crushed stones of sizes less than 20mm. The sieve analysis of the aggregates is shown in table 5.1.

Ordinary Portland cement manufactured by the Ashaka Cement Company was used throughout the research. 1:2:4 mix proportion was adopted as the most popular and the most economical mix design for ordinary concrete structures. This means one part by weight of cement, two parts by weight of fine aggregate, and four parts by weight of coarse aggregate. Based on the mix proportion, the summary of the concrete mix per beam is as follows:

Cement 380 kg.m3.

Fine aggregate 770 kg/m3.

Coarse aggregate 1530 kg/m3.

The water:cement ratio was varied in each batch depending on the moisture content of the aggregates in order to achieve good workability. Water:cement ratio for all the mixes was between 0.55-0.61. All the batching was done by weight. Mixing of the concrete was carried out using rotating drum mixer.

5.1.1 TEST BEAMS

A total of six reinforced concrete beams of rectangular cross section were cast. Three of the beams has cross sectional dimensions of 300mm by 100mm and the other three has cross-sectional dimensions of 100mm by 300mm. The overall length of each beam is 4.0m. The limitation of testing equipment and handling were the main factors that governed the selection of the cross-sectional dimensions and span of the specimens. The quantity of the main reinforcement in each beam was established by assuming the reinforcement percentage to vary between 0.4 percent to 1.2 percent of the cross sectional area. All the main reinforcement are deformed high yield bars. Each beam contain compressive reinforcement comprising of two mild steel bars of 6.0mm diameter. Stirrups were provided throughout the length of the beams using mild steel bars of 4.0mm diameter. Figures 5.1 and 5.2 shows schematically the general layout of reinforcements and the beams cross-sections.

The variable parameters in the beams are: percentage of reinforcement and the bar diameter. However, in each beam the quantity of reinforcement does not vary in the longitudinal direction. The data relating to all the beams are summarized in table 5.2.

5.1.2 FABRICATION OF BEAMS

The beams were cast using timber forms. Two batches of concrete was used to cast each beam. When placing and vibrating of the first batch , the mixing of the second batch was normally continued. In this way, a continuity of mixing, pouring and vibrating was maintained for each beam. Two beams were cast per day. Thorough compaction of the concrete was achieved using "kango" hammer. Three control cubes of sizes 150mm * 150mm *150mm and three cylinders of sizes 150mm diameter and 300mm long were cast along with each pair of beams.

The control cubes and cylinders were used for determining the concrete strength at the age of testing. The beams, the cubes and cylinders were usually left overnight before they are removed from the mould. Dismantled mould and the formwork were reassembled for further use. The beams, the cubes and cylinders were cured for 28 days before testing. Wet bags were used for curing beams, the cubes and the cylinders. They were covered with the bags and watered for 28 days before testing.

5.1.3 TEST ARRANGEMENT

The testing arrangement comprised of the so-called four-point bending test, in which the 4.0 m beams were supported on rollers spaced at centre-centre distance of 3.80 m. The two concentrated loads consisting the loadings were applied at points situated 2.0 m apart, symmetrically disposed in relation to the centre of the beam.

Table 5.1 AGGREGATE SIEVE ANALYSIS

Sieve Sizes (mm)	Percentage Passing	
19.05	-	99.04
9.52	-	15.3
4.76	-	10.6
2.36	83.5	-
1.18	66.5	-
600μm	21.4	-
300μm	4.39	-
150μm	0.57	-

The corresponding grading curve is shown in appendix. The result indicate that the coarse aggregate grading falls within the zone 'C' of the grading reauirement in accordance with the British Standard B.S.882:1973.

Table 5.2: **GENERAL DETAILS OF TEST BEAMS**

Beam No	Tensile reinforcement	Area of tensile reinforcement (mm^2)	Percentage of tensile reinf ω	Modulus of elasticity of steel E_s	Modulus of elasticity of concrete E'_{bo} KN/m^2	Average Cube strength of concrete N/mm^2
B-I	2Y16	402	1.340			
B-II	2Y10	157	0.523			
B-III	2Y8	101	0.337	2.1e8	1.9e7	15.2
B-IV	5Y10	393	1.310			
B-V	3Y10	236	0.787			
B-VI	4Y10	314	1.046			

All the experiments were carried out in the Concrete and Structures Laboratory, Department of Civil Engineering ABU Zaria. The machine used is the "MFL UTSYSTEM". The main features of the machine are as follows;

a) a cabin from which the jacks are controlled hydraulically through hoses.

b) a dial gauge from which the load level can be read.

c) jacks which be adjusted depending on the beam span.

The loads were applied using two hydraulic jacks of total capacity equal to 100kN.

Hence there is a region of pure, constant bending moment in the beam where the deflection was measured. Figure 5.3 show schematically the test arrangement, the bending moment, and shear force diagrams showing the region of pure constant bending moment. The distribution of the applied concentrated loads is at 45 degrees to the neutral axis. Due to this distribution, the bending moment diagram at the points of load application is not angular, rather a smooth curve is obtained. Therefore, the region which is completely devoid of shear force and torsion is less than 200 cm. Figure 5.4 shows the arrangement of the apparatus used for the tests.

5.1.4 CUBE TESTS/CYLINDER TESTS

The crushing loads of the cubes specimens were determined using the compression machine. The machine applies load on the cubes until a maximum load (which corresponds to the ultimate compressive strength of the cube) is reached. The specimens subsequently fails by crushing.The failure load was the recorded.

The compressive strength at failure is obtained by dividing the failure load by the surface area of the cube: Thus

Compressive strength=Load at failure/surface area.

The specimen used were cubes of sizes 150mm by 150mm by 150mm. The tests were performed after curing for 28 days using wet jute bags. The results of cube/cylinder tests were plotted as shown in figures 5.5-5.7.

The modulus of elasticity of concrete was determined using the compresometer. The average value of the modulus of elasticity or the concrete which is 1.9*10 KN/mm was used for the evaluation of all the beams.

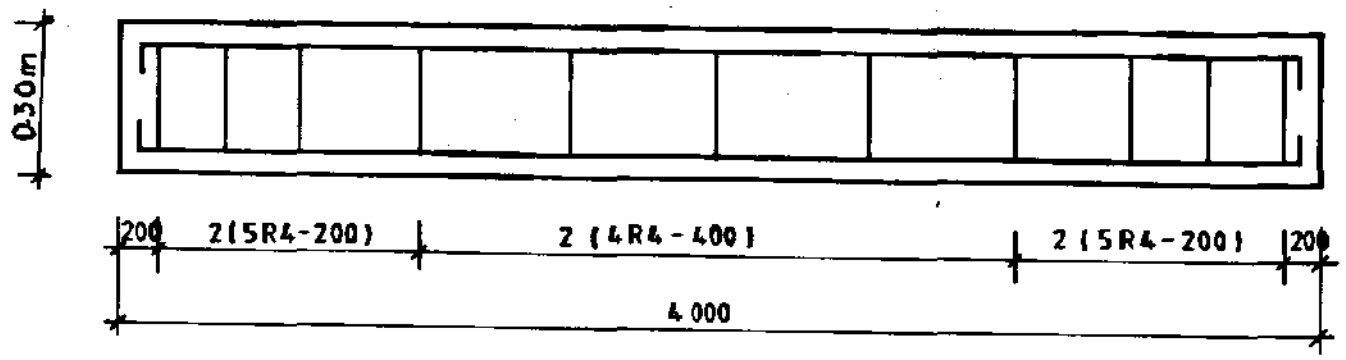


Fig. 5.1(a) Typical layout of reinforcements for Beams B-I, B-II and B-III.

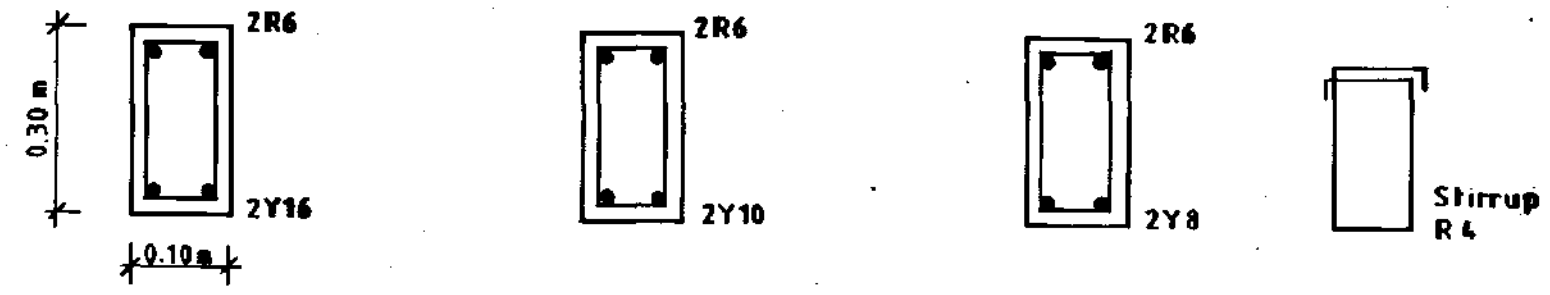


Fig. 5.1(b). Cross-sections of beams B-I, B-II and B-III.

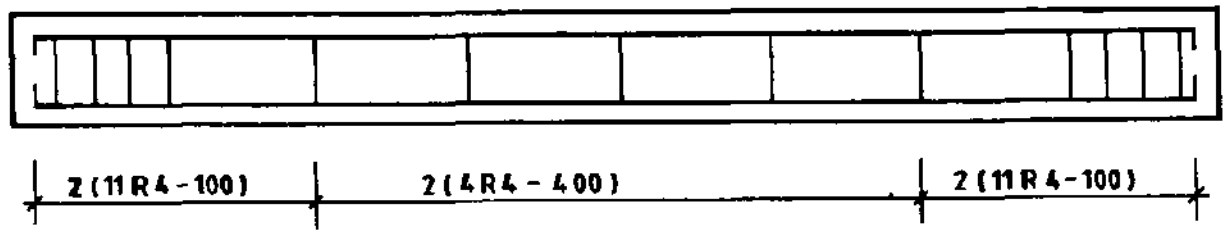


Fig. 5.2(a) Typical layout of reinforcements for beam-IV, beam-V, beam VI.

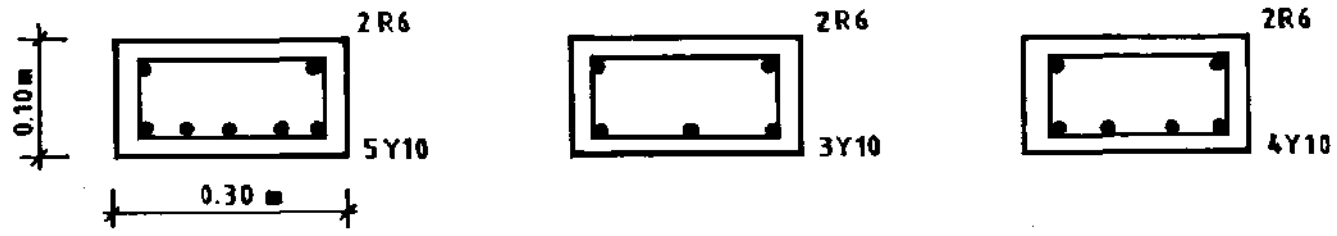


Fig. 5.2(b). Cross-sections of beams B-IV, B-V, B-VI.

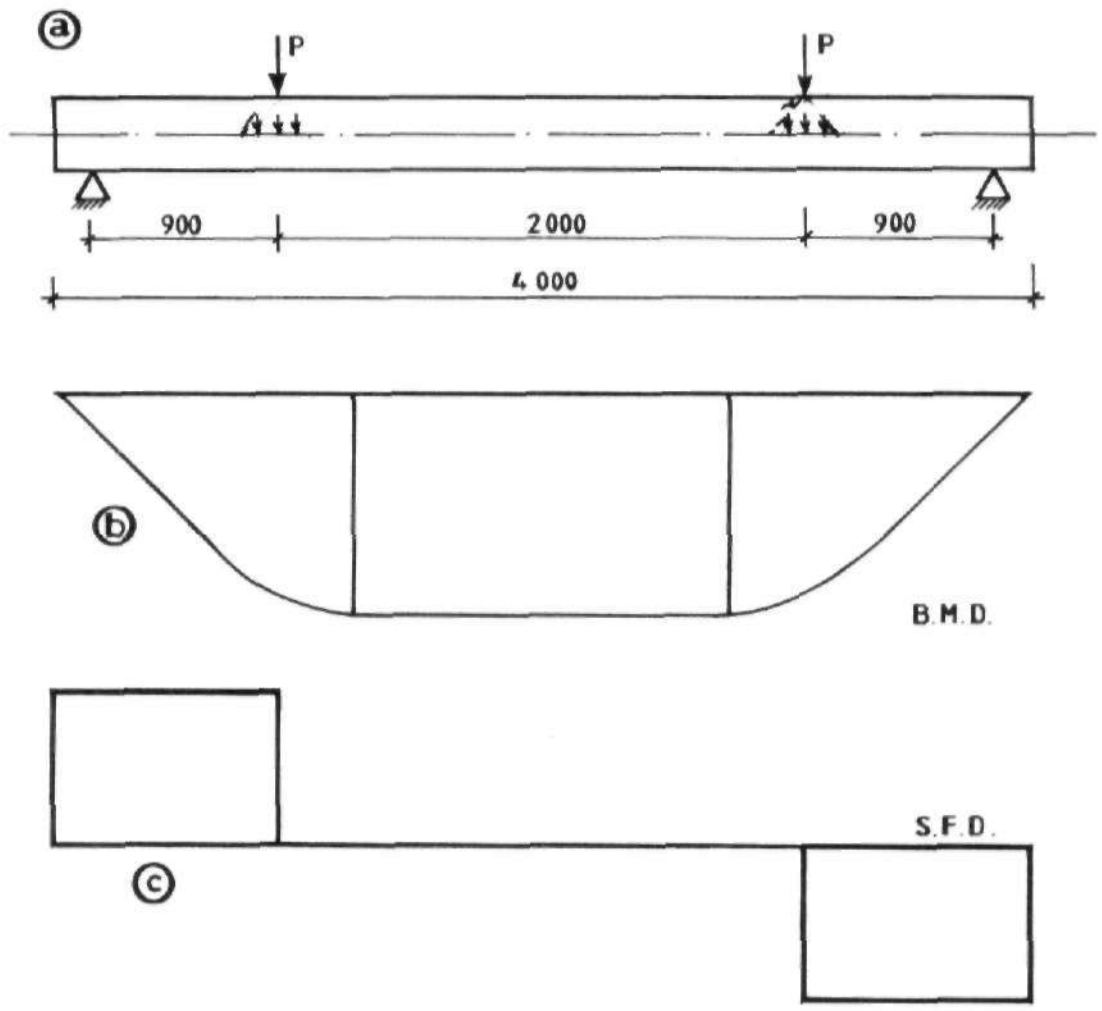


Fig. 5.3. Test arrangement showing bending moment and shear force diagrams.

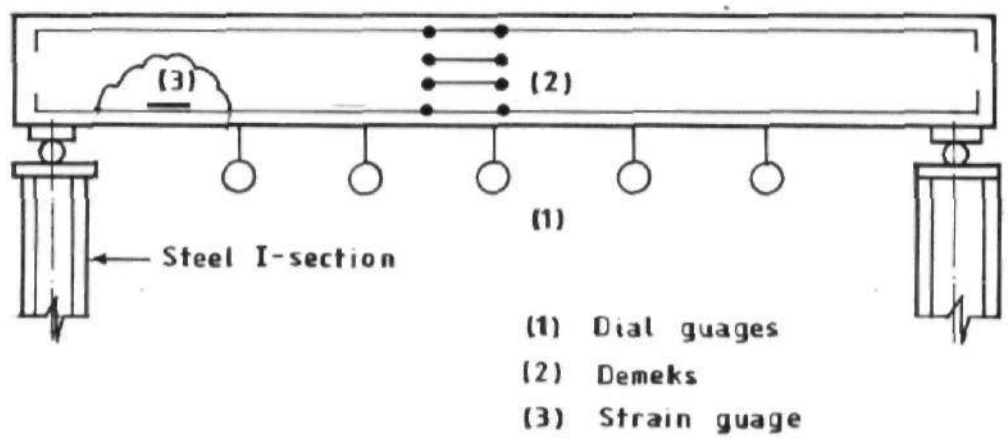


Fig. 5.4. Arrangement of measuring instruments.

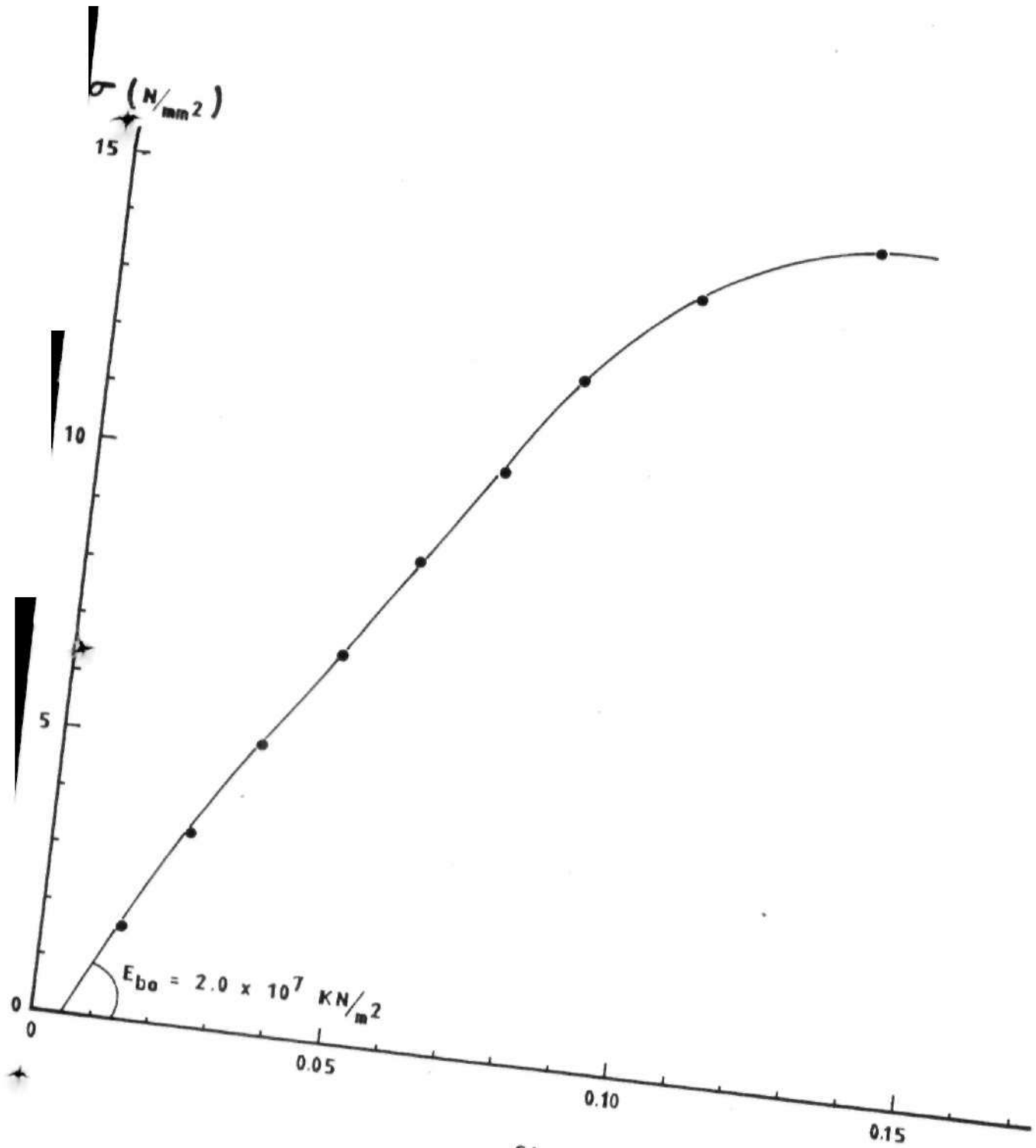


Fig. 5.5 Stress - strain curve for beams I and IV

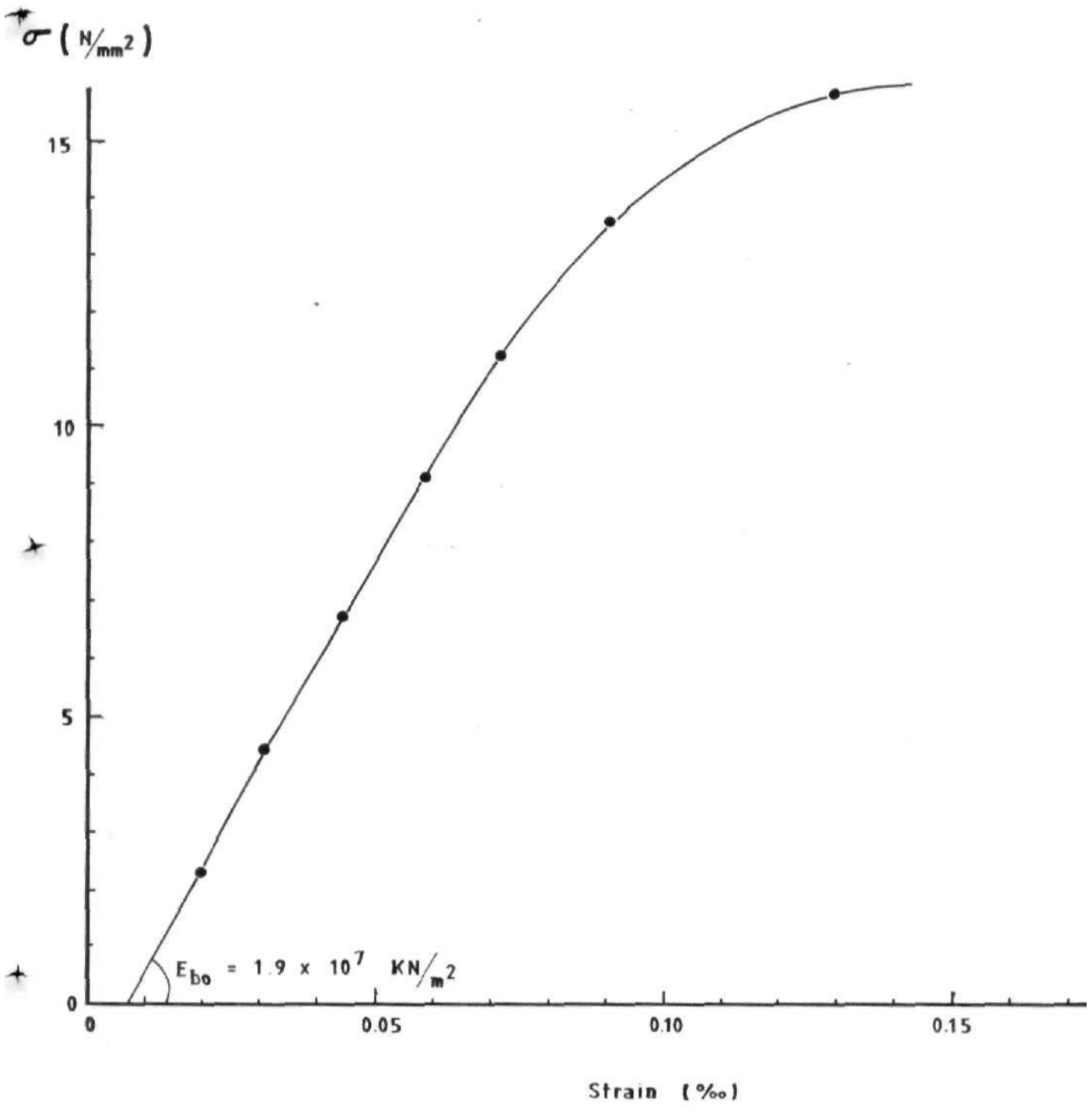


Fig. 5.6 Stress-strain curve for beams II and V.

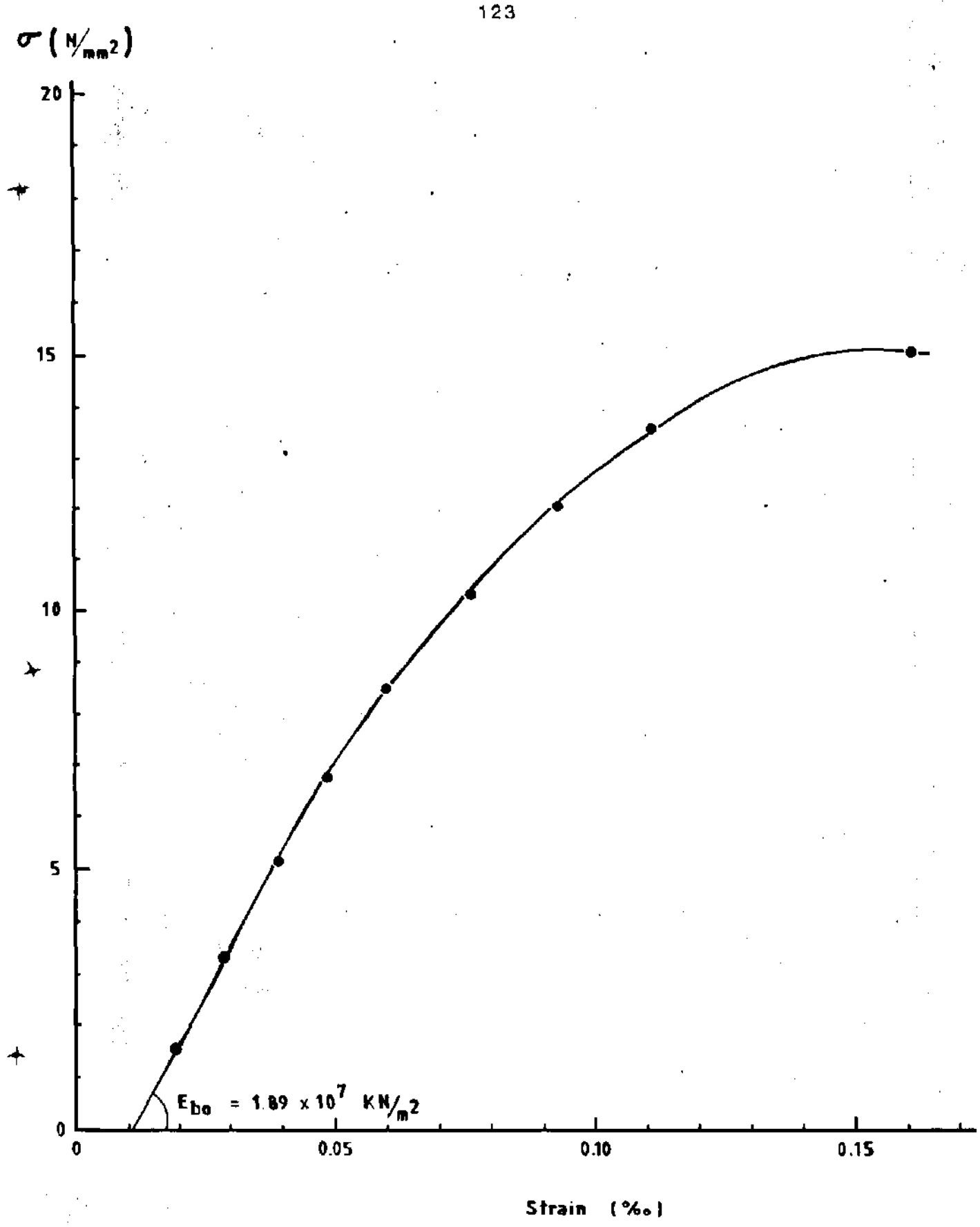


Fig. 5.7. Stress-strain curve for beams III and VI .

5.1.5 EVALUATION OF THE MEASURED DATA AND THE RESULTS

The data obtained from the experimental measurements were evaluated and utilized to give the required M-κ diagrams. Simple or circular bending was assumed. This is the type of bending produced by equal and opposite pure couples in which shear is absent. However, for analytical purposes, a parabola was used having same radius as the circle.(See fig 5.8). From the figure we can write that:

$$y = \frac{x_1^2}{2R}; \qquad R = \frac{x_1^2}{2y_1}$$

where y_i is the deflection and x_i is the distance from the origin.

The equation for the parabola was therefore solved to find its radius and hence the radius of curvature. The computer program used for this solution is attached in the appendix. The values thus obtained were plotted against the magnitude of the associated bending moment in the region of constant moments. Figures 5.6 - 6.2 embody the results for the beams BI - BVI.

5.1.6 OBSERVATIONS

For all the beams, deflection measurements were carried out using 1.0 cm dial gauges mounted at 50 cm intervals in the region of constant bending moment. The gauges were of different types: some are graduated in imperial units while some are in S.I. unit. This situation created some difficulties in reading the instruments because readings from the instruments which are graduated in imperial unit have to be converted to the S.I unit using appropriate conversion factor.

All the beams failed by flexure except Beam BI which failed due to shear failure. In slabs, the expected deflection was greater than in beams. The dial gauges alone was not sufficient to measure the deflection. Dumpy level and a half meter rule was used when the beam deflection was well over 1.0cm. The accuracy of the results obtained through these readings cannot be expected to be high because it was not possible to read tenths of millimetres as in the case of dial gauges.

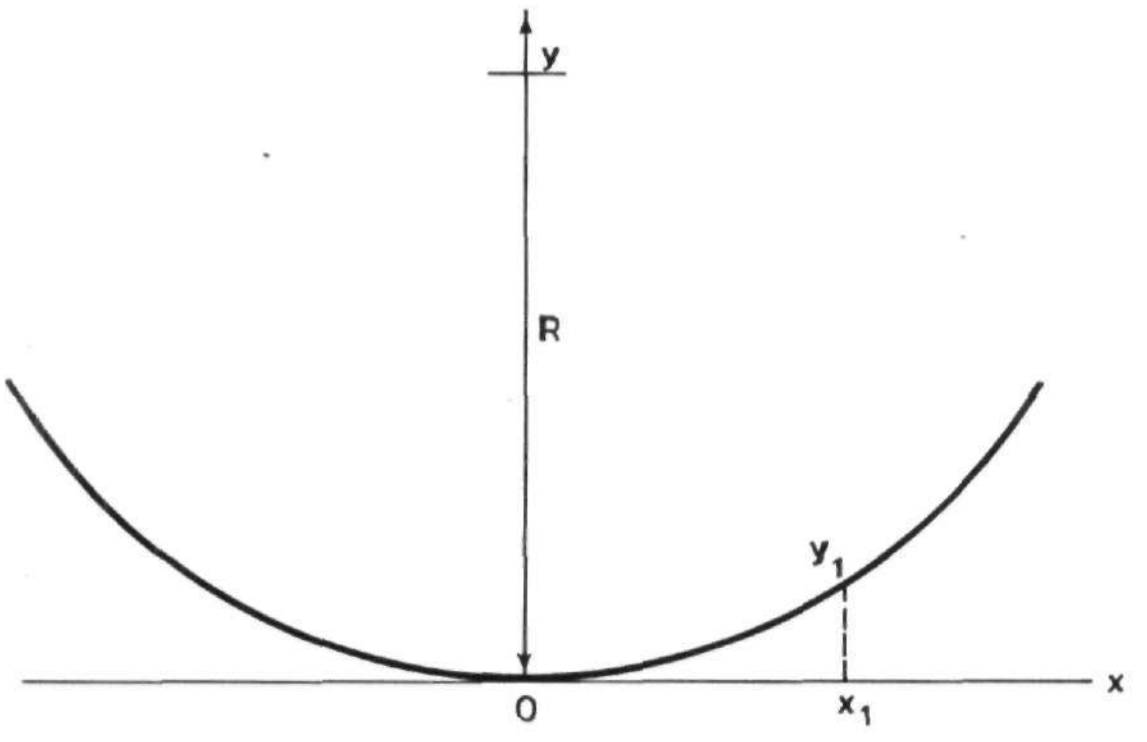


Fig. 5.8. Assumed parabola for analysing the experimental data .

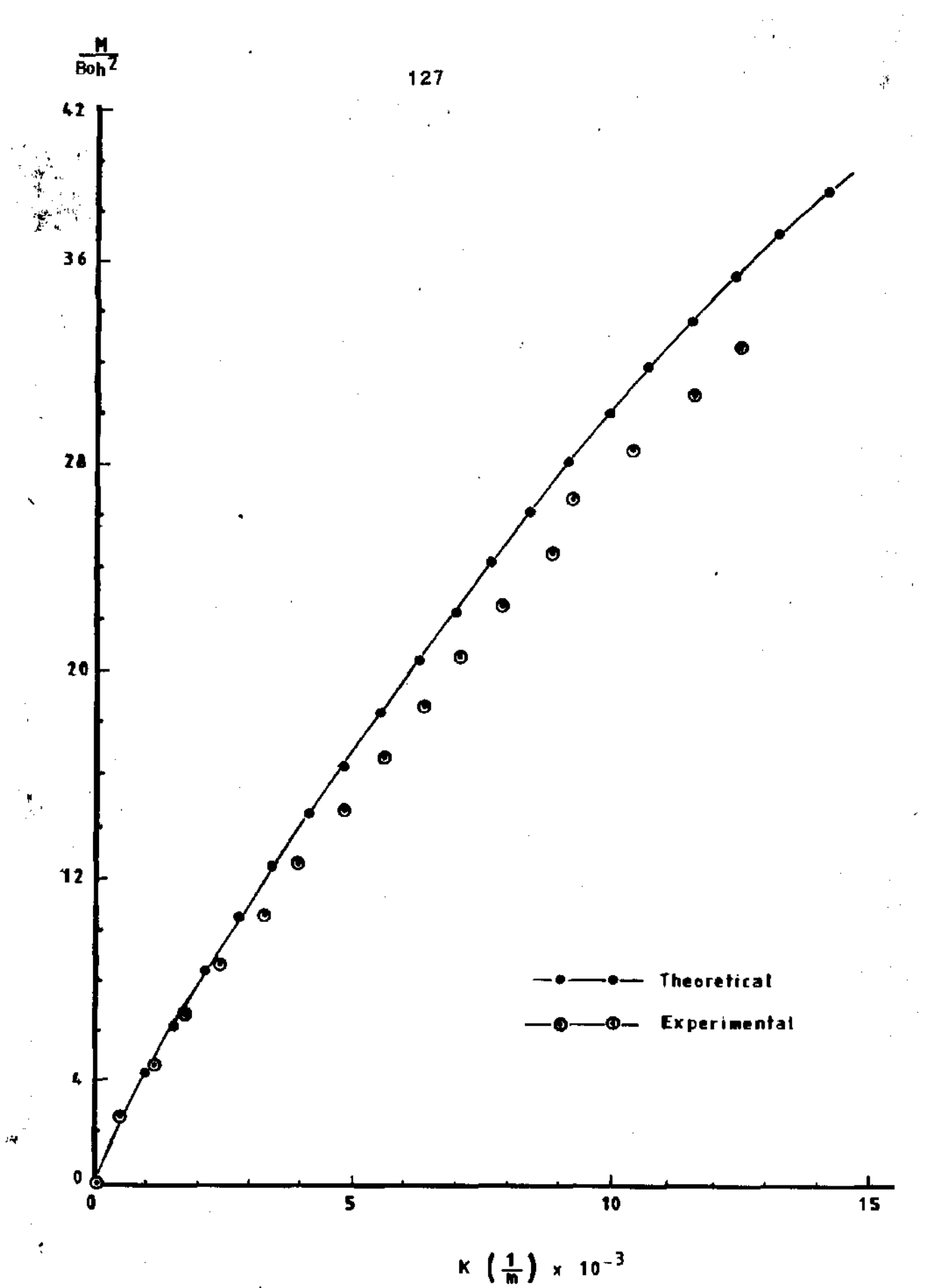


Fig. 5.9. Beam 1,2Y16, Wo= 1.340

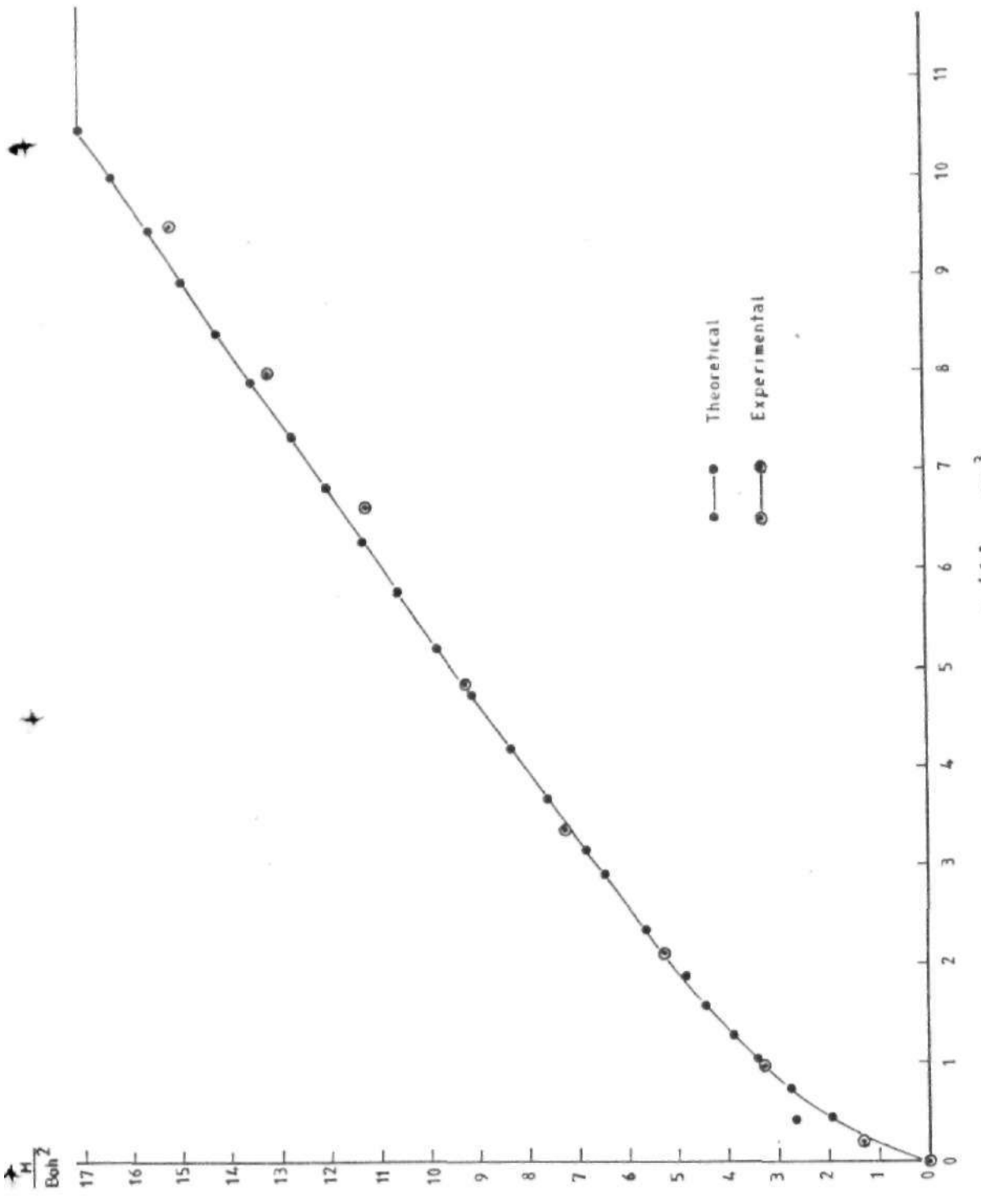


Fig. 5.10. Beam II, 2Y10, W_o = 0.523

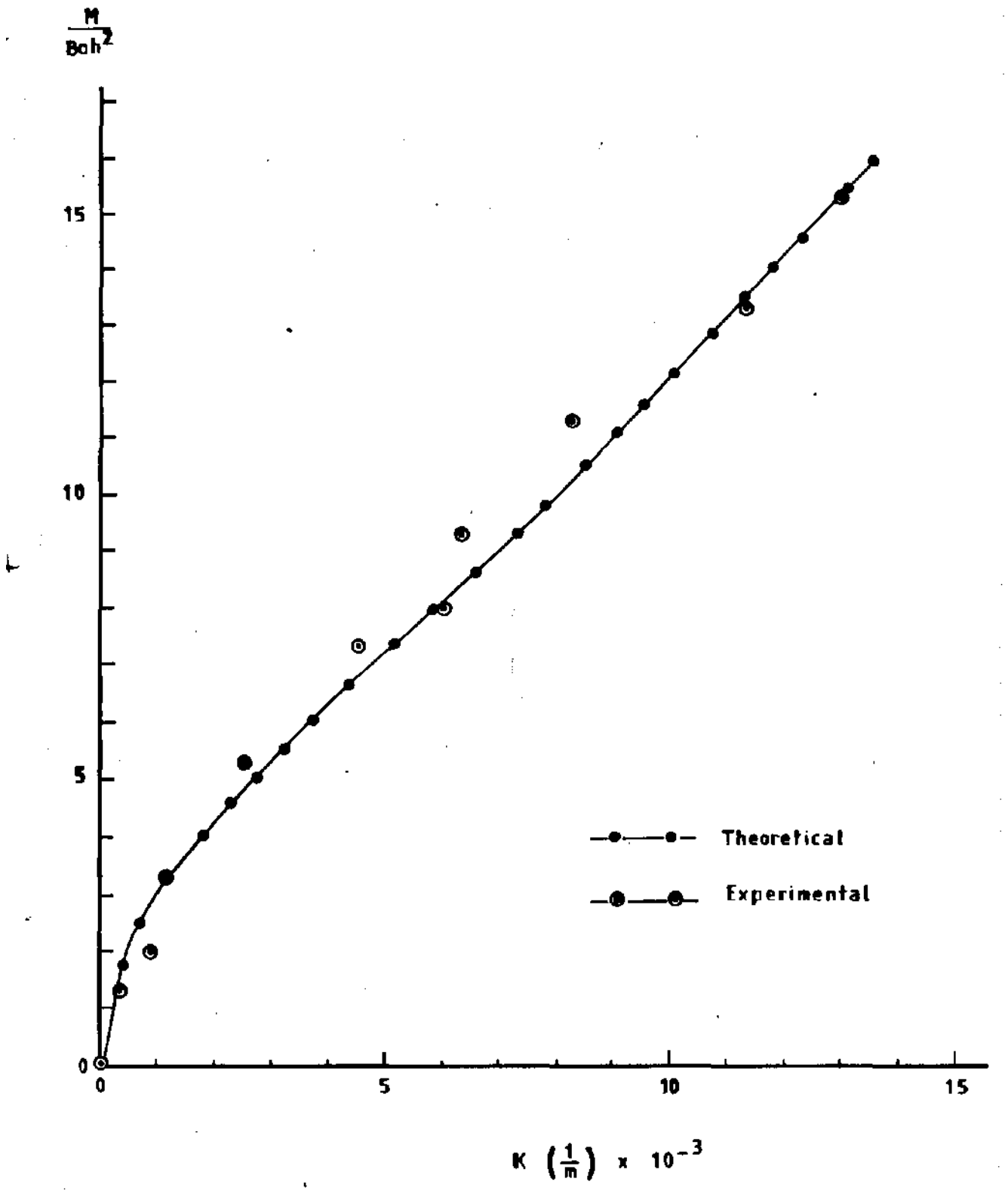


Fig. 5.11. Beam III, 2Y8, Wo = 0.337.

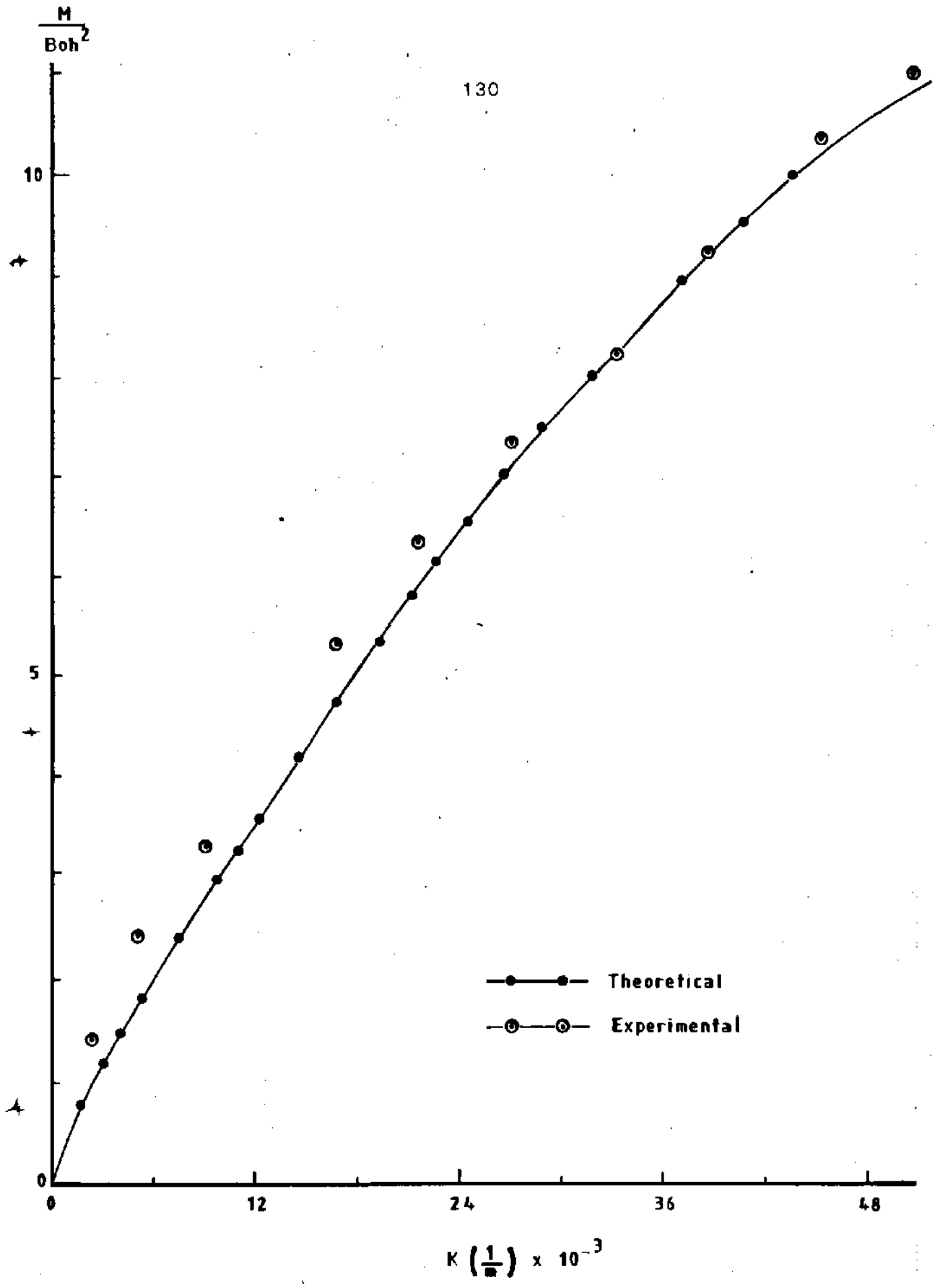


Fig. 5.12 Beam IV, 5Y10, Wo = 1.310.

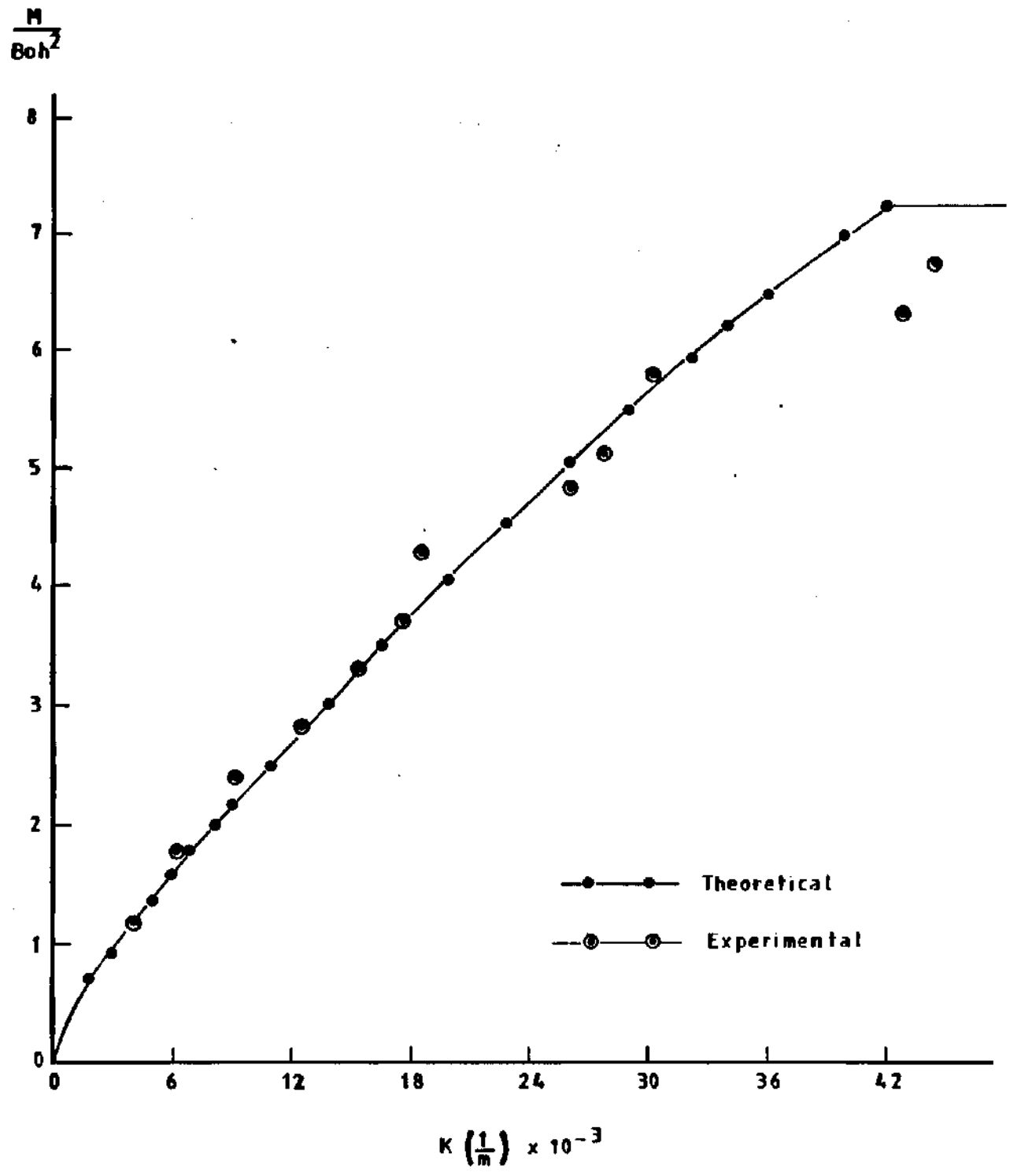


Fig. 5.13. Beam V, 3Y10, Wo = 0.787

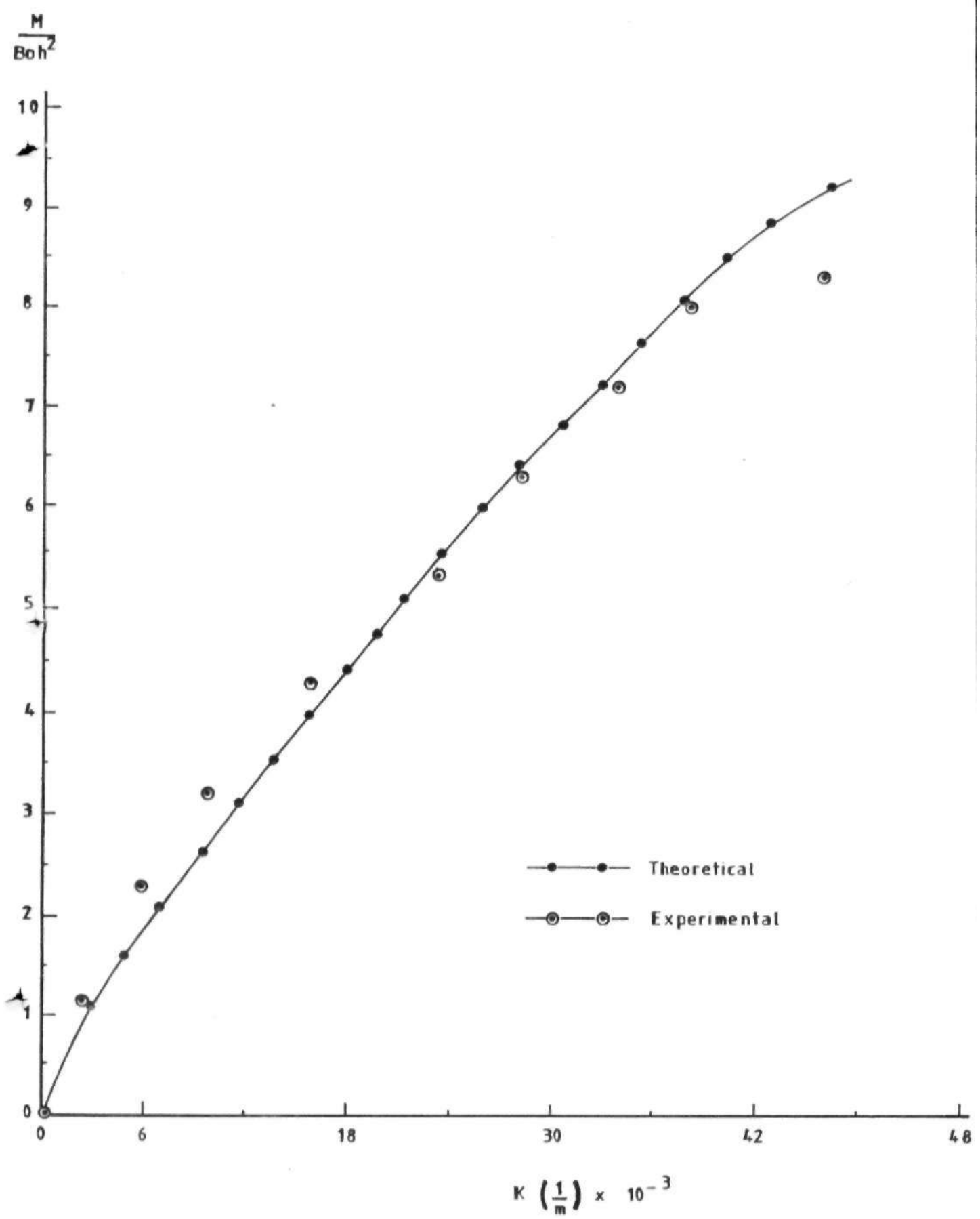


Fig. 5.14. Beam VI, 4Y10, Wo = 1.046.

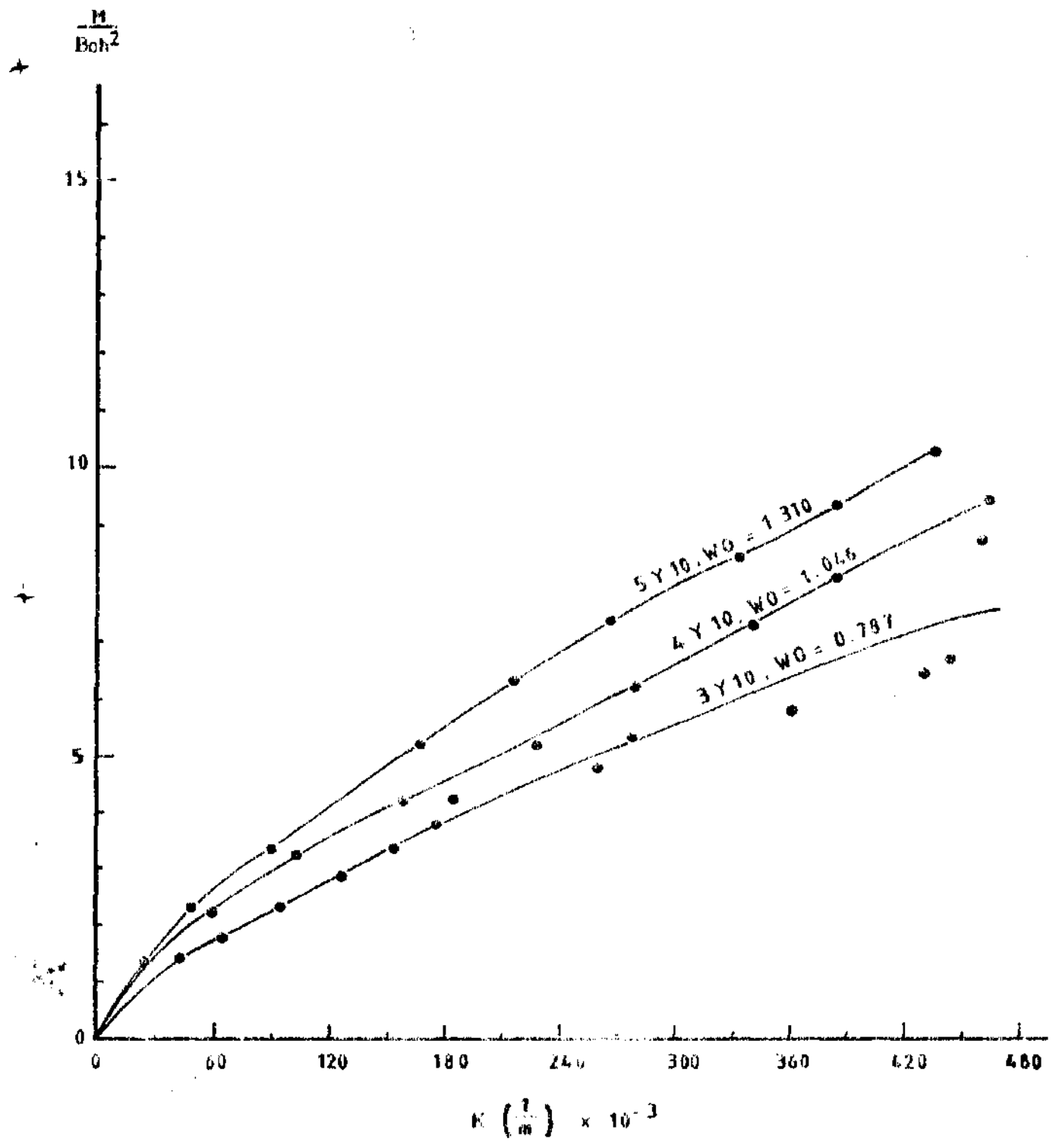


Fig. 5.15. Comparison of experimental results for beams cross-section b x h = 300 mm x 100 mm

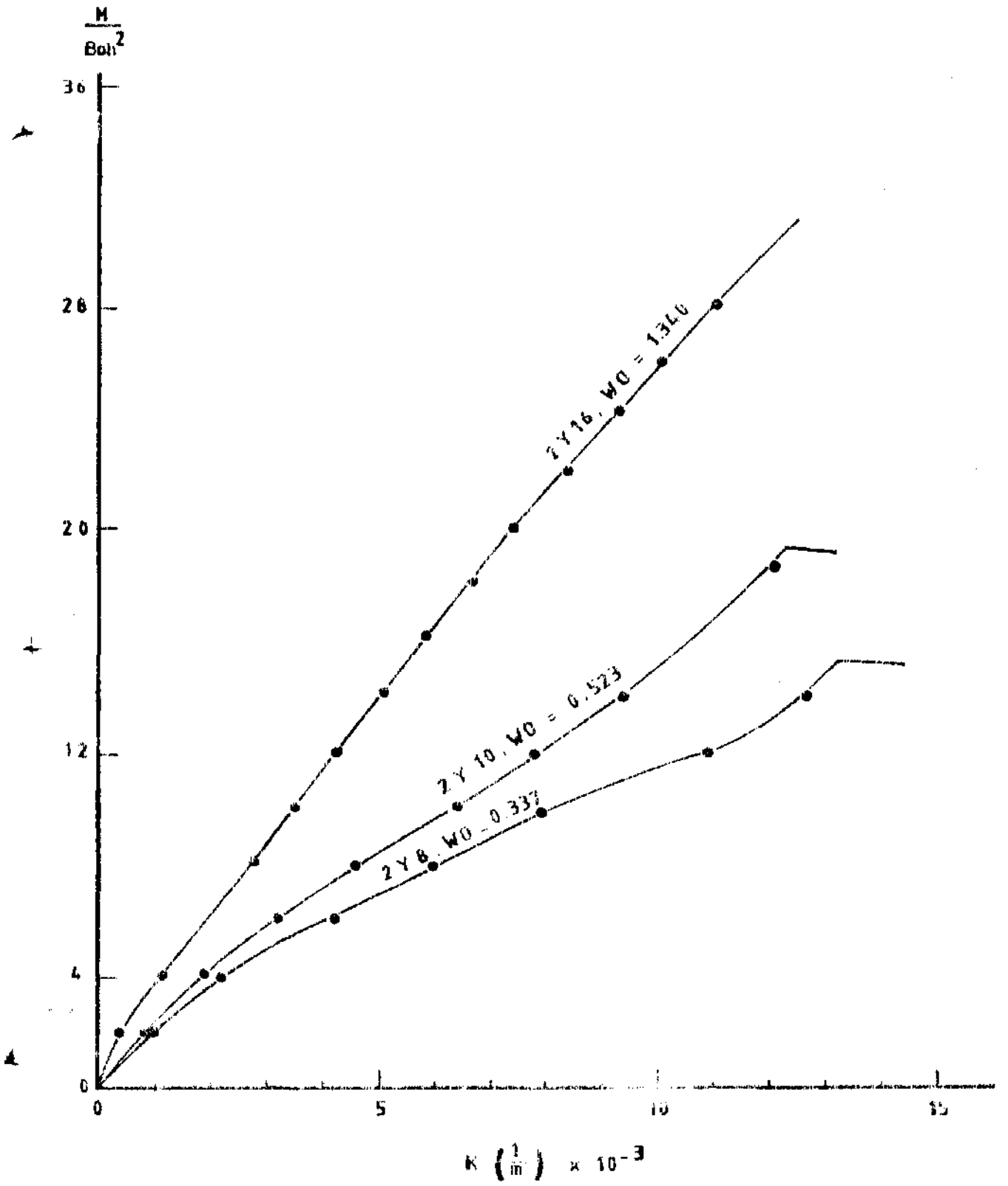


Fig. 5.16. Comparison of experimental results for beams cross-section b x h = 100mm x 300 mm.

5.2 CONCLUSIONS AND RECOMMENDATIONS

5.2.1 CONCLUSIONS

1 There are many factors which influences the shape of the moment-curvature relationship. Some of these factors have been fully discussed in chapter one. They include:

- the shape of stress-strain curve of concrete in tension and compression.
- the $\sigma(\varepsilon)$ relationship of steel reinforcement.
- geometry of the cross-section and the placement of steel reinforcement.
- environmental factors, loading history, concrete constituents, duration of loads etc.

2 However, the most difficult factor to be taken into consideration was the stress-strain relationship of concrete in tension and compression. All the analytical formulae used to represent the stress-strain diagram of concrete in both tension and compression are complicated and difficult to use for any practical purposes. For this reason, it was necessary to use simplified shapes to represent the stress-strain relationships of concrete.

The progressive micro-cracking in reinforced concrete beams under increasing loads was accounted for by considering concrete to have a non-zero tensile carrying capacity.

This was achieved by using stress-strain diagram which includes strain softening (gradual descending tail).

In order to approach reality as close as possible, the stress-strain curve of concrete in compression was assumed a second degree parabola. Tensile stress-strain curve was approximated to a bilinear curve. These approximations led to a third degree equation according to the equilibrium of internal forces. The equation was easily solved using a computer program to determine the position of the neutral axis. Having the position of the neutral axis, it was possible to calculated the moments and the curvatures for an assumed value of strain in the tensile reinforcement. In this way and for increasing values of tensile steel strain, the $M(\kappa)$ diagram was obtained. Accuracy of this approach was good enough for practical purposes for determining the deflections of reinforced concrete beams subjected to short-time loading. This claim was confirmed by experimental results obtained both by the author and by previous researchers.

4 The method presented in this research work is accurate enough to be used for the purposes of determining the $M(\kappa)$ relationship and deflections instead of the oversimplified methods recommended in most literature and codes of practices. This assertion is confirmed by the theoretical and experimental results obtained both by the author and other researchers.

In most reinforced concrete textbooks and codes of practice, control of deflections is usually based on the effective span-depth ratios. This method is primarily a rule-of-thumb approach based mainly on experience. However, it gives good results due to the fact that structures seldom receive their full design loads. In concrete structures where deflection control is a design criterion, the method presented in this thesis gives more realistic solutions because materials behaviours are more realistically accounted for.

In the model proposed by Bazant and Oh (1984), the general $\sigma(\varepsilon)$ curve for concrete in compression was used which is complicated and therefore difficult to use for analytical purposes. Moreover, the computational effort needed for the theory proposed in this work is much less compared with the model proposed by Bazant and Oh. The computational work needed to solve this theory consists of solving a third degree equation to determine the depth of neutral axis. Whereas in the case of Bazant and Oh model, the solution is complicated with integral.

The presented theory has broader application compared to Branson's formula which is limited to the serviceability range of loads. Whereas the presented theory can predict deflection up to the ultimate load.

5 Moment-curvature curves obtained in this research work tend to "bend-over" at higher moment levels due to the stress-strain behaviour of concrete and the percentage of

steel reinforcement.

Lightly reinforced cross-sections

results in s-shaped moment-curvature curves up to the point of yielding of tensile reinforcement. In heavily reinforced sections, the moment-curvature curves are steep: almost a straight line from the origin to the point of yield stress of tensile reinforcement.

5.2.2 RECOMMENDATIONS

1. The Nigerian Code of Practice NCP 1 1973 section 3.10.3 which deals with calculation of deflection should be reviewed. The formula given in the Code was based on the I-effective method of evaluating deflections. However, all the components of the formula cannot be expressed in the unit of stiffness. Moreover, the formula does not contain any variable bending moment hence the I-effective as expressed in the formula is not for the entire span of the beam but appears to be just for a particular value in the beam. The error should be looked into and corrected.

2. Further investigation should be made in order to determinate more accurately the value of cracking moment M_{cr} It is generally known that in concrete, micro-cracking is a continuous process hence no value of bending moment can be assigned to its formation.

However, if the value of the cracking moment can be obtained accurately, use of bilinear M-κ relations would be more realistic in the evaluation of deflections.

3. The effect of long time behaviour of concrete on the M-κ relationship of concrete should be further investigated.

4. Although the theory was developed for T-beams, only one case was solved; that is the case when the neutral is on web. Various other cases of the positions of the neutral axis on the flange, as well as the lines of tensile stress peaks and of points where the stress is reduced to zero relative to the bottom flange should be investigated.

REFERENCES

ACI Committee 435. "Deflection of reinforced concrete flexural members." (ACI 435-2R-66). Reaffirmed in 1979. American Concrete Institute, Detroit 1966, 29pp.

Ahmad, S.H., and Shah, S.P., "Stress-Strain curve of concrete confined by spiral reinforcement." ACI Journal Vol. 79, Nov- Dec 1982 pp 484-490.

Ahmad, S.H., and Shah, S.P., "Complete triaxial stress-strain curve for concrete." ASCE Proceedings Vol. 108 st.4 April 1982. pp 728-742.

Alexander, S., "A simple equation for the stress-strain curve of concrete."Indian Concrete Journal (Bombay) Vol. 39, No. 7 July, 1965 pp 274-277.

Alwis W.A.N., "Trilinear moment-curvature relationship for reinforced concrete beams. "ACI Structural Journal Vol. 87, May -June, 1990 pp 276-283.

Ansan, F., "Stress-Strain response of micro-cracked concrete in direct tension". ACI Material Journal Vol.84, No 6 Nov- Dec 1987 pp 481-490.

Astil, A.W., and Martin, L.N, "Elementary Structural Design to CP 110." Pitman press Great Britain. pp 272.

Bach and Graf. "Versuche mit Eisenbetonbalken zur ermittlung der Beziehungzwischen formanderungswinkel und Biegungsmoment"
Bulletin No 38, Deutcher Ansschuss fur Eisenbeton 1917 Berlin.

Balavadze, B.K, "Influence of reinforcement on the characteristics of tensile concrete." Beton i Zhelezobeton USSR. pp 462-465.

Barnard, P.R, "Researches towards the complete stress-strain curve of concrete." Magazine of Concrete Research Vol. 16, No 49 Dec 1964 pp 203-210.

Bazant, Z.P, and Oh, Byung. H., "Deformation of progressively cracking reinforced concrete beams." ACI Journal, Proceedings Vol. 81 May-June 1984 pp 268-278.

Bazant, Z.P, and Chern, J.C. "Strain-Softening with creep and exponential algorithm."Journal of Engineering Mechanics ASCE Vol III, ST-3, 1985 pp 391-415.

Beeby, A.W, "A note on an aspect of variability of deflection." Magazine of Concrete Research Vol.26, No 88 1974, pp 161-168.

Branson, D.E. and Trost, H., "Unified procedures for predicting the deflection and centroidal axis location of partially cracked non prestressed and prestressed concrete member." ACI Journal, Proceedings Vol. 93 March - April 1983, pp 119 - 130.

Branson, D.E., "Deformation of Concrete Structures." MaGraw - Hill Book Co. New York, pp 546.

Berg, O.Y., and Voprosu, K., "O prochnosti i plastichnosti betona."Dokladi Akademi Nauk Moscow. Vol. 70, No. 4 pp 617.

Bosco et al "Minimum reinforcement in high strength concrete." Journal of structural Engineering ASCE Vol. 116, No 2; 1990 pp 427-437.

Brock, G. " Concrete complete stress-strain curves" Engineering Vol. May 1962 pp 606-608

Carreira, D.J.; Chu, Kuang-Han. "Stress-Strain relationship for plain concrete in tension" ACI Journal Proceedings Vol. 83 Jan-Feb 1986 pp 21-28.

Carreira, D.J.;Chu, Kuang-Han. "The moment-curvature relationships of reinforced concrete members". ACI Journal March-April, 1986. pp 191-198.

Cognini, S; et al "Viscoelastic moment-curvature diagrams". ACI Material Journal Vol. 84, Nov. 1987 pp 519-524.

Desayi, P and Krishan, S; "Equation for stress-strain curve of concrete" ACI Journal Vol. 61, No. 23, 1964 pp 345-350.

Desayi, P and Viswanatha, C.S.; "The deflection of reinforced concrete beams in short-time loading tests". Indian Concrete Journal, Vol. 39, No.7 1965, pp 111-115.

Evans, R.H.; and Marathe, M.S.; "Micro-cracking and stress-strain curve for concrete in tension". Materials and Structures/research and Testing (RILEM) Paris Vol. 1, No 1, 1968 pp 61-64

Everard, K.A. "The flexural rigidity of reinforced concrete". Magazine of concrete research, Vol 14, No 42 1963 pp 165-170.

Gilkey, H.J.; Murphy, G.; "Stress-strain characteristics of mortars and concretes". Proceedings ASTM Vol.38 Part I, 1963 pp 318- 326.

Gopolarotnam, V.S.; Shah S.P., "Softening response of plain concrete in direct tension". ACI Journal Proceedings Vol. 82, May-June 1985. pp 310-323.

Guo-Zhen-hai;and Zhang Xin-qin: "Investigation of complete stress-deformation curves for concrete in tension"
ACI Journal Proceedings Vol. 84, No 4, 1987. pp 278-285.

Hognestad et al; "Complete stress distribution in ultimate strength design". ACI Journal, Proceedings Vol. 52, No 4, 1955 pp 455-479.

Hsu C.T.T. "Reinforced concrete members subjected to combined biaxial bending and tension. ACI Journal Vol 83 No 10, 1986 pp 200-205.

Hsu C.T.T., et al " Microcracking of plain concrete and the shape of the stress-strain curve. ACI Journal Vol. 63 No 6, 1960 pp 209-223.

Hughes, B.P. and Chapman G.P., "The deformation of concrete and microconcrete in compression and tension with particular reference to aggregate size". Magazine of Concrete Research Vol 18 No 54, 1966 pp 19-24.

Jones, R. "A method of studying the formation of cracks in materials subjected to stresses". British Journal of applied Physics (London) Vol. 3, No. 7, 1952. pp 229-232.

Kucynski, W. "The problem of variable stiffness of reinforced concrete beams as due to the non-linear elasticity of concrete".
Bulletin de l'academia Polonaise Des Sciences series des science techniques. Vol.9 pp 371-381.

Kent, D.C., and Park, R., " Flexural members with confined concrete". Journal of structural division ASCE Vol.,97, St. 7, 1969 pp 1969-1990.

Kakuta, Y. et al "Moment-Curvature relationship of reinforced concrete slabs". Transactions of Journal of Structural Engineering ASCE Vol.14, No 3 pp 369-373.

Kriz, L.B., and Lee, S.L., "Ultimate strength of over-reinforced beam". Proceedings ASCE Vol.16, EM 3 pp 95-105.

Kotsovos "Effect of testing techniques on the post-ultimate behaviour of concrete in compression". Materials and Structures Vol.16, No 91, 1983. pp 3-12.

Kaminska, M., Czkwianianc A, "Method of Analysis of Prismatic Members and its Pracical Applications".
Prace Naukowe Instytutu Budownictwa Politechniki Nr 18, 1993. pp 65-68.

McNeedy, O.J and Lash, S.O., "Tensile strength of concrete"
ACI Journal Proceedings Vol 60, No. 6, 1963. pp 751-761.

Monnier, Th. "The Moment-Curvature relation of reinforced concrete beams". Heron, Vol.17 No 2, Delft.

Mander, J.B et al "Observed stress-strain behaviour of confined concrete". Journal of Structural Division ASCE Vol. 114, No. 8 1988. pp 1469-1471.

Neville, A.M., "Properties of Concrete". Pitman Publishing Ltd, London. 779 pp.

Neville, A.M, "Deflection control by Span/Depth ratio". Magazine of Concrete Research Vol 29, No. 98, 1977. pp 45-52

Nigerian Standard Code of Practice. Part 1; 1973. "The structural use of concrete in Building". Nigerian Standard Organisation, Lagos.

Park, R and Paulay, T. "Reinforced concrete structures, John Wiley and sons New York, 1975 pp 769.

Popovics, S "A review of stress- strain relationships for concrete". ACI Journal Vol. 67. No 14. 1970 pp 243-248.

Popovics, S "The fracture mechanism in concrete: How much we know" ?. Proceedings, ASCE Vol 93, 1969 EMS pp 531-544.

Prakhya, G.K.V. and Morley C.T. "Tension - stiffening and moment - curvature relation of reinforced concrete elements" ACI structural Journal Vol 87, No. S-61 1990 pp 507-605.

Reynolds C.E. and Stleadman, J.C. "Reinforced Concrete Designers Manual" Billing and sons Ltd, Surrey 1980 pp 890.

Richart, F.E. et al " A study of failure of concrete under combined compressive stresses". Bulletin No 185 University of Illinois Eng. Experimental station, Urbana III.

Saenz "Discussion of equation for stress - strain curve of concrete" by Desayi and Kristinan. ACI Journal Proceedings Vol. 61 No 9, 1964 pp 1229-1236.

Sakai, K and Kakuta, Y "Moment - curvature relationship of reinforced concrete members subjected to combined bending and axial forces". ACI Journal, Proceedings Vol. 77, No 3.1980 pp 189-194.

Smith and Young "Ultimate flexural analysis based on stress - strain curves of cylinders". ACI Journal Proceedings Vol 53, No 6 1956, pp 597-610.

Sinh and Gerstile "Stress - strain response of singly reinforced beams under cyclic loading". ACI Journal Proceedings Vol. 61, No 7. 1964 pp 1021-1038.

Shah, S.P. and Sankar, R. "Internal cracking and strain softening response of concrete under uniaxial compression". ACI Material Journal Vol 84, No 3. 1987. pp 200-212.

Srinivasa, P.R. and Subrahmanyan, B.U "Trisegmental moment - curvature relation for reinforced concrete member. ACI Journal No. 70, 1973 pp 346-351.

Turner, P.W and Barnard, P.R "Stiff constant strain rate testing machine" The Engineer (London) No. 5557. 1962 pp 146-148.

Vebo, A and Ghali, A "Moment - Curvature relation of reinforced concrete slabs". Journal of Structural Division ASCE
Vol. 103, No St 3. 1977 pp 515 - 531.

Wang, P.T. et al "Stress - strain curve of normal and lightweight concrete in compression". ACI Journal Vol. 75 1978. pp 603 - 611.

Warner, P.T. et al "Reinforced concrete". Pitman Publishing, New Zealand. 1982, 473pp

Yu, N.W. and Winter, G. "Instantaneous and long - time deflections of reinforced concrete beams under working loads".
ACI Journal Vol. 57, No.1 1960. pp 29 - 50.

C.P 110: 1972 "Code of practice for use of concrete", British standards Institutions.

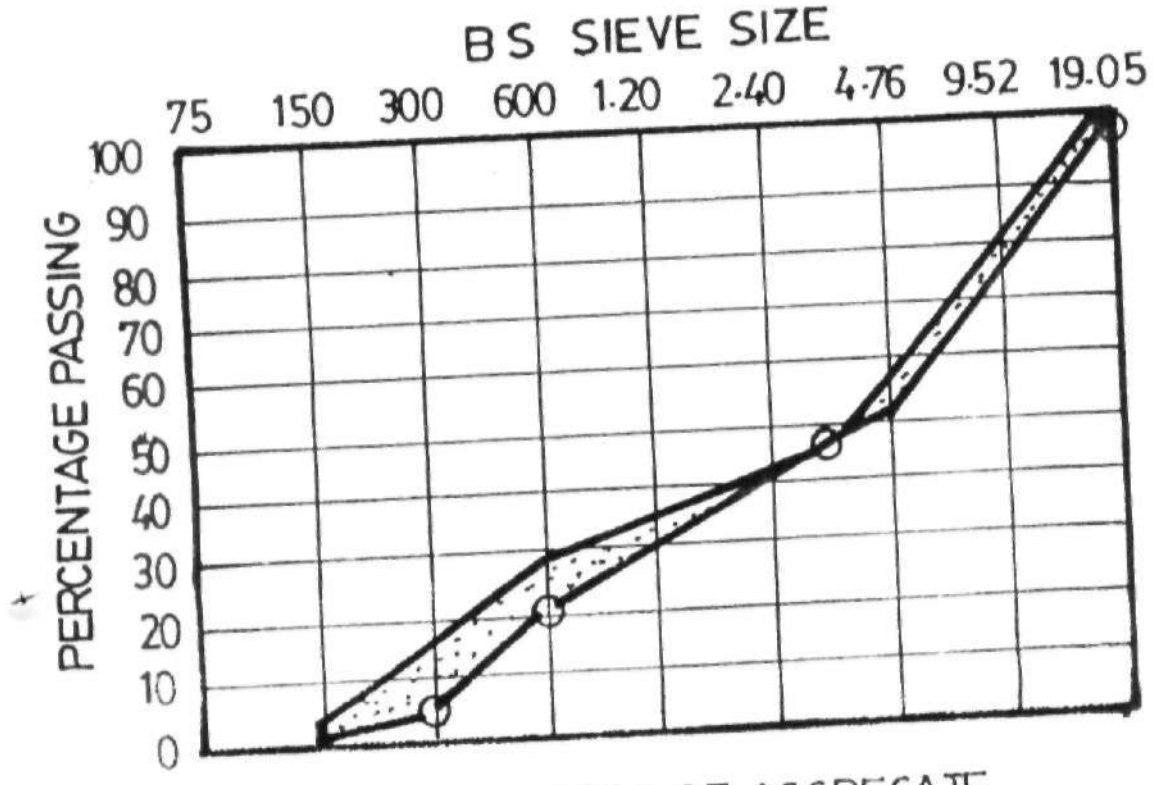


FIG. 5.0 : GRADING OF AGGREGATE

APPENDIX II
SOME SELECTED PHOTOGRAPHS



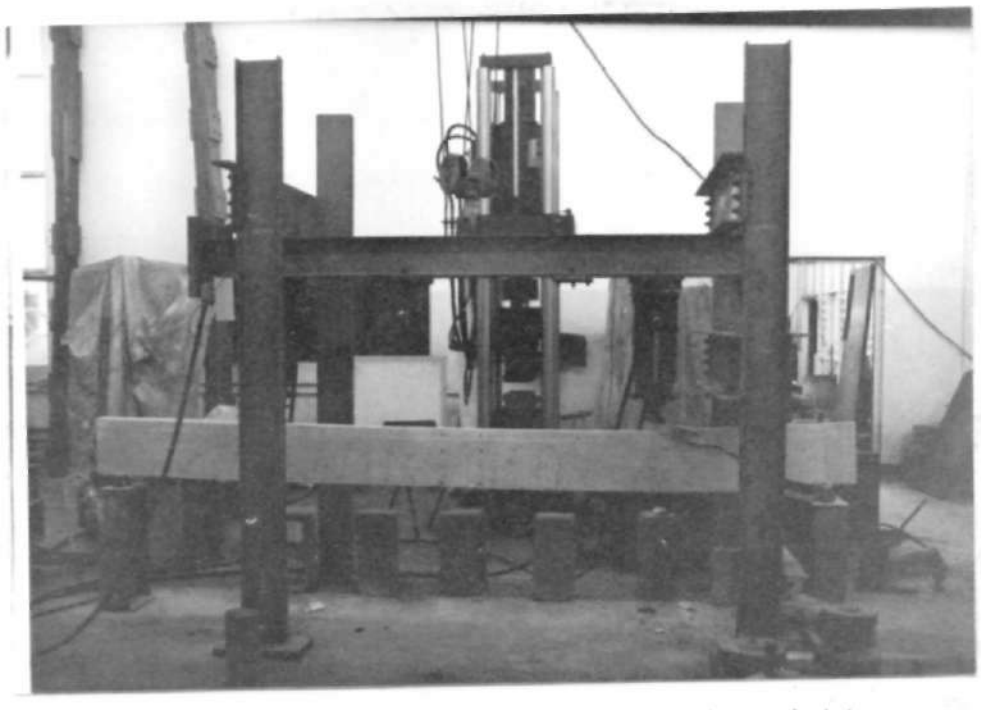
Cylinder Test



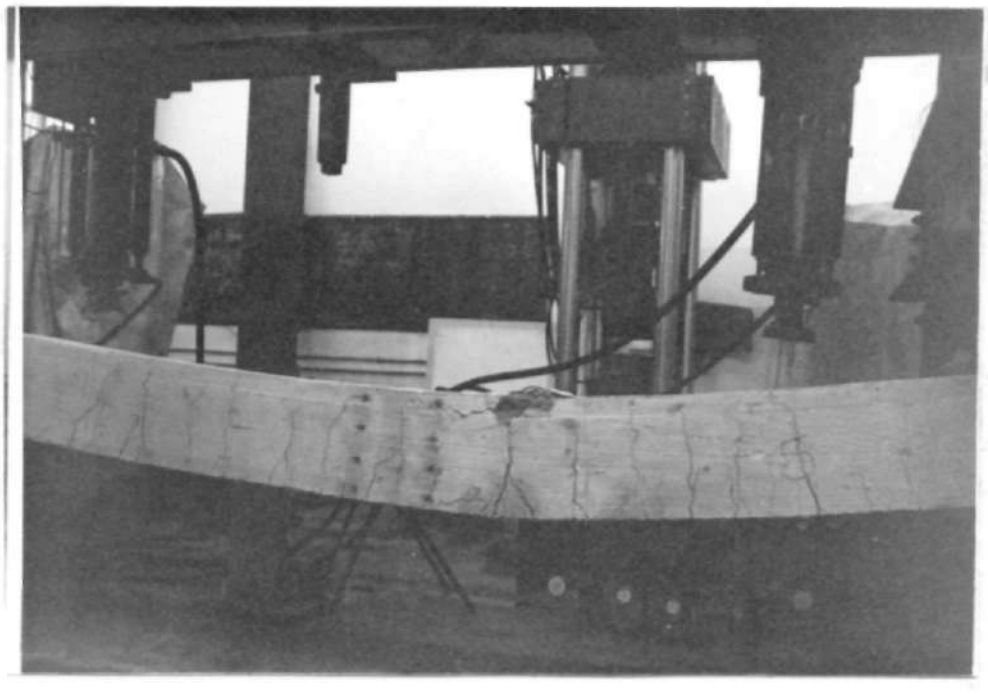
Formwork used for casting



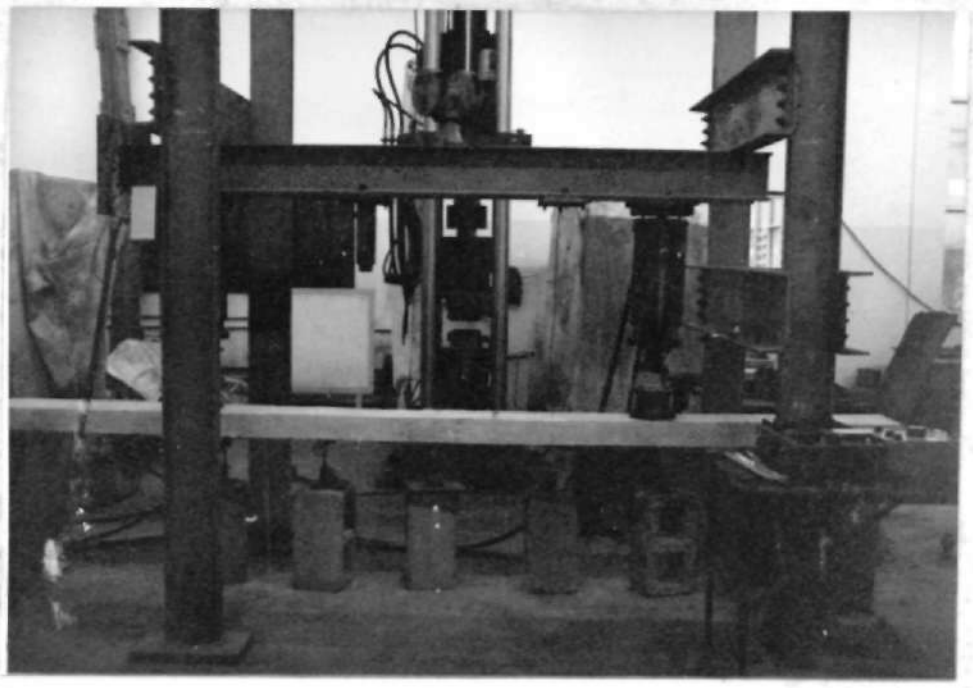
Getting ready for casting



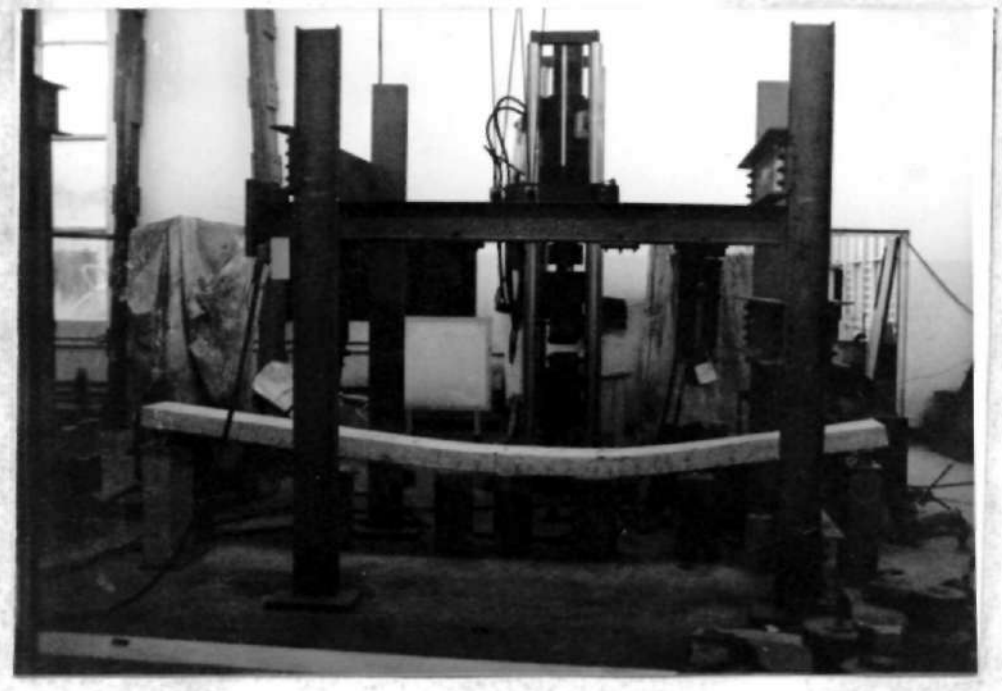
Beam B-I Showing Shear failure at the right support



Tested Beam



Beam Ready for testing



Tested Beam

APPENDIX III

LISTED PROGRAMS FOR CALCULATING MOMENT-CURVATURE RELATIONSHIP

```
10 ' PROGRAM FOR THE  COMPUTATION OF MOMENT-CURVATURE RELATIONS
20 'OKOLI, OBUMNEME GODWIN.
30 'Monnier equation first scheme (Full Triangle over tensile z
40 '
50 CLS
60 KEY OFF
70 'INPUT  OF DATA
80 INPUT "depth of beam";DO
90 INPUT "effective depth of beam";H
100 INPUT "BREADTH OF FLANGE"; BO
110 INPUT "Thickness of flange ";KHOH
120 INPUT "thickness of web"; KBOB
130 INPUT  "cover of compression reinforcement";KDH
140 INPUT "area of tension reinforcement";AS
150 INPUT "area of compression reinforcement ": ASPRIME
160 INPUT "MODULUS OF ELASTICITY OF STEEL";EA
170 INPUT  "modulus of elasticity of concrete": EB
180 INPUT "concrete compressive strain at max. stress";EPSILONE
190 INPUT "concrete ultimate strain in tension";EPSILONT
200 INPUT "concrete tensile strain at max. tensile strength";EP
210 '
220 PRINT
230 KBO = KBOB/BO:'PRINT "KBO =";KBO
240 KD =KDH/H :'PRINT "KD =": KD
250 KHO=KHOH/H:'PRINT "kho=";kho
260 OMEGAONE = AS/(BO*H):'PRINT "OMEGAONE =": OMEGAONE
270 OMEGATWO = ASPRIME /(BO*H):'PRINT "OMEGATWO =";OMEGATWO
280 NO =EA/EB:'PRINT "NO =";NO
290 '
300 ' main loop
310 '
320 P=1
330 OPEN "con" FOR OUTPUT AS #1
340 PRINT #P,"  ra      kx      kappa     rd    sigmaa   moment
350 FOR EPSILONA =.0000525 TO .00105 STEP .0000525
360 '  PRINT"epsilona=";EPSILONA
370    RA = EPSILONA/EPSILONBPRIME
380 FT=EB*EPSILONM
390 SIGMAA = EA*EPSILONA
400 ' PRINT "sigmaa=": SIGMAA
410 'COMPUTATION OF CO-EFFICIENTS OF THIRD DEGREE EQUATION
420 A= -((3+RA)-(1-KBO)*(3+RA))+3*NO*FT/SIGMAA*KBO*EPSILONA/EPS
430 B= 3*(1-(1-KBO)*(1+KHO*(2+RA)))-6*(NO-1)*OMEGATWO-6*NO*OMEG
AA*KBO*EPSILONA/EPSILONM*(1+2*DO/H)
440 C=3*KHO*(1-KBO)*(2+KHO*(1+RA))+6*(NO-1)*(1+KD)*OMEGTWO+12*N
T/SIGMAA*KBO*EPSILONA/EPSILONM*DO/H^2*(2*H+DO)
450 D=-(KHO^2*(1-KBO)*(3+KHO*RA)+6*(NO-1)*KD*OMEGATWO+6*NO*OMEG
MAA*KBO*EPSILONA/EPSILONM*DO^2/H^2
460    X = .3
470    XMIN = 0
480    XMAX =1
490    IF A*X^3 + B*X^2 + C*X+ D > .000001 THEN 840
500    IF A*X^3 + B*X^2 + C*X +D <-.000001  THEN 880
510 '   PRINT " KX=": X
520    KAPPA =RA*EPSILONBPRIME/(1-X)/H
530 '   PRINT  "KAPPA=": KAPPA
540    RD=X*RA/(1-X):'PRINT "RD=";RD
550 M1=BO*H^2*SIGMAA/24/NO/(1-X)/X*((4*(3-RD)-(4-RD)*X)*X^3-(1-
*(1-KHO)*(3*X-RD*(X-KHO))-(4*X-RD*(X-KHO))*(X-KHO))+24*OMEGATWO
(1-KD))
560 M2=BO*H^2*SIGMAA/24/NO/(1-X)/X*(24*NO*FT/SIGMAA/H^3*KBO*EPS
O-X*H)^2*X*(1/6*(DO-X*H)-1/2*(DO-H)))
570  M=M1-M2
580 'PRINT
```

depth of beam .25
height of beam .235
BREADTH OF FLANGE .29
Thickness of flange 0
Thickness of web .29
cover of compressive reinforcement .015
area of tension reinforcement .000151
area of compression reinforcement .000151
modulus of elasticity of steel 2.7E+07
modulus of elasticity of concrete 2.7E+07
concrete compressive strain at max. stress .002
concrete ultimate strain in tension .0018
concrete tensile strength 1350
concrete tensile strain at max. tensile strength .00005

ra	kx	kappa	rd	sigmaa	moment
0.026	0.552	0.00050	0.032	11025	5.88
0.053	0.554	0.00100	0.065	22050	11.74
0.079	0.556	0.00151	0.099	33075	17.59
0.105	0.557	0.00202	0.132	44100	23.41
0.131	0.559	0.00253	0.167	55125	29.22
0.157	0.561	0.00305	0.201	66150	35.01
0.184	0.563	0.00358	0.237	77175	40.77
0.210	0.565	0.00411	0.273	88200	46.52
0.236	0.567	0.00464	0.309	99225	52.24
0.263	0.569	0.00519	0.347	110250	57.94
0.289	0.571	0.00573	0.385	121275	63.61
0.315	0.574	0.00629	0.424	132300	69.26
0.341	0.576	0.00685	0.464	143325	74.88
0.367	0.579	0.00742	0.504	154350	80.47
0.394	0.581	0.00800	0.546	165375	86.04
0.420	0.584	0.00859	0.589	176400	91.57
0.446	0.587	0.00919	0.634	187425	97.07
0.472	0.590	0.00980	0.679	198450	102.54
0.499	0.593	0.01043	0.726	209475	107.97
0.525	0.596	0.01107	0.776	220500	113.35

STAGE II

depth of the beam .25
height of beam .235
BREADTH OF FLANGE .29
Thickness of flange 0
thickness of web .29
cover of compression reinforcement .015
area of tension reinforcement .000151
area of compression reinforcement .000151
MODULUS OF ELASTICITY OF STEEL 2.1E+08
modulus of elasticity of concrete 2.7E+07
concrete compressive strain at max. stress .002
concrete ultimate strain in tension .0018
concrete tensile strength 1350
concrete tensile strain at max. tensile strength .00005

ra	kx	kappa	rd	sigmaa	moment
0.026	0.531	0.00048	0.030	11025	5.05
0.053	0.482	0.00086	0.049	22050	7.35
0.079	0.442	0.00120	0.062	33075	8.56
0.105	0.412	0.00152	0.073	44100	9.39
0.131	0.388	0.00183	0.083	55125	10.03
0.157	0.369	0.00212	0.092	66150	10.55
0.184	0.353	0.00242	0.100	77175	10.98
0.210	0.339	0.00270	0.108	88200	11.36
0.236	0.327	0.00299	0.115	99225	11.69
0.263	0.316	0.00327	0.121	110250	11.99
0.289	0.307	0.00354	0.128	121275	12.26
0.315	0.298	0.00382	0.134	132300	12.51
0.341	0.291	0.00409	0.140	143325	12.74
0.367	0.284	0.00437	0.145	154350	12.95
0.394	0.277	0.00464	0.151	165375	13.15
0.420	0.271	0.00490	0.156	176400	13.34
0.446	0.266	0.00517	0.162	187425	13.52
0.472	0.261	0.00544	0.167	198450	13.69
0.499	0.256	0.00571	0.172	209475	13.86
0.525	0.252	0.00597	0.176	220500	14.01
0.551	0.247	0.00623	0.181	231525	14.16
0.578	0.243	0.00650	0.186	242550	14.30
0.604	0.240	0.00676	0.190	253575	14.44
0.630	0.236	0.00702	0.195	264600	14.58
0.656	0.233	0.00728	0.199	275625	14.71
0.683	0.230	0.00754	0.204	286650	14.83
0.709	0.227	0.00780	0.208	297675	14.95
0.735	0.224	0.00806	0.212	308700	15.07
0.761	0.221	0.00832	0.216	319725	15.19
0.788	0.219	0.00858	0.221	330750	15.30
0.814	0.216	0.00884	0.225	341775	15.41
0.840	0.214	0.00909	0.229	352800	15.52
0.866	0.212	0.00935	0.233	363825	15.63
0.893	0.209	0.00961	0.237	374850	15.73
0.919	0.207	0.00987	0.240	385875	15.83
0.945	0.205	0.01012	0.244	396900	15.93
0.971	0.203	0.01038	0.248	407925	16.03
0.998	0.202	0.01063	0.252	418950	16.13
1.024	0.200	0.01089	0.256	429975	16.22

STAGE III

height of beam .235
BREADTH OF FLANGE .29
Thickness of flange 0
thickness of web .29
cover of compression reinforcement .015
area of tension reinforcement .000151
area of compression reinforcement .000151
MODULUS OF ELASTICITY OF STEEL 2.1E+08
modulus of elasticity of concrete 2.7E+07
epsilonbprime .002
epsilont .0018
concrete tensile strength 1350
concrete tensile strain at max. tensile strength .00005

ra	kx	kappa	rd	sigmaa	moment
0.263	0.381	0.00361	0.161	110250	26.01
0.289	0.361	0.00385	0.163	121275	23.71
0.315	0.344	0.00409	0.165	132300	21.86
0.341	0.329	0.00433	0.167	143325	20.37
0.367	0.316	0.00457	0.170	154350	19.15
0.394	0.304	0.00481	0.172	165375	18.17
0.420	0.293	0.00506	0.174	176400	17.37
0.446	0.284	0.00531	0.177	187425	16.72
0.472	0.276	0.00555	0.180	198450	16.21
0.499	0.268	0.00580	0.183	209475	15.80
0.525	0.261	0.00605	0.186	220500	15.48
0.551	0.255	0.00630	0.189	231525	15.24
0.578	0.250	0.00655	0.192	242550	15.07
0.604	0.244	0.00680	0.195	253575	14.95
0.630	0.240	0.00705	0.199	264600	14.89
0.656	0.236	0.00731	0.202	275625	14.86
0.683	0.232	0.00756	0.206	286650	14.88
0.709	0.228	0.00781	0.209	297675	14.93
0.735	0.225	0.00807	0.213	308700	15.00
0.761	0.222	0.00832	0.217	319725	15.11
0.788	0.219	0.00858	0.221	330750	15.23
0.814	0.216	0.00884	0.225	341775	15.38
0.840	0.214	0.00909	0.229	352800	15.54
0.866	0.212	0.00935	0.233	363825	15.72
0.893	0.210	0.00961	0.237	374850	15.91
0.919	0.208	0.00987	0.241	385875	16.12
0.945	0.206	0.01013	0.245	396900	16.34
0.971	0.204	0.01039	0.250	407925	16.57
0.998	0.203	0.01065	0.254	418950	16.81
1.024	0.201	0.01091	0.258	429975	17.05
1.050	0.200	0.01117	0.263	441000	17.31
1.076	0.199	0.01143	0.267	452025	17.57
1.103	0.198	0.01170	0.272	463050	17.84
1.129	0.197	0.01196	0.276	474075	18.12
1.155	0.196	0.01222	0.281	485100	18.40
1.181	0.195	0.01248	0.286	496125	18.68
1.208	0.194	0.01275	0.290	507150	18.97
1.234	0.193	0.01301	0.295	518175	19.27
1.260	0.192	0.01327	0.300	529200	19.57
1.286	0.191	0.01354	0.305	540225	19.87
1.313	0.191	0.01380	0.309	551250	20.18
1.339	0.190	0.01407	0.314	562275	20.49
1.365	0.190	0.01433	0.319	573300	20.80
1.391	0.189	0.01460	0.324	584325	21.12
1.418	0.188	0.01486	0.329	595350	21.43